

**Study on Degradation of a Commercial
Rigid Polyurethane Foam Used for Filling
of Process Gas Equipment (PGE) and Pipes
and Corrosion Behavior of Pipes at K-25/K-27**

Nuclear Engineering Division

About Argonne National Laboratory

Argonne is a U.S. Department of Energy laboratory managed by The University of Chicago under contract W-31-109-Eng-38. The Laboratory's main facility is outside Chicago, at 9700 South Cass Avenue, Argonne, Illinois 60439. For information about Argonne, see www.anl.gov.

Availability of This Report

This report is available, at no cost, at <http://www.osti.gov/bridge>. It is also available on paper to the U.S. Department of Energy and its contractors, for a processing fee, from:

U.S. Department of Energy

Office of Scientific and Technical Information

P.O. Box 62

Oak Ridge, TN 37831-0062

phone (865) 576-8401

fax (865) 576-5728

reports@adonis.osti.gov

Disclaimer

This report was prepared as an account of work sponsored by an agency of the United States Government. Neither the United States Government nor any agency thereof, nor The University of Chicago, nor any of their employees or officers, makes any warranty, express or implied, or assumes any legal liability or responsibility for the accuracy, completeness, or usefulness of any information, apparatus, product, or process disclosed, or represents that its use would not infringe privately owned rights. Reference herein to any specific commercial product, process, or service by trade name, trademark, manufacturer, or otherwise, does not necessarily constitute or imply its endorsement, recommendation, or favoring by the United States Government or any agency thereof. The views and opinions of document authors expressed herein do not necessarily state or reflect those of the United States Government or any agency thereof, Argonne National Laboratory, or The University of Chicago.

Study on Degradation of a Commercial Rigid Polyurethane Foam Used for Filling of Process Gas Equipment (PGE) and Pipes and Corrosion Behavior of Pipes at K-25/K-27

for
Bechtel Jacobs Company, LLC
Oak Ridge, TN

by
D. Singh, N. Chen*, C. Lorenzo-Martin*, and J.L. Routbort*
Nuclear Engineering Division and *Energy Systems Division, Argonne National Laboratory

K. Pagilla and M. Urgan-Demirtas
Department of Chemical and Environmental Engineering, Illinois Institute of Technology

K. Reddy and J. Gangathulasi
Department of Civil and Materials Engineering, University of Illinois at Chicago

G.D. Del Cul, C.M. Simmons, and A.S. Icenhour
Nuclear Science and Technology Division, Oak Ridge National Laboratory

August 2006

EAST TENNESSEE TECHNOLOGY PARK CLASSIFICATION REVIEW REQUEST FORM

PERSON REQUESTING ACTION Bob Seigler / Vickie Hughes	TELEPHONE 241-4922 241-5082	FACSIMILE 241-2852
PARK ADDRESS K2527-Q MS 7313	PAGER 873-6200	ORGANIZATION K-25/K-27

Request: Routine Urgent (Requests will be prioritized on the basis of urgency and date.)
 Log In Date 7/25/2006 Log Out Date 7/25/2006 (CICO Use Only) (Standard processing time is 10 working days. Some documents require special review and the processing time will be longer.)

Action Requested: Classification Opinion Other

DOCUMENT DESCRIPTION (TO BE COMPLETED BY REQUESTER)

Document Classification: Secret Confidential RD FRD NSI Classified, Pending Review Unclassified

DOCUMENT NUMBER: ANL-06/?? PAGES: DATE: 7/24/06

DOCUMENT TITLE: Study on Degradation of a Commercial Rigid Polyurethane Foam Used for Void Filling of Process Gas Equipment (PGE) and Corrosive Behavior of Pipes

AUTHOR(S): (Indicate other organizations, if applicable.)
 DOCUMENT TYPE: REPORT MEMO LETTER PHOTO DRAWING OTHER (See Remarks)

REMARKS: Argonne National Laboratory/Energy Technology Division

REASON FOR REVIEW:
 Newly Created Document Litigation Executive Order Privacy Act Request Freedom of Info Act (No.: _____)
 Request for Info. (No.: _____) ALL OTHER, Indicate: _____

RECOMMENDATION OF ETPP AUTHORIZED DERIVATIVE CLASSIFIER (TO BE OBTAINED BY REQUESTER)

ACTION RECOMMENDED: UNCLASSIFIED
 REMARKS:

ETPP ADC SIGNATURE: J. D. [Signature] / BJC Engr. DATE: 7/24/06

CLASSIFICATION OFFICE ACTION (TO BE COMPLETED BY CLASSIFICATION OFFICE IF FURTHER ACTION REQUIRED)

ACTION AUTHORIZED: REPORT IS NOT SENSITIVE
 REMARKS:

ETTP CLASSIFICATION OFFICE ADC/ADD SIGNATURE: [Signature] DATE: 7/25/06
 SOURCE AUTHORITY (IF REQUIRED): DATE:

ADDITIONAL COMMENTS/ACTIONS

12.500. CO-06 (RC)
 B. Seigler - 1p fax to 241-2852

CONTENTS

ACKNOWLEDGEMENTS.....	ix
ACRONYMS AND ABBREVIATIONS.....	xi
EXECUTIVE SUMMARY	xiii
1 INTRODUCTION.....	1
2 URETHANE FOAM.....	3
2.1 Urethane Foam Sample Description.....	3
2.2 Configuration of Urethane Foam Test Samples.....	3
2.3 Microstructural Evaluation of the As-received Constrained Rise Foam	4
2.4 Density.....	6
2.5 Unconfined Compressive Strength.....	7
2.6 Triaxial Compressive Strength	10
3 EFFECT OF TEMPERATURE ON THE MECHANICAL PROPERTY OF URETHANE FOAM.....	15
4 THERMAL AGING EFFECTS ON URETHANE FOAM	17
4.1 Effect of Temperature Aging on the Structural Integrity of Urethane Foam	17
4.2 Effect of Water Immersion on Structural Integrity of Urethane Foam.....	19
5 EFFECT OF THERMAL CYCLING ON STRUCTURAL INTEGRITY OF URETHANE FOAM.....	23
6 COMPRESSION PROPERTIES OF URETHANE FOAM	27
7 COMPRESSION BEHAVIOR OF HIGHER DENSITY FOAMS	31
7.1 Baseline Characterization	31
7.2 Compression Testing of Higher Density Foams.....	33
7.3 Creep Testing.....	33
8 BIODEGRADATION OF URETHANE FOAM.....	39
8.1 Literature Review.....	40
8.2 Materials and Methods.....	41
8.3 Results and Discussion	46
8.4 Conclusions.....	50

CONTENTS (Cont.)

9	RADIOLYTIC DEGRADATION OF URETHANE FOAM	55
10	CORROSION OF STEEL PIPES	57
10.1	Material and Experimental Procedure	57
10.2	Corrosion Study Results	59
10.2.1	Corrosion in Leachate Solution	59
10.2.2	Corrosion in Soil Mixed with Leachate (open condition)	59
10.2.3	Corrosion in Soil Mixed with no Leachate (sealed condition)	64
10.2.4	Corrosion in Soil Mixed with Leachate (sealed and open conditions).....	64
10.2.5	Corrosion in Anaerobic Soil	64
10.3	Summary	68
11	SUMMARY	71
12	REFERENCES	73
	APPENDIX 1: Test Data for As-received Urethane Foam Samples.....	75
	APPENDIX 2: Triaxial test data on longitudinal (V) and transverse (H) cut urethane foam (3.1 pcf).....	79
	APPENDIX 3: Effect of Temperature on Urethane Foam Compression Strength.....	83
	APPENDIX 4: Thermal Aging Test Results	85
	APPENDIX 5: Confined Compression Test on 3.1 pcf Foam	103
	APPENDIX 6: Compression and Creep Testing Data (New Higher Density Foams) Unconfined Compression Tests	110
	APPENDIX 7: Biodegradation Literature Review	127
	APPENDIX 8: Corrosion Test Results.....	141

FIGURES

2.1	As-received constrained-rise urethane foam cylinders.....	4
2.2	As-received urethane foam machined in (A) longitudinal and (B) transverse directions to the cylinder axis for aging study	4
2.3	Surface porosity on the as-machined test sample (a) curved surface and (b) edge.....	5
2.4	SEM photomicrograph of urethane foam surface Showing the cellular structure. Notice the damage resulting from sample machining.....	6
2.5	Density variations of urethane foam samples as a function of sample location, orientation, and processing condition.....	7
2.6	Compression test being conducted on Instron machine	8
2.7	Typical load-extension variations for constrained-rise samples tested for compression.....	8
2.8	Average compressive strength variations of unconfined urethane foam samples as a function of sample location, orientation, and processing condition.....	9
2.9	Compressive strength of unconfined individual urethane foam samples as a function of sample location, orientation, and processing condition.....	9
2.10	Experimental set-up used for triaxial tests of urethane foam.....	10
2.11	Stress-strain variations for transverse machined urethane foam at varying confining pressures.....	11
2.12	Failed urethane foam sample during triaxial test (left) compared with an untested sample (right)	12
2.13	Stress-strain variations for longitudinal machined urethane foam at varying confining pressures.....	12
3.1	Set-up for high-temperature compression	15
3.2	Effect of test temperature on the compressive strength of urethane foam	16
4.1	Oven used for aging studies of urethane foam	17

FIGURES (Cont.)

4.2	Density variation with high-temperature dry aging at 70°C (158°F) (circles) and 90°C (194°F) (squares).....	18
4.3	Compressive strength of urethane foam (transverse direction) aged at 70°C (158°F) and 90°C (194°F) in air.....	19
4.4	Samples for room-temperature water immersion test	20
4.5	Density variation with wet aging at various temperatures	20
4.6	Compressive strength of urethane foam (transverse direction) aged at 70°C (158°F) and 90°C (194°F) in air.....	21
4.7	Wet aging samples after 60-day exposure. Samples at 90°C (194°F) showed change in color (foreground) compared to 23°C (73°F) and 70°C (158°F) samples (background).....	22
5.1	(a) Freeze-thaw cycling chamber and (b) Interior of the chamber.....	24
5.2	Change in urethane foam density during dry freeze-thaw cycling.....	25
5.3	Compression stress-strain curves for five urethane foam samples after dry freeze-thaw cycling.....	25
5.4	Change in urethane foam density during wet freeze-thaw cycling	26
5.5	Compression stress-strain curves for five urethane foam samples after wet freeze-thaw cycling.....	26
6.1	(a) Consolidometer set-up and (b) foam sample in rigid ring.....	28
6.2	Typical compression vs. time plots obtained during a consolidation test at fixed applied stress	29
6.3	Consolidation behavior (volumetric strain) of urethane foam in (a) transverse and (b) longitudinal directions.....	30
7.1	Compressive strength of foams tested for consolidation behavior.....	32
7.2	Compressive strength vs. density behavior of foams tested for consolidation behavior.....	32

FIGURES (Cont.)

7.3	Compression behaviors (volumetric strain) of urethane foams A, B, C, and D as a function of applied stress and hold times	35
7.4	Compressive creep behaviors of foams A and B at a constant stress of 64 psi (4.6 tsf)	37
7.5	Consolidation of foam B (6.6 pcf) as a function of time at 75 psi (5.4 tsf)	37
8.1	FT-IR spectrum of treated (single arrow) and untreated (double arrows) PU foams	50
8.2	Growth assay of the anaerobic bacteria during the bioassay.....	51
8.3	FT-IR spectrum of treated (single arrow) and untreated (double arrows) PU foams	54
10.1	As-received ASTM A53 steel sample coupon	58
10.2	Corrosion samples in leachate solution. Note the corrosion product at the bottom	58
10.3	Corrosion rates (C.R.) of (a) as-cut and (b) polished samples directly suspended in solution and tested at room temperature.....	60
10.4	Corrosion rates of (a) as-cut and (b) polished samples directly suspended in solution and tested at 60°C (140°F)	61
10.5	Corrosion rates of (a) as-cut and (b) polished samples directly suspended in solution and tested at 80°C (176°F)	62
10.6	Corrosion rates of samples placed in soil mixed with leachate (open condition) and tested at 23°C (73°F), 60°C (140°F), and 80°C (176°F).....	63
10.7	Corrosion samples in Oak Ridge soil under open condition.....	63
10.8	Corrosion rates for samples placed in soil, in sealed condition, and tested at 23°C (73°F), 60°C (140°F), and 80°C (176°F).....	65
10.9	Corrosion samples in Oak Ridge soil in sealed condition.....	65
10.10	Corrosion rates of samples placed in soil, in open condition, and tested at room temperature	66

FIGURES (Cont.)

10.11	Corrosion rates of samples placed in soil, in sealed condition, and tested at room temperature.....	66
10.12	Steel samples suspended in leachate solution for 90 days at (a) 23°C (73°F), (b) 60°C (140°F), and (c) 80°C (176°F).....	67
10.13	Corrosion rates of samples placed in Oak Ridge soil, in anaerobic condition, and tested at room temperature	68
A.7.1	Structure of polyurethane (Nakajima-Kambe et al., 1999)	128

TABLES

2.1	Results of triaxial test conducted on urethane foam machined in transverse (H) and longitudinal (V) directions	13
8.1	Composition of the basal medium (pH=7.2)	42
8.2	Tensile strength of untreated PU plugs.....	45
8.3	Weight loss during bioassay experiments.....	47
8.4	Tensile strength of treated plugs during bioassay experiments	49
8.5	Cumulative weight loss during soil burial experiments.....	52
8.6	Tensile strength of treated plugs during soil burial experiments.....	53
10.1	Compositional make-up of corrosion fluid.....	59
10.2	Summary of corrosion rates in various test conditions.....	69
A7.1	Raw materials used during the synthesis of PUs.	129
A7.2	Polyurethane (PU)-degrading microorganisms (PE = polyether, PS = polyester) (Nakajima-Kambe et al., 1999).....	132
A7.3	Sensitivity of analytical balance used for weighing the PU foams.....	139
A7.4	The effectiveness of the drying procedure used for the weight change determination	140

ACKNOWLEDGEMENTS

The work at Argonne National Laboratory was supported by Bechtel Jacobs Company (BJC) under Memorandum Purchase Order 23900-MP-0154. Valuable insights and discussions with various BJC personnel including A Dada, R. Seigler, E. Strassburger, R. James, and J. Gadd are appreciated.

ACRONYMS AND ABBREVIATIONS

ANL	Argonne National Laboratory
AODC	Acridine Orange Direct Count Method
BJC	Bechtel Jacobs Company
CERCLA	Comprehensive Environmental Response, Compensation, and Liability ACT
DOE	Department of Energy
EMWMF	Environmental Waste Management Facility
HRT	Hydraulic Retention Time
ISA	Inner Surface Area
MCNP	Monte Carlo N-Particle Transport Code System
NCFI	North Carolina Foam Industries
ORNL	Oak Ridge National Laboratory
ORR	Oak Ridge Reservation
PGE	Process Gas Equipment
PU	Polyurethane
SBR	Sequencing Batch Reactor
SEM	Scanning Electron Microscope
SRT	Sludge Retention Time
UPBR	Upflow Packed Bed Reactor

EXECUTIVE SUMMARY

This study has been undertaken to investigate the degradation behavior of a commercial urethane foam. Bechtel Jacobs Company (BJC) plans to use urethane for infiltrating segmented process gas equipment (PGE) at the K-25/K-27 plants to restrict the mobility of the various radionuclides. Subsequently, the infiltrated PGE will be sent to the Environmental Management Waste Management Facility (EMWMF) at the Oak Ridge Reservation (ORR) for disposal.

The objective of this study was to generate test data to be used in evaluating the long-term performance of the urethane foam in the landfill environment. The longevity of the foam was evaluated under plausible degradation scenarios that may lead to foam failure, which could then compromise the integrity of the final cap during the life of the landfill. The degradation effects of various conditions such as mechanical stresses, heat, moisture, temperature cycling, biodegradation, and radiation exposure were studied.

All urethane foams in this study were fabricated and supplied by North Carolina Foam Industries (NCFI). The unconfined compressive strength of the as-received urethane foam, which had a density of 3.1 pounds per cubic feet (pcf), was found to be anisotropic. Compressive strengths were 50 psi in the direction of foam rise (longitudinal) and 31 psi in the direction perpendicular to foam rise (transverse). The aging study focused on the transverse (i.e., weaker compressive strength) mechanical properties. The compressive strength of the urethane foam degraded with test temperature up to 90°C (194°F). Strength dropped by 40% at 90°C (194°F), to 19 psi, as compared with the room-temperature compressive strength of 31 psi.

Dry and wet aging of urethane did not degrade compressive strength for tests conducted at temperatures as high as 90°C (194°F) and exposure times as long as 60 days. However, foam density did decrease (by as much as 15%) with such long-term exposure at elevated temperature. The density changes were mainly attributed to sample dimensional changes.

Dry and wet freeze-thaw cycling also did not degrade the compressive strength for 30 cycles between -5°C and 50°C (23°F and 122°F).

Confined compression tests conducted on 3.1-pcf density foam showed that at 75 psi stress (corresponding to 90-ft burial depth), strains were 50 to 60%. Based on this observation, BJC selected higher density foams (4-7 pcf) for study of potential landfill overburden loads. No aging studies were conducted on the higher density foams. However, since the compositional makeup for the higher density foam is same as the low (3.1 pcf) foam (according to NCFI), its aging behavior is expected to be similar to the low-density foam.

Unconfined compressive strengths of four higher density foams showed that with increasing density, compressive strength increases. These foams also showed anisotropic behavior in their mechanical properties. For the foam with density of 7 pcf (foam B), compressive strengths were approximately 200 psi and 120 psi in the longitudinal and transverse directions, respectively.

Confined compression tests on urethane foam showed that foam B satisfies BJC's initial consolidation condition of <10% volumetric strain at stresses of 75 psi (5.4 tsf or equivalent to 90-ft soil depth corresponding to the maximum overburden pressures). In time-dependent confined compression testing at 75 psi (5.4 tsf), foam B deformed <8% in over 1800 h of testing.

A biodegradation study showed the urethane foam (3.1 pcf) to be non-biodegradable under anaerobic conditions. This rigid foam is resistant to microbial attack due to its chemical and physical structure. Since there is no difference in chemical composition of the higher density (6.6 pcf) foam, it is likely that the denser foam will have similar biodegradability properties as the less denser (3.1 pcf) foam.

Irradiation and testing of the urethane foam (3.1 pcf), performed at Oak Ridge National Laboratory, indicated no significant degradation of the foam and minimal gas generation during a gamma irradiation to a "1000-year alpha and gamma" dose on the entire sample volume.

Another aspect of this study was to investigate the corrosion behavior of the PGE steel pipes. The objective was to determine the corrosion rates of the steel in various disposal scenarios. The data obtained will help EMWFMF in establishing the durability of steel structures and in assessing the potential of subsidence due to structural collapse. This information will be used in assessing the structural integrity of steel objects relative to the design life of the EMWFMF.

Corrosion tests on the ASTM A51 steel were conducted in four conditions: (a) sample suspended in leachate, (b) sample buried in soil mixed with leachate and soil open to air, (c) sample buried in soil mixed with leachate in a sealed container, and (d) sample buried in soil to create anaerobic conditions. Corrosion rates at room temperature for the above test conditions were 0.065 mm/yr, negligible, 0.03 mm/yr, and negligible, respectively.

1 INTRODUCTION

Currently, the U.S. Department of Energy (DOE) and its contractor, Bechtel Jacobs Company (BJC), are undertaking a major effort to clean up the former gaseous diffusion facility (K-25) located in Oak Ridge, TN. One need is for disposal of tons of steel pipes and other process gas equipment (PGE) that are contaminated by various radionuclides, including UO_2F_2 . The approach BJC is taking is to infiltrate the PGE with an urethane foam to restrict the mobility of the radionuclides during handling and demolition process.

Most of the infiltrated PGE will be ultimately disposed of in the Environmental Management Waste Management Facility (EMWMF). The EMWMF is an above ground disposal facility for Comprehensive Environmental Response, Compensation and Liability Act (CERCLA) waste generated from remediation of DOE facilities on the Oak Ridge reservation (ORR). The landfill accepts both hazardous and low-level radioactive wastes. The 1.7 million cubic yard facility is designed with a maximum waste depth of 75 feet, and the entire facility is overlain by 15 feet thick impermeable cap. The maximum overburden pressure at the base of the landfill is 75 psi or 5.4 tons per square foot (tsf).

The long-term integrity of urethane foam in the disposal environment has not been established. In this regard, BJC contracted Argonne National Laboratory (ANL) to evaluate the urethane foam in a laboratory test program.

The objective of this study was to generate test data to be used in evaluating the long-term performance of the urethane foam in the landfill environment. The longevity of the foam was to be evaluated under plausible degradation scenarios that may lead to failure of the foam material which could then compromise the integrity of the final cap on the EMWMF. Of particular concern is loss of foam integrity that leads to excessive subsidence or excessive differential subsidence of the cap over a 1,000-year period.

The focus of the proposed study was to isolate the specific degradation mechanism of interest for the urethane foam and study its effect on the urethane property(s) by accelerated tests, and use predictive modeling to assess a useful life-time of urethane. To ascertain what degradation mechanisms could affect the foam, the foam was exposed to extreme environments not likely to be experienced in real applications. However, these extreme measures are required to accelerate the degradation process. By determining the rate constants of the degradation process, it is then possible to simulate the foam behavior over long periods based on the relative short period of time of this study. This predictive modeling is valid only if there is some degradation in the foam property is observed and the degradation mechanism remains the same during accelerated testing.

Aging and potential degradation of polymers are expected to be caused by numerous natural weathering factors, including heat, sunlight, moisture, temperature cycling, micro-organisms, radioactivity, and chemical pollutants, etc. However, in the disposal scenario, not all the degradation mechanisms will be operable. It is important to identify the critical degradation causes and their effect on the material properties under environments that simulate the actual weathering conditions. Moreover, accelerated tests have to be conducted to determine useful

lifetimes of the materials of interest. Based on review of the disposal environment, the following properties were of interest:

- Temperature Effects - Once buried, the temperature of the foam is expected to remain constant at about 55°F. However, prior to burial, large temperature variations may be experienced. This aspect of the study concentrated on higher temperatures and thermal cycling.
- Water Immersion - While the landfill will be capped and long-term immersion is a remote possibility, moisture will be available in the landfill. The foam must thus maintain integrity in a moist environment.
- Freeze-Thaw Cycling - Foam will only be subjected to mild freeze-thaw cycling prior to burial.
- Mechanical Strength - The foam will be compressively loaded soon after burial or at some time in the future based on degradation of the surrounding PGE. Strength was investigated for confined and unconfined short-term compressive strength and long-term confined compressive strength and creep.
- Biodegradation – The susceptibility of the foam to attack and degradation by biological growth can be expected.
- Radiation – The effect of radiation on foam integrity is important because of contact of foam with the contaminated surfaces of PGE.
- Ultraviolet Radiation - UV is known to break down urethane foam, but as the foam is inside the PGE prior to disposal and buried following disposal, this aspect of foam integrity did not justify evaluation.

Before exposure of the foam to significant loading within the landfill, the surrounding PGE (i.e., pipe or other metal structure) must first structurally degrade. Therefore, another aspect of this study was to evaluate the corrosion behavior of the steel pipes in a simulated environment and accelerated aging conditions. Corrosion was determined under several representative environmental conditions, which are expected to exist over time within the EMWMF.

2 URETHANE FOAM

2.1 URETHANE FOAM SAMPLE DESCRIPTION

Urethane foam samples were fabricated by North Carolina Foam Industries (NCFI), Mount Airy, North Carolina, and shipped to Argonne National Laboratory. The samples were fabricated in June 2005. The standard urethane foam was a two-component system of resin and polymeric isocyanate mixed one-to-one by volume. Urethane foam was fabricated in two forms: constrained-rise and free-rise. Constrained rise foam samples were produced in pipes dimensionally similar to PGE. As-received cylindrical shaped samples had a diameter of 8 in (20.3 cm) and length of 4 ft (122) as shown in Fig. 2.1. Notice the surface inhomogeneity in some of the cylinders. These constrained-rise samples were used for aging studies.

In addition to constrained-rise urethane foam samples, NCFI also supplied a box (2 ft × 1 ft × 1 ft) of free-rise urethane foam.

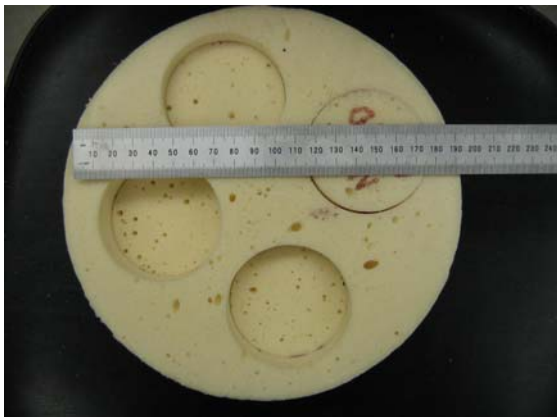
2.2 CONFIGURATION OF URETHANE FOAM TEST SAMPLES

For the constrained-rise urethane, a baseline study was conducted to establish any variations in the property of the urethane foam based on the location from where the test sample was extracted from the cylinder. It was assumed that all the cylinders had been processed in an identical manner, and that the material characteristics did not vary from cylinder to cylinder. However, the material properties could vary depending on the location within each cylinder such as center, top or bottom. In this regard, properties such as density, microstructure, and compressive strength were determined along the cylinder length to discern any differences from the baseline.

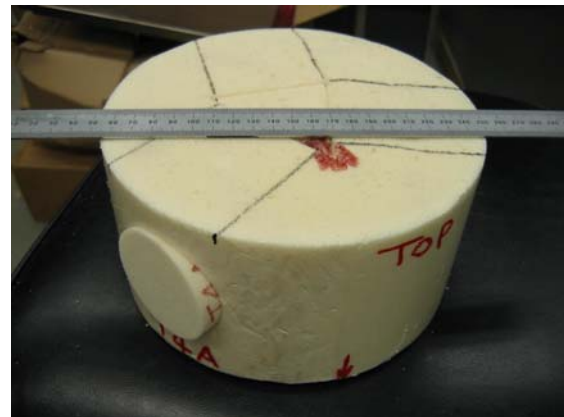
In addition, we investigated the effect on the physical property of the orientation of the test sample at a particular location along the cylinder length. This test was done by machining samples that were parallel (longitudinal) and perpendicular (transverse) to the cylinder's length, as shown in Figs. 2.2(a) and 2.2(b), respectively. Samples were machined by hot-wire and core-drill techniques at a commercial facility.



FIGURE 2.1 As-received constrained-rise urethane foam cylinders



(a)



(b)

FIGURE 2.2 As-received urethane foam machined in (A) longitudinal and (B) transverse directions to the cylinder axis for aging study

2.3 MICROSTRUCTURAL EVALUATION OF THE AS-RECEIVED CONSTRAINED RISE FOAM

Figures 2.3(a) and 2.3(b) show higher magnification pictures of the surface of a constrained-rise sample. Circular pores as large as 1-2 mm were randomly distributed on both the flat and curved surfaces of the cylinder. Figure 2.4 shows a high-magnification scanning electron photomicrograph of the urethane foam surface. There were no discernible differences between the urethane foam microstructure in the transverse and longitudinal directions.



(a)



(b)

FIGURE 2.3 Surface porosity on the as-machined test sample
(a) curved surface and (b) edge

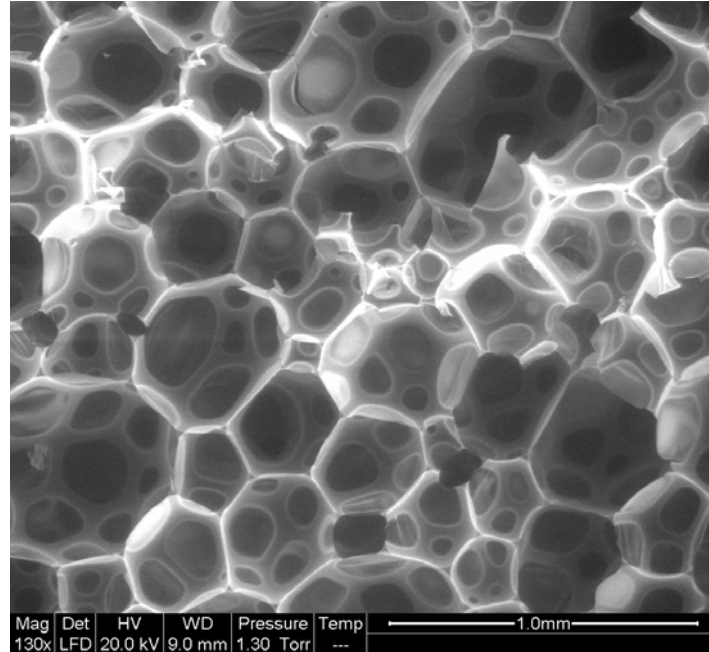


**FIGURE 2.4 SEM photomicrograph of urethane foam surface
Showing the cellular structure. Notice the damage resulting
from sample machining**

2.4 DENSITY

Densities were determined for samples machined from free-rise urethane foam and were compared with those of constrained-rise foam. ASTM D 1622-03 (Standard Test Method for Apparent Density of Rigid Cellular Plastics) was used to determine the density of the samples, which was calculated by taking the ratio of the sample weight and measured volume. Typical samples were cylindrical (2.375-in. diameter and 2.375-in. length). Averages were obtained from measurements on at least three samples at each condition (location and orientation). All measurements were made in a standard laboratory environment [$\sim 23^{\circ}\text{C}$ (73°F), 45-50% RH].

Figure 2.5 shows the variations in the density of the various samples along with the standard deviations. As expected, free-rise urethane foam had the lowest density, 2.62 lb/ft³. The constrained-rise foam had slight orientation dependence. The average density for transverse-cut samples (3.13 lb/ft³) was slightly higher than that of the longitudinal-cut samples (2.95 lb/ft³). Furthermore, for a same sample orientation, we found no significant density variations based on the location (top, middle, or bottom) of the sample in the cylinder. Raw data for the density measurements are listed in Appendix 1.

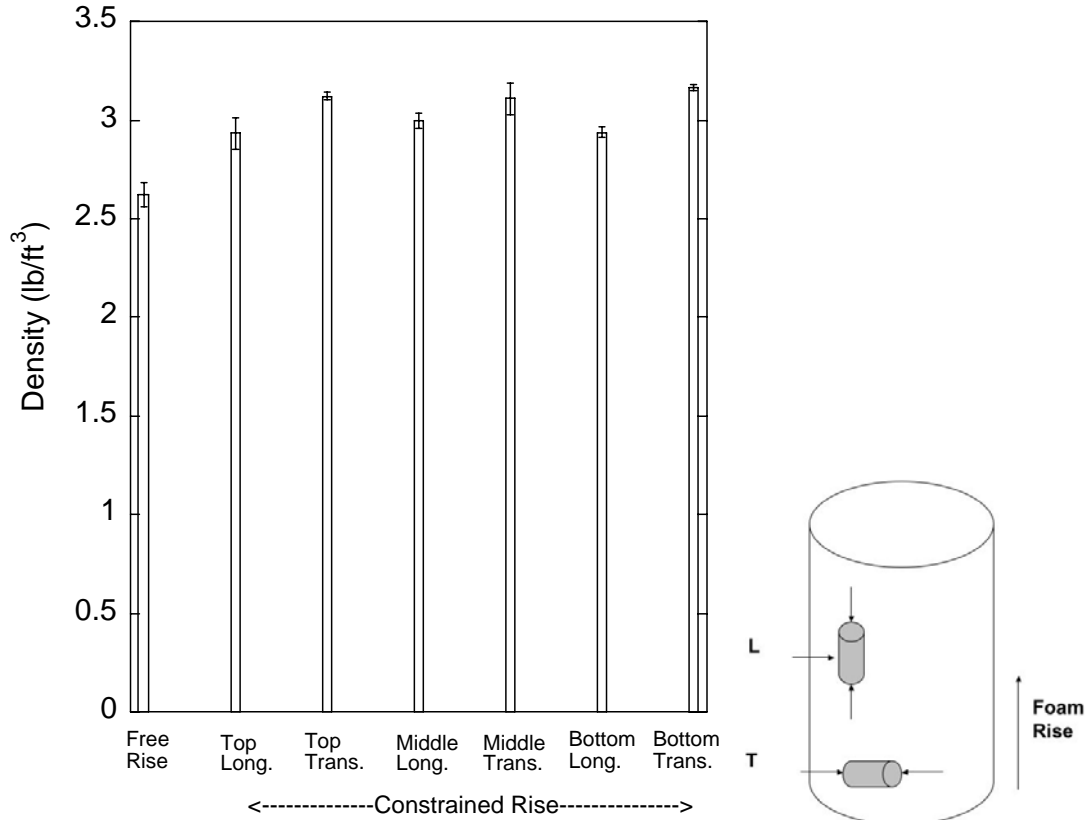


FIGURE 2.5 Density variations of urethane foam samples as a function of sample location, orientation, and processing condition

2.5 UNCONFINED COMPRESSIVE STRENGTH

Compressive strength tests on the foam (free-rise and constrained-rise) samples were conducted per ASTM D 1621 (Standard Test Method for Compressive Properties of Rigid Cellular Plastics). These samples were the same as those on which the density variations were evaluated. Typical samples were cylindrical with 2.375-in. (6.03 cm) diameter and 2.375 in. (6.03 cm) length. Tests were conducted under standard laboratory atmosphere. Compressive strength was measured on a Model 4505 Instron Universal Testing System (Fig. 2.6), which has a rate of cross-head movement of 0.24 in./min. Load versus cross-head displacement were recorded. In accordance with the ASTM standard, samples were deformed until they reached the yield point or were compressed approximately 13% of its original thickness, whichever came first. Compressive strength was calculated by taking the load at 10% deformation (if no yielding) or the yield load (if yielding observed) and dividing by the initial sample cross-sectional area, as shown in the raw load-deflection plot for constrained-rise samples in Fig. 2.7. Longitudinal-cut samples exhibit the characteristic yield point, whereas transverse samples do not.

Figure 2.8 shows the average compressive strength and standard deviation of the as-received urethane foam samples. Figure 2.9 shows the individual strength values of the data in



FIGURE 2.6 Compression test being conducted on Instron machine

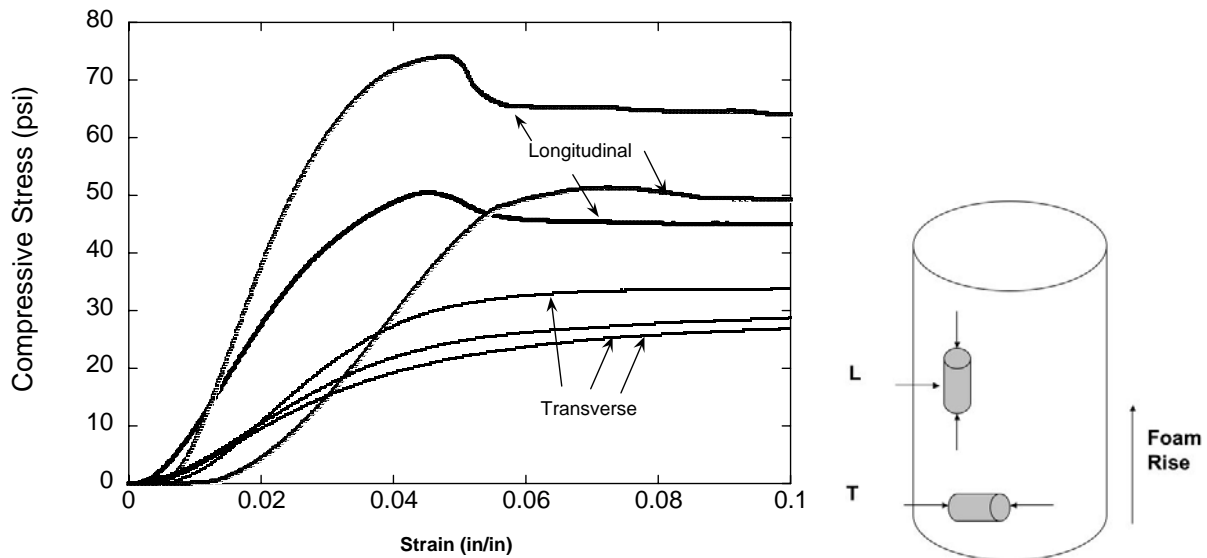


FIGURE 2.7 Typical load-extension variations for constrained-rise samples tested for compression

Fig. 2.8. Clearly, the average strength of free-rise foam is significantly lower than that of the constrained-rise foam, which exhibits anisotropic behavior with regard to compressive strength. Also, the average strength in the longitudinal direction is higher (56 psi) than in the transverse direction (31 psi). Thus, for all the subsequent aging tests, we decided (with consent of BJC) to study only samples in the transverse or the weaker direction. Appendix 1 contains the raw compressive strength data for the samples shown in Fig. 2.9.

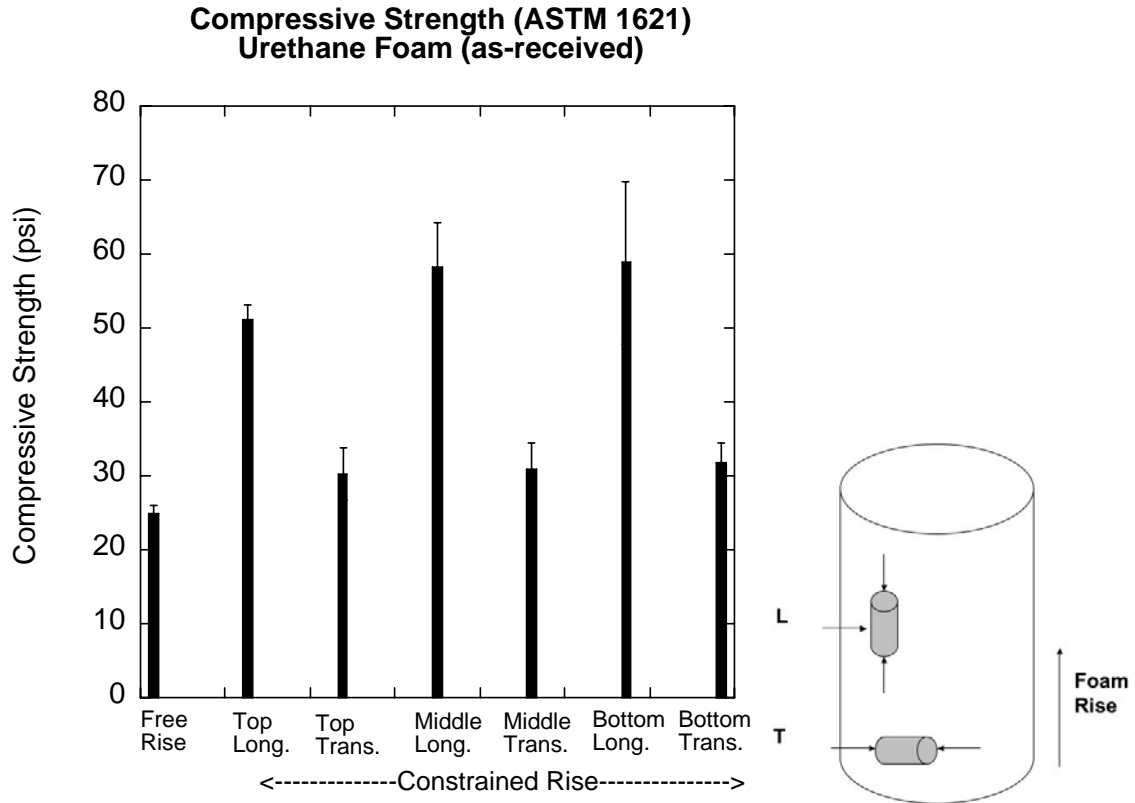


FIGURE 2.8 Average compressive strength variations of unconfined urethane foam samples as a function of sample location, orientation, and processing condition

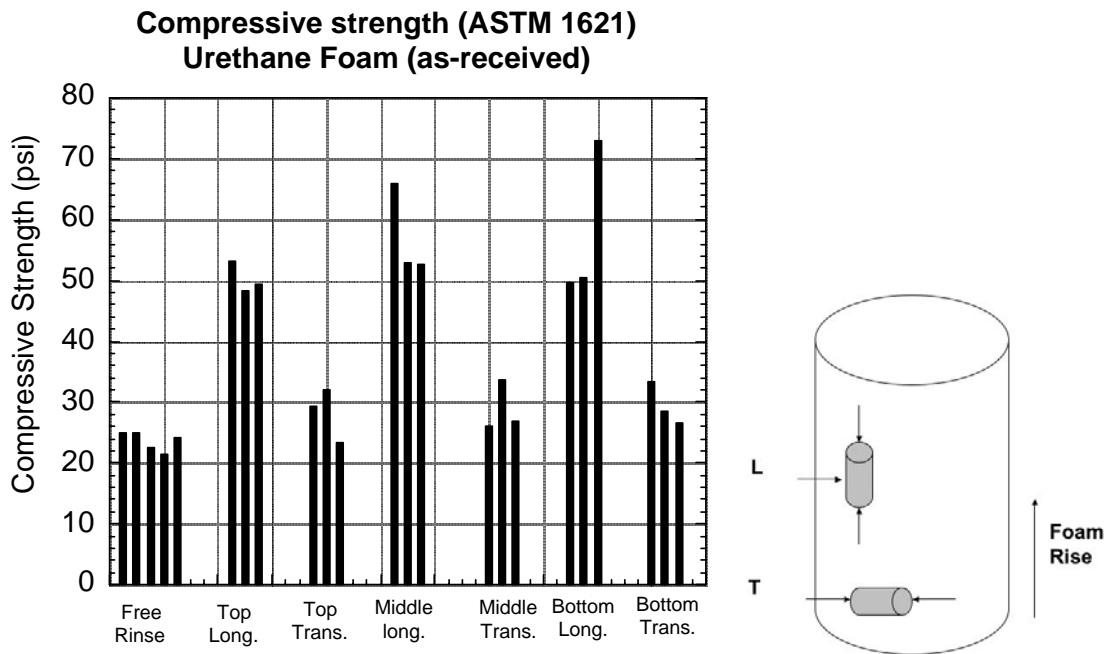


FIGURE 2.9 Compressive strength of unconfined individual urethane foam samples as a function of sample location, orientation, and processing condition

2.6 TRIAXIAL COMPRESSIVE STRENGTH

The unconfined compression tests reported above provided an engineering index. However, in use, the foam will be completely surrounded by waste, soil, etc., and the shear stresses are expected to be relatively low – the slopes are 4H:1V or less, and the highest stresses on the foam are applied vertically. However, at depth, the lateral loads created by the overburden may be significant [1]. Thus, to include the effects of lateral pressures exerted upon the foam by the surrounding materials in the landfill, triaxial compression tests were performed on the foam. The test method followed was ASTM Standard D 2850–03 (Standard Test Method for Unconsolidated-Undrained Triaxial Compression Test on Cohesive Soils).

Tests were conducted in a standard triaxial compression chamber, as shown in Fig. 2.10. A cylindrical sample (5.5-in. long \times 2.5-in. dia) was enclosed in a rubber membrane (Fig. 2.10a) and then placed in a triaxial chamber (Fig. 2.10b). The desired confining pressure was gradually applied using air pressure. The sample was then placed on a compression loader (Fig. 2.10c) under a constant deflection rate (0.06 in./min) until either significant deformation occurred or vertical stress decreased. The axial strain versus vertical stress was plotted. The mode of failure (shear, bulging, etc.) was recorded. All tests were conducted in a laboratory ambient environment. The same procedure was repeated at three confining pressures. Two sets of machined samples were tested: transverse and longitudinal. For each set, two or three samples were tested.

Figure 2.11 plots the stress-strain behavior of transverse-machined samples tested at confining pressures ranging from 10 psi to 30 psi. As shown, the peak stress decreases with increasing confining pressures. Failure was usually accompanied with buckling of the sample, as shown in Fig. 2.12.

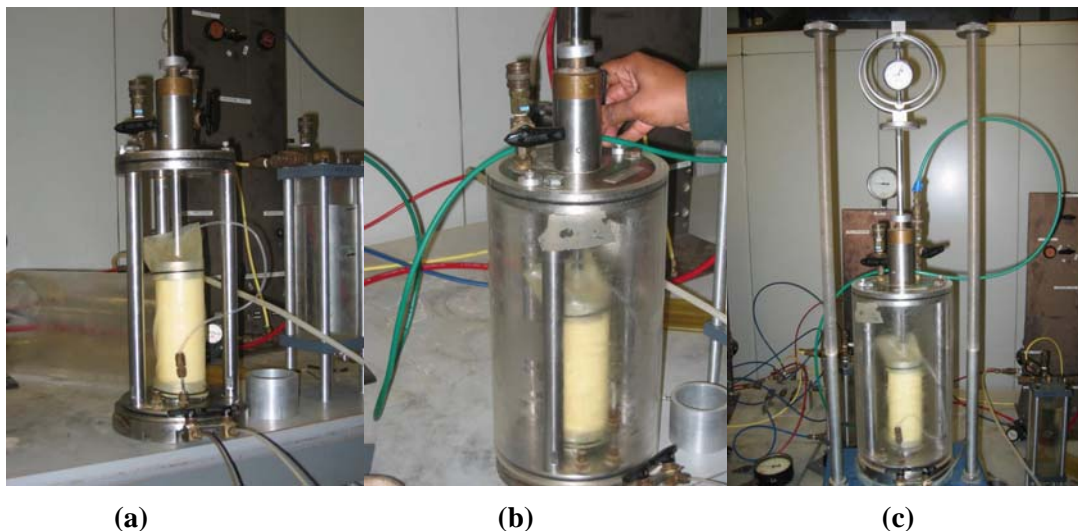


FIGURE 2.10 Experimental set-up used for triaxial tests of urethane foam

Figure 2.13 plots the stress-strain behavior of longitudinal-machined samples tested at confining pressures of 20-60 psi. The triaxial strength of foam appears to be higher in the longitudinal than the transverse direction. This observation is consistent with the evaluation of unconfined compressive strength.

Table 2.1 lists the tests conducted on all the samples. Raw data are presented in Appendix 2. The major principal failure stresses are calculated as a function of confining pressures for the transverse- and longitudinal-machined samples. The results do not exhibit distinct dependency on the level of confining pressure. No distinct shear failure planes were observed in any of the tested samples.

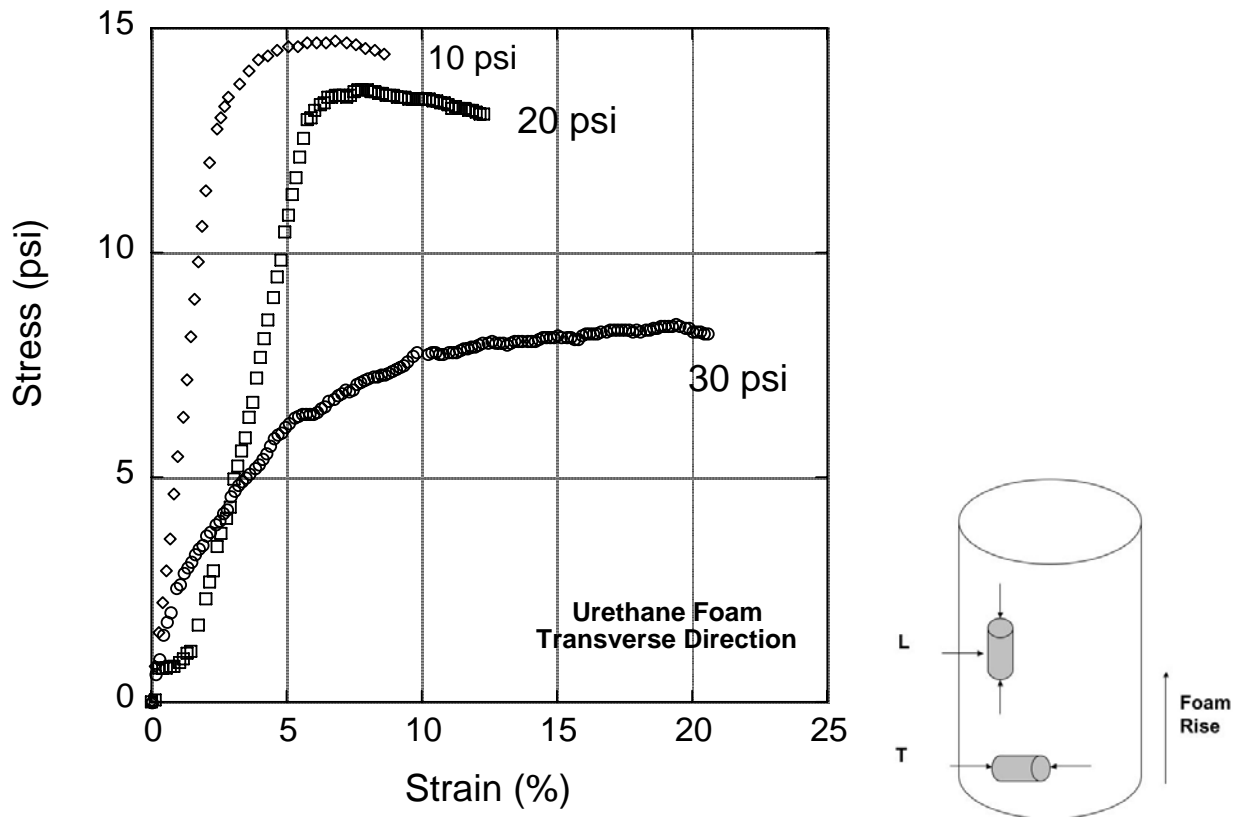


FIGURE 2.11 Stress-strain variations for transverse machined urethane foam at varying confining pressures



FIGURE 2.12 Failed urethane foam sample during triaxial test (left) compared with an untested sample (right)

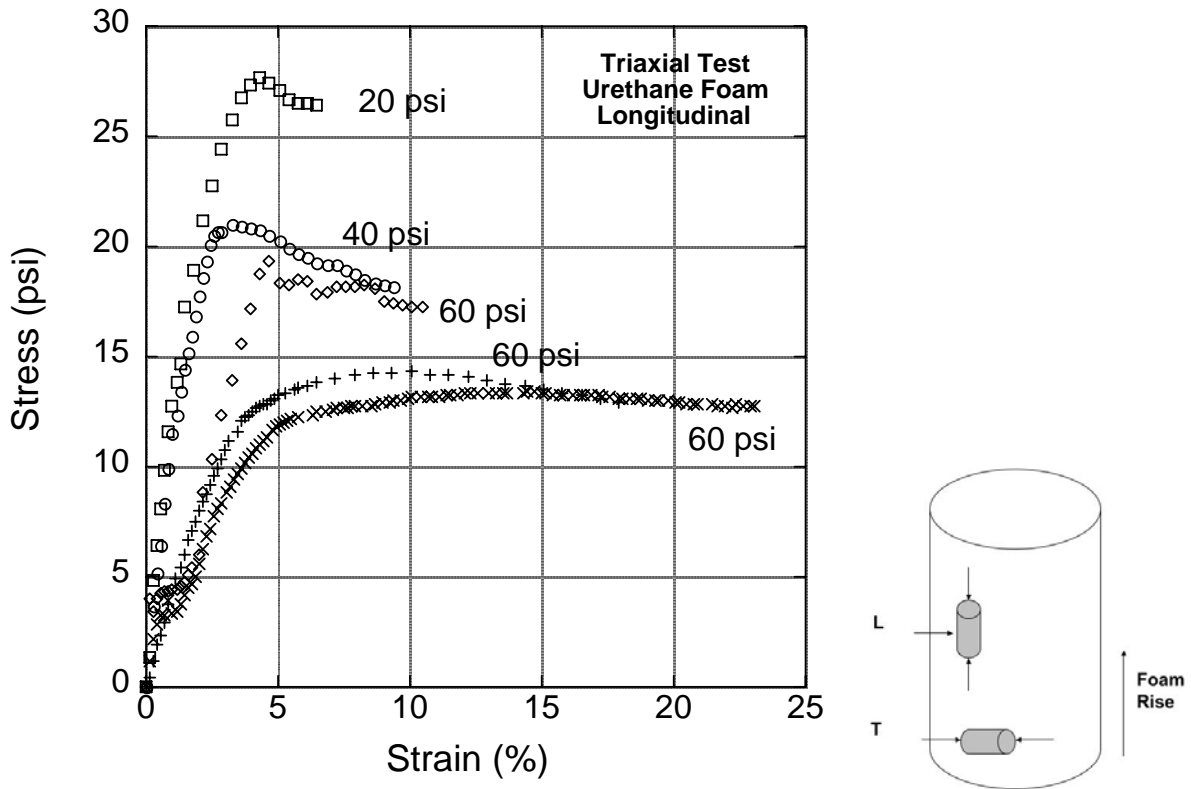


FIGURE 2.13 Stress-strain variations for longitudinal machined urethane foam at varying confining pressures

TABLE 2.1 Results of triaxial test conducted on urethane foam machined in transverse (H) and longitudinal (V) directions

Sample No	Confining Pressure (psi) (σ_3)	Axial Stress at Failure (psi) ($\sigma_1 - \sigma_3$)	Major Principal Stress (psi) (σ_1)
H 6	10	15.2	25.2
H 2	20	13.6	33.7
H 1	30	8.4	38.4
V3	20	20.9	40.9
V4	20	27.9	47.9
V5	20	19.4	39.5
V2	40	13.4	53.4
V1	60	14.2	74.3

The results from the triaxial tests were unexpected, in that the foam material lost strength with increased confining pressure. As shown in Fig. 2.12, samples failed by buckling and not by shearing or crushing. The increased confining pressure apparently increased the stress upon the foam structure and induced a buckling type failure. This failure type was not observed in the unconfined compression tests. Because of this different behavior, the results were recorded and discussed with BJC personnel. BJC decided that conditions under which the samples failed were not representative of field conditions and precluded any further triaxial testing.

3 EFFECT OF TEMPERATURE ON THE MECHANICAL PROPERTY OF URETHANE FOAM

The compressive strengths of urethane foams per ASTM D 1621 standards were measured as a function of test temperature. The purpose of this test was to determine the baseline strength at a selected temperature. The temperatures were 23°C (73°F), 70°C (158°F), and 90°C (194°F). It is recognized that under landfill conditions such high temperatures will not be seen.

These tests were conducted in a furnace mounted on the Instron Universal Testing System (as shown in Fig. 3.1). Samples were loaded after the furnace temperature stabilized for 10 min. The loading rate was 0.24 in./min. Strength as a function of sample deflection was recorded. At least three samples were tested at each of the three test temperatures. All tests were for transverse-oriented samples.

Figure 3.2 shows the variation in strength as a function of test temperature. With increasing temperature, compressive strength drops. From an average value of about 31 psi at room temperature, strength declines to 19 psi for samples tested at 90°C (194°F). The decrease in strength at elevated temperatures is probably due to polymer softening [2, 3]. Raw data is presented in Appendix 3.

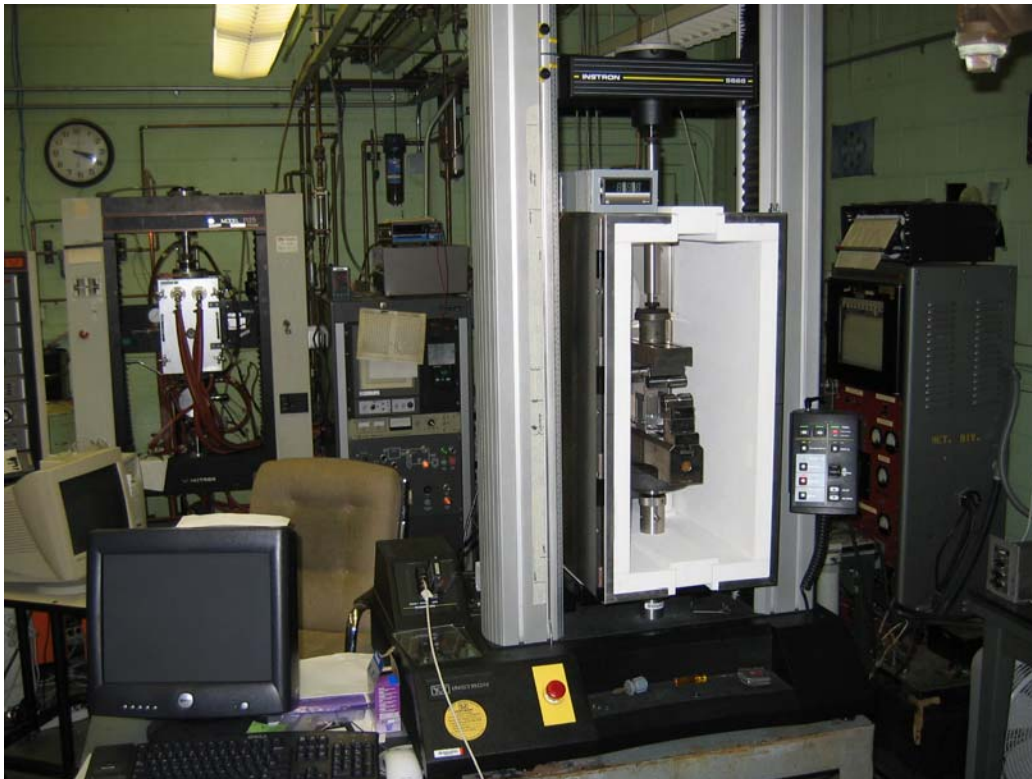


FIGURE 3.1 Set-up for high-temperature compression

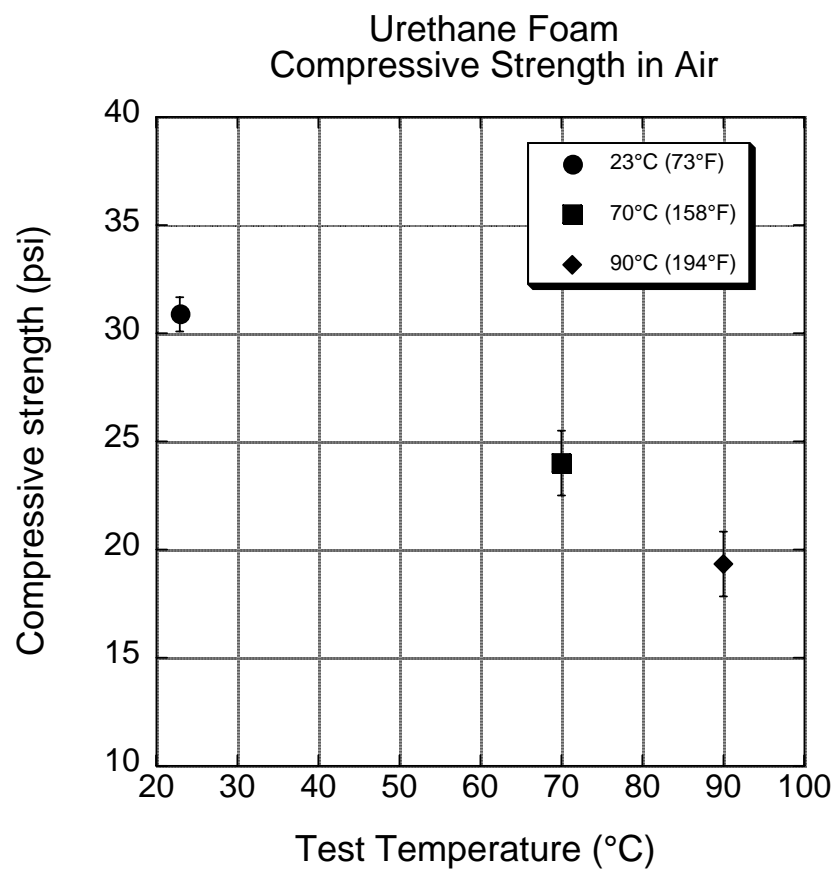


FIGURE 3.2 Effect of test temperature on the compressive strength of urethane foam

4 THERMAL AGING EFFECTS ON URETHANE FOAM

4.1 EFFECT OF TEMPERATURE AGING ON THE STRUCTURAL INTEGRITY OF URETHANE FOAM

The structural integrity of urethane foam was established as a function of temperature and time by the test method specified in ASTM D 2126 (Standard Test Method for Response of Rigid Cellular Plastics to Thermal and Humid Aging). Compressive-strength samples (2.3-in. dia \times 2.3-in. long), machined in the transverse direction, were placed in ovens, as shown in Fig. 4.1. Samples were exposed at $70^{\circ}\text{C} \pm 2^{\circ}\text{C}$ (158°F) and $90^{\circ}\text{C} \pm 2^{\circ}\text{C}$ (194°F) for various intervals: 24 h, 1 week, 2 weeks, 30 days, and 60 days. Humidity for these exposures was laboratory ambient. At the conclusion of each exposure, three samples were examined for any visual changes, as well as density and strength. Before the compression test, samples were conditioned at laboratory ambient (approximately $23^{\circ}\text{C}/73^{\circ}\text{F}$, 50% RH) for at least 24 h. Dimensional, weight, density, and appearance changes were recorded and are provided in Appendix 4.

Figure 4.2 shows the variations in the sample density as a function of temperature and time of aging. For the initial 14 days of exposure, the density changes for the three samples tested at each temperature showed $\pm 2\%$ change. All weight and dimensional measurements were made after the samples had been cooled to room temperature and conditioned at laboratory ambient for 24 h. However, for longer exposure times (30 and 60 days), density mostly showed a reducing trend, with decreases as high as 6% for the 90°C (194°F) exposure. This lower density is probably due to sample dimension changes and any further foam polymerization that occurs with increasing temperature. No change in surface appearance was observed for any of the samples.



FIGURE 4.1 Oven used for aging studies of urethane foam

Figure 4.3 shows the compressive strength measured on samples aged at 70°C (158°F) and 90°C (194°F) in air for 1 to 60 days. As shown, with increasing aging time, the compressive strength increases over the as-received strength of 30 psi. Compressive strengths reach as high as 40-50 psi (or a 33% increase). However, no significant effect of the aging temperature on the compressive strength appears to occur for longer periods of aging. Apparently, during high-temperature exposure, any unreacted polymer precursor undergoes polymerization, thereby increasing the compressive strength of the foam. No effort was made to establish this effect conclusively as part of this study.

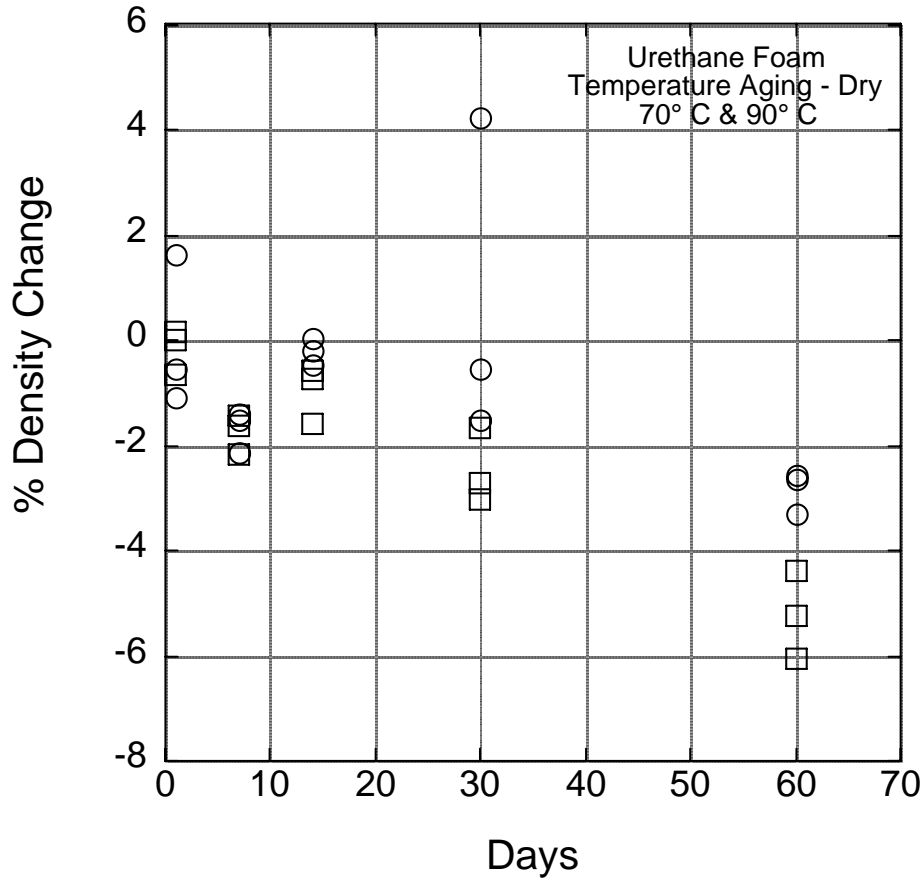


FIGURE 4.2 Density variation with high-temperature dry aging at 70°C (158°F) (circles) and 90°C (194°F) (squares)

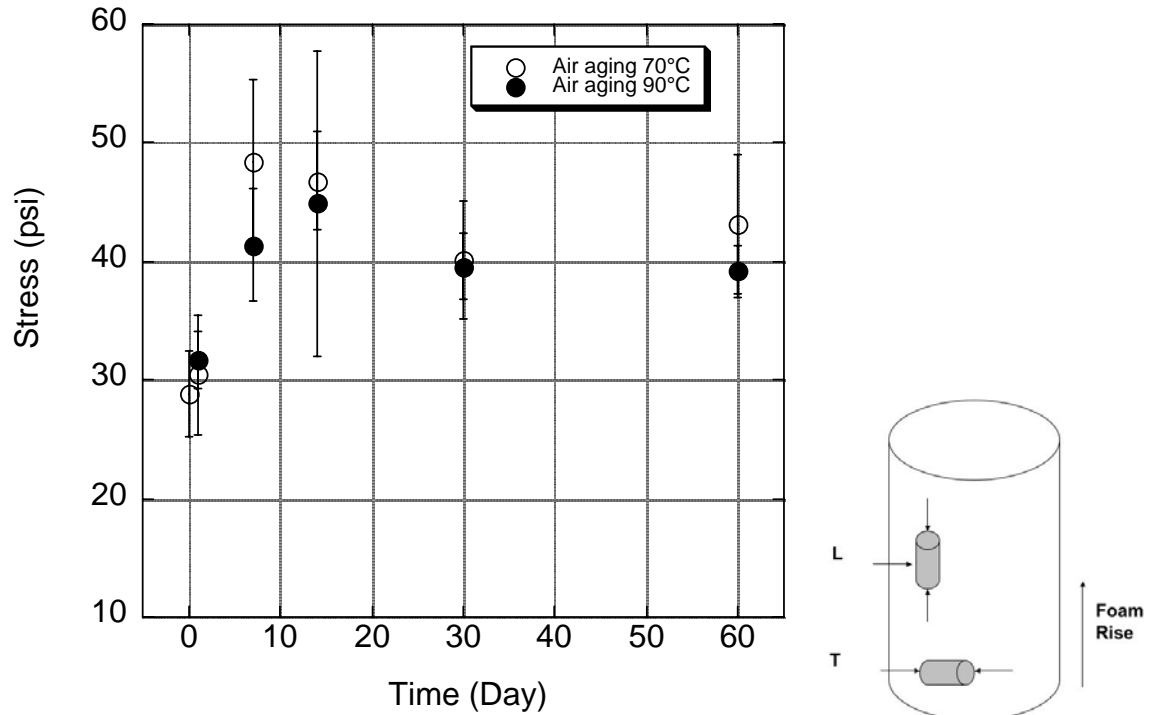


FIGURE 4.3 Compressive strength of urethane foam (transverse direction) aged at 70°C (158°F) and 90°C (194°F) in air

4.2 EFFECT OF WATER IMMERSION ON STRUCTURAL INTEGRITY OF URETHANE FOAM

Effect of water on the structural integrity of urethane foam was determined as a function of temperature and time by following procedures similar to those in ASTM D 870-02 (Standard Practice for Testing Water Resistance of Coatings Using Water Immersion). Compressive strength samples (transverse-machined) were placed in deionized water at 23°C (73°F), 70°C ± 2°C (158°F), and 90°C ± 2°C (194°F). Figure 4.4 shows the containers in which the samples were placed. Samples were exposed at the above conditions for 24 hours, 1 week, 2 weeks, 30 days, and 60 days. At the conclusion of each exposure, three samples were tested under ambient laboratory condition (23°C, 50% RH) after drying of samples in a vacuum drying oven. Before the mechanical tests, samples were conditioned at the laboratory ambient condition for at least 24 h. Dimensional, weight, density, and appearance changes were recorded and are provided in Appendix 4.

Density changes were most significant for the samples exposed to 90°C (194°F), as shown in Fig. 4.5. The density of urethane foam was found to reduce significantly (by 5-15%) within the first few weeks and thereafter did not change. For the 23°C (73°F) and 70°C (158°F) exposures, the density reduction was much less than that of the 90°C exposure.



FIGURE 4.4 Samples for room-temperature water immersion test

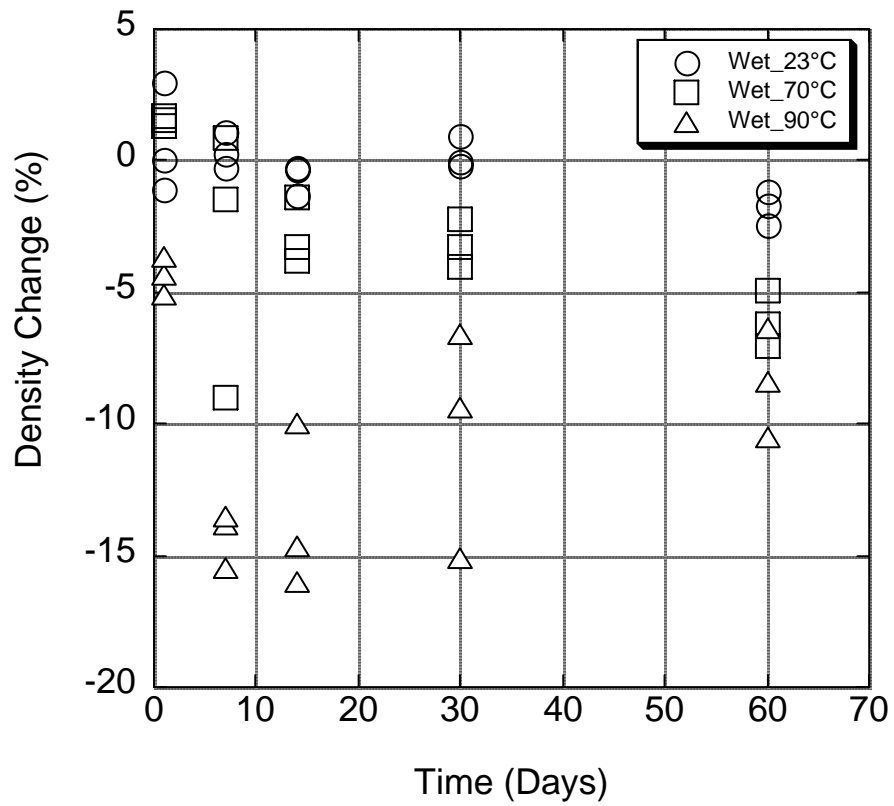


FIGURE 4.5 Density variation with wet aging at various temperatures

Figure 4.6 shows the compressive strength of the urethane foam measured after wet aging for various intervals at room temperature, 70°C (158°F), and 90°C (194°F). As observed for dry aging, the compressive strength initially increased. For longer exposures, strength did not degrade. For the 60-day exposure in water at 70°C (158°F) and 90°C (194°F), the compressive strength was about 30 psi, which is similar to that for as-received urethane foam in the transverse direction. Thus, no noticeable degradation occurred over the 60-day exposure of urethane foam in water. Tests at 70°C and 90°C were continued for 90 days, and the results were similar to those of the 60-day tests (attached in Appendix 4).

As a result of the long-term water exposure, the urethane foam samples exhibited some change in color, as shown in Fig. 4.7. This discoloration was quite apparent for the 90°C (194°F) samples. The color change appears to be due to interaction between water and polymer [4].

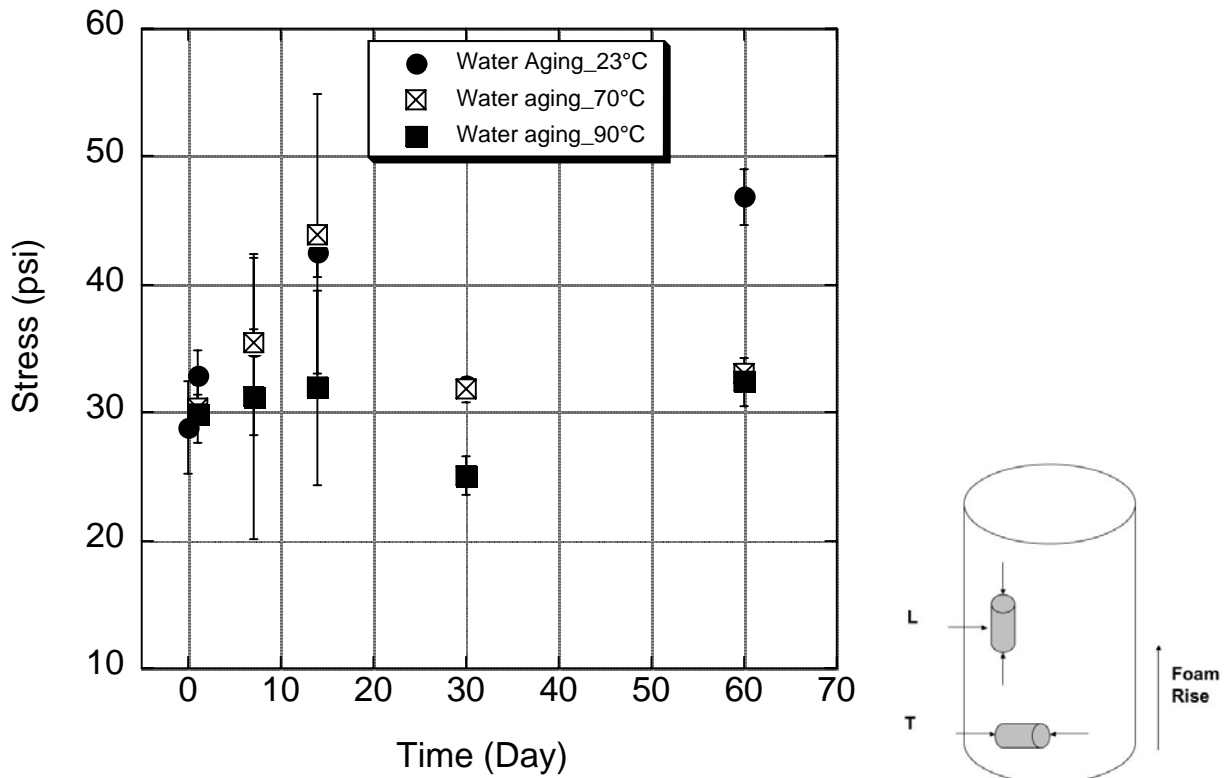


FIGURE 4.6 Compressive strength of urethane foam (transverse direction) aged at 70°C (158°F) and 90°C (194°F) in air



FIGURE 4.7 Wet aging samples after 60-day exposure. Samples at 90°C (194°F) showed change in color (foreground) compared to 23°C (73°F) and 70°C (158°F) samples (background)

To summarize the elevated-temperature aging tests,

- The urethane foam compressive strength does not appear to degrade in air or water.
- The reduction in the density of the post-water-aged samples was primarily due to dimensional changes; however, the compressive strengths were as high as those of the as-received material.
- These aging tests indicated that temperature does not accelerate the aging of urethane foam as determined by compressive strength measurements.

5 EFFECT OF THERMAL CYCLING ON STRUCTURAL INTEGRITY OF URETHANE FOAM

The purpose of this test was to gain insight into how the urethane material responds to thermal excursions. This test was conducted to assess urethane foam material's response to the thermal cycling that it may encounter prior to burial. However, this test is not intended to provide a quantitative measure of the service life. Freeze-thaw cycling tests were conducted on the urethane foam samples between $-5^{\circ}\text{C} \pm 3^{\circ}\text{C}$ (23°F) and $50^{\circ}\text{C} \pm 3^{\circ}\text{C}$ (122°F) for 30 cycles in air. Hold times were 16 h at -5°C (23°F) and 8 h at 50°C (122°F). Ramping between the temperatures was within 2 h. Both wet and dry test protocols were employed per ASTM D 6944-03 (Standard Test Method for Resistance of Cured Coatings to Thermal Cycling). Five samples (2.3 in. dia. \times 2.3 in. long) were tested for compressive strength in a freeze-thaw temperature cycling chamber. All the test samples were transverse machined. After exposure, dimensional, weight, density, and appearance changes were recorded. Compressive strength tests were performed and compared with the baseline data to determine any degradation.

Figure 5.1(a) shows the ESPEC Model ECT-2 thermal cycling chamber that was used for freeze-thaw cycling. Figure 5.1(b) shows the interior of the chamber with samples. For wet thermal cycling, five samples were soaked in water and placed in a plastic bag to retain the moisture in the sample. At the freezing temperature, a thin coating of ice formed on the samples placed in the bag. For dry cycling, five samples were kept open in the chamber environment.

Figure 5.2 shows the variation in density of five urethane foam samples prior to the tests compared to dry freeze-thaw cycling after 30 days. Within the standard deviation, the densities are the same before and after dry thermal cycling.

Figure 5.3 shows the compressive strength plots of the urethane foam after 30 days of dry freeze-thaw cycling. The average strength for the five samples tested was 35.9 ± 7.4 psi. These values are quite similar to the as-received transverse compressive strength of the foam of 31 psi, as shown in Fig. 2.8. Thus, dry freeze-thaw cycling between -5°C and 50°C (23°F - 122°F) for 30 cycles does not degrade the compressive strength of the urethane foam material.

Figure 5.4 shows the density change after the wet thermal cycling. Again, based on the standard deviation, the density did not change after 30 days of wet thermal cycling. Figure 5.5 shows the compressive strength plots of the urethane foam after 30 days of wet thermal cycling. The average strength for the five samples was 35.6 ± 3.3 psi, which is quite similar to the as-received transverse compressive strength of the foam of 31 psi, as shown in Fig. 2.8, and to the dry thermal cycling results, as shown in Fig. 5.3. Thus, wet freeze-thaw cycling between -5°C and 50°C (23 - 122°F) for 30 cycles does not degrade the compressive strength of the urethane foam material.



(a)



(b)

FIGURE 5.1 (a) Freeze-thaw cycling chamber and (b) Interior of the chamber

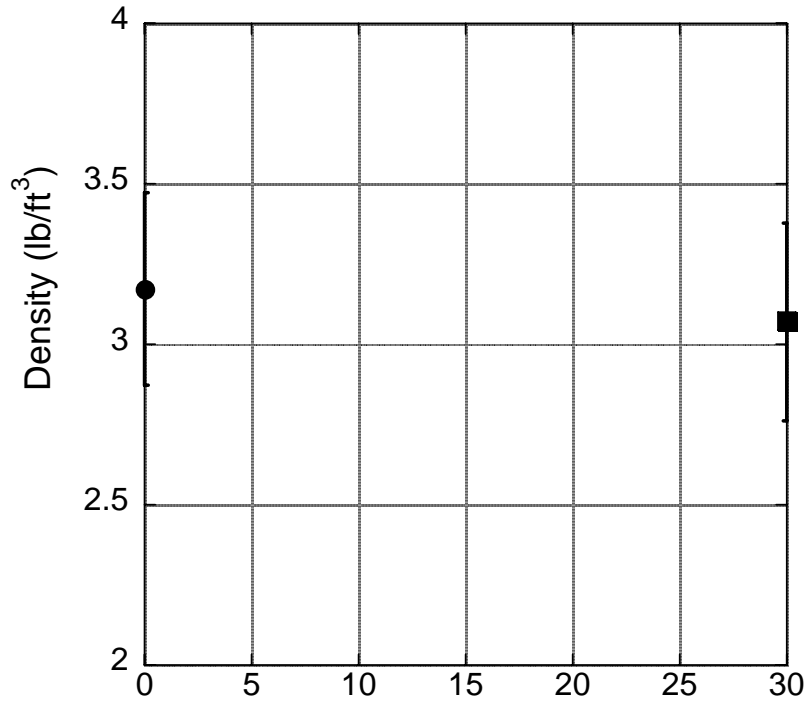


FIGURE 5.2 Change in urethane foam density during dry freeze-thaw cycling

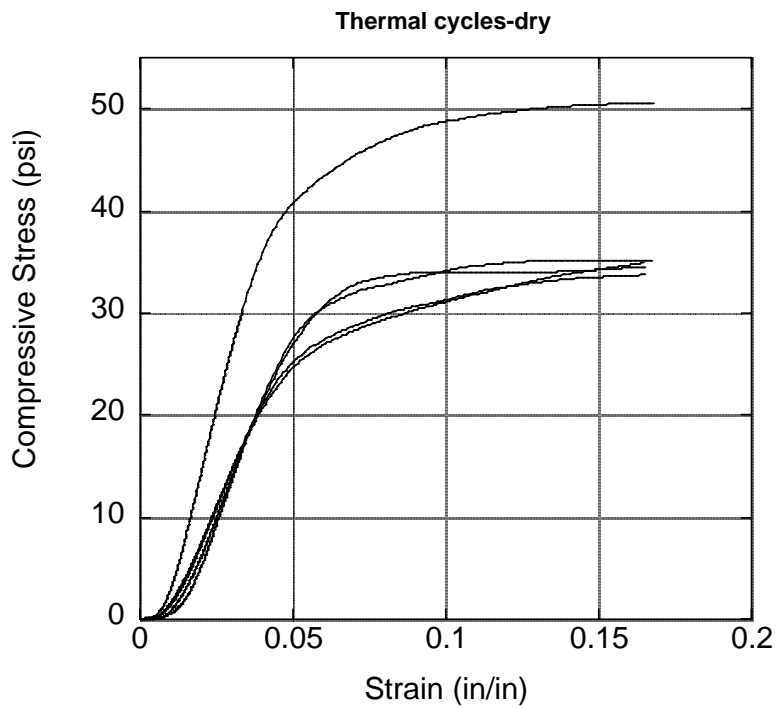


FIGURE 5.3 Compression stress-strain curves for five urethane foam samples after dry freeze-thaw cycling

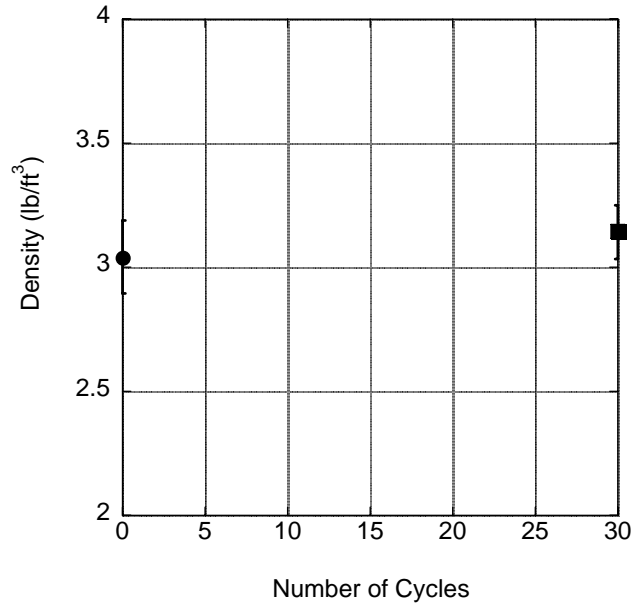


FIGURE 5.4 Change in urethane foam density during wet freeze-thaw cycling

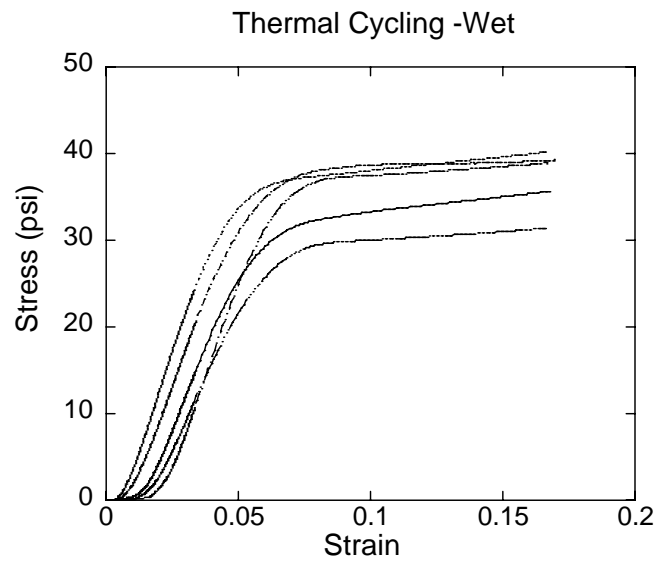


FIGURE 5.5 Compression stress-strain curves for five urethane foam samples after wet freeze-thaw cycling

6 COMPRESSION PROPERTIES OF URETHANE FOAM

The last of the engineering properties of the foam to be investigated was confined compression. Since the foam will be confined in the landfill and the major principal load will be applied vertically, a consolidometer test was run to investigate the vertical compressive properties of a laterally confined sample. For this testing, a consolidometer device borrowed from geotechnical testing was used. Samples were tested by the standard method given in ASTM D-2435 (“Standard Test Methods for One-Dimensional Consolidation Properties of Soils Using Incremental Loading”), adjusted to investigate the properties of the foam under compressive loads.

Foam samples were cut to fit inside the confining ring (2.5-in. dia, 1-in. high), pore stones were placed on the upper and lower surfaces, and the foam sample was set in a dry state into the consolidometer. A typical machine setup and sample are shown in Fig. 6.1. Samples were loaded by pneumatic piston, and recordings of deflection (strain) with time were made for various applied stresses. The increments of time and loading typically used for soils were not rigorously followed, as the behavior of the foam is not related to the drainage rate of the sample.

Foam samples with density of approximately 3.1 pcf were tested initially. The tests were run on 3.1-pcf foam at load increments of about 15 psi (1.1 tsf), with readings of deflection recorded at increments of time until no further change in deflection was observed (as shown in Fig. 6.2) in a reasonable period of time (few hours). For each load increment, a stress-strain plot was then created by plotting the strain at the last reading for that load vs. the applied load. The raw data are presented in Appendix 5. As can be seen in Fig. 6.3(a) and (b), the foam generally showed resistance to strain under light loads, crushed under moderate loads, and ceased to strain appreciably more under successively higher loads. The maximum strain obtained on any sample was about 60% strain. Comparison of Figs. 6.3(a) and 6.3(b) indicates a degree of anisotropy – the longitudinal-oriented samples were always more resistant to crushing than the transverse-oriented samples.

Results from the 3.1 pcf foam showed higher compression than desired for use by the project (as indicated by BJC). Under the maximum EMWMF load of 75 psi, the measured strain was on the order of 50 to 60%. Owing to the failure of the foam to support the higher loads, we did not subject this foam to creep testing.

Because the foam failed to support the potential overburden loads for the landfill, BJC decided to add other more-dense foams to the study. They anticipated that more-dense foams should provide higher unconfined strength and greater resistance to crushing under the axial compressive loading. However, the other properties investigated for the 3.1-pcf foam (as described above) are judged to be appropriate, if the higher density foam has the identical chemical makeup as the 3.1-pcf foam.



(a)



(b)

FIGURE 6.1 (a) Consolidometer set-up and (b) foam sample in rigid ring

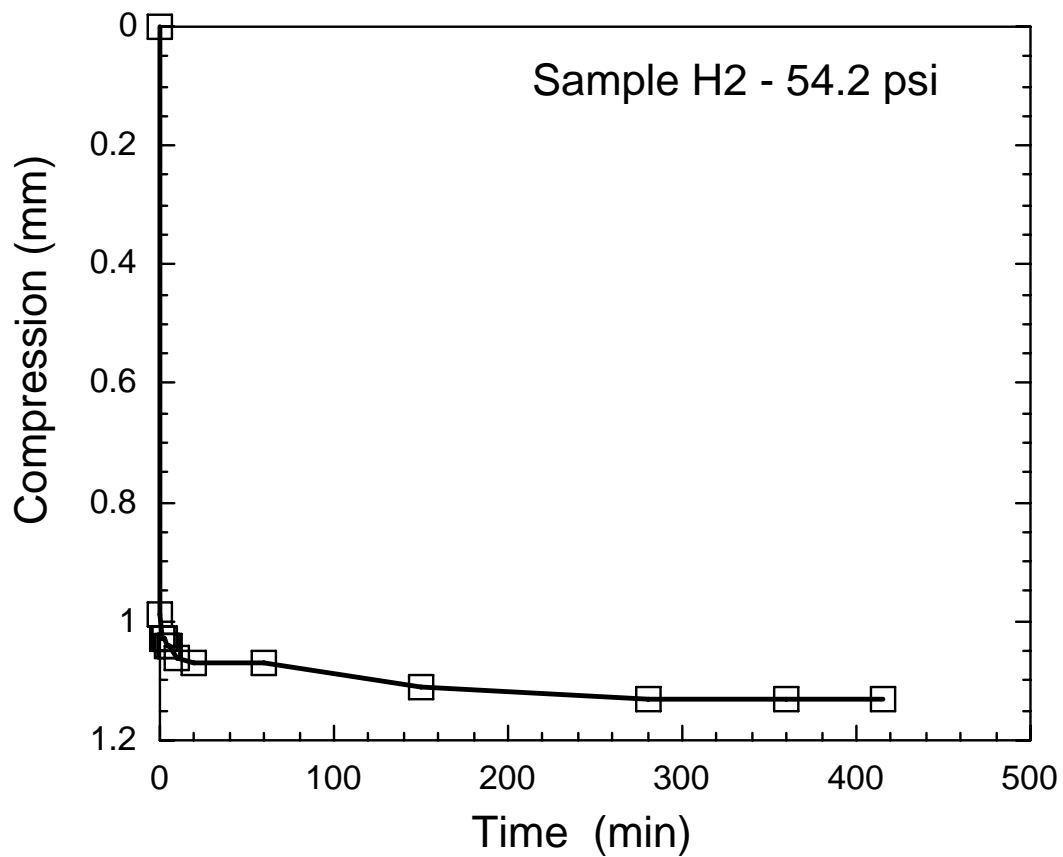
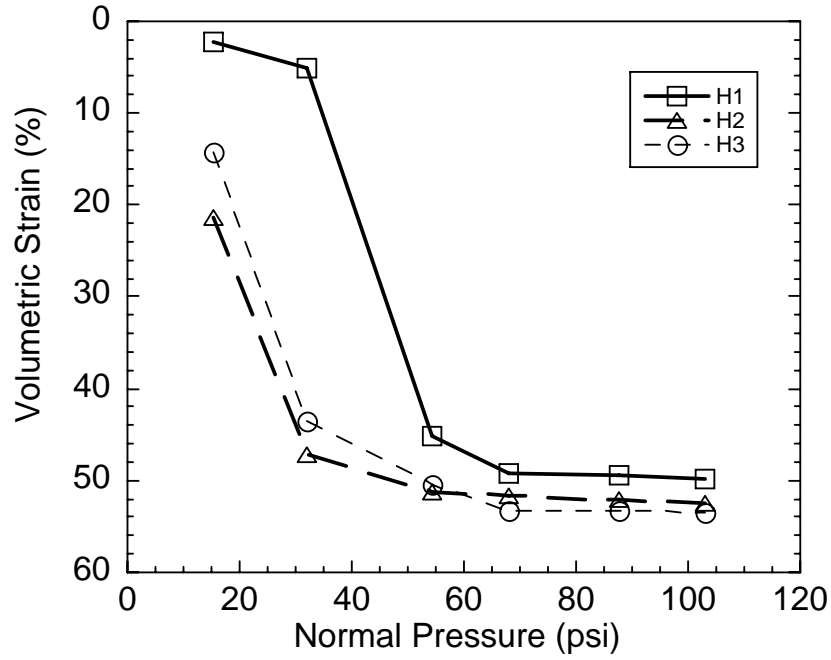
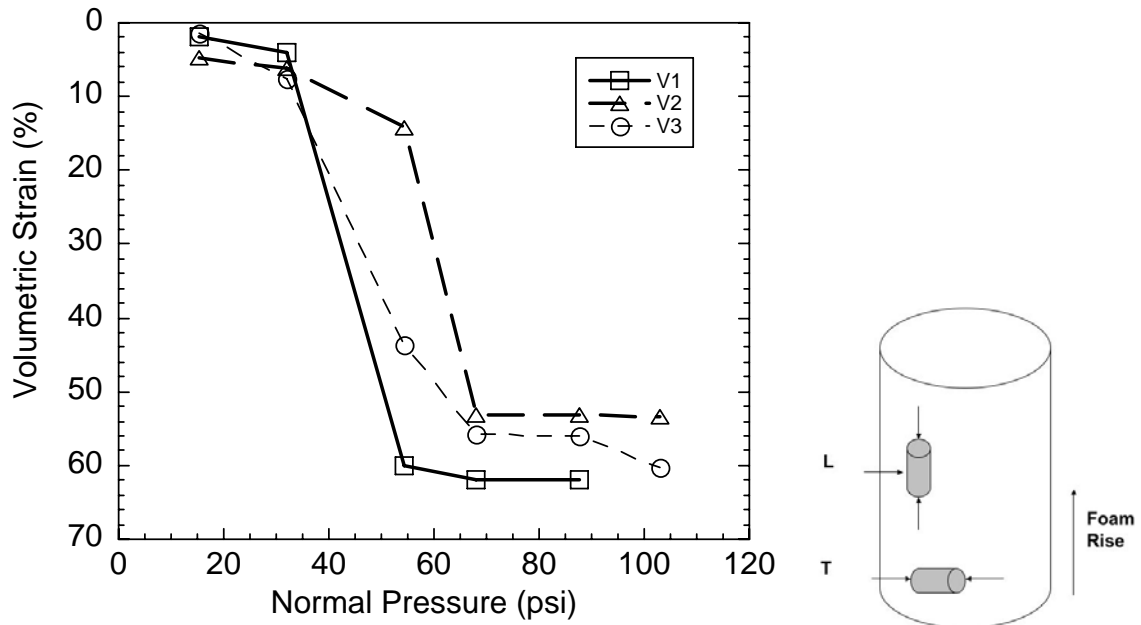


FIGURE 6.2 Typical compression vs. time plots obtained during a consolidation test at fixed applied stress



(a)



(b)

FIGURE 6.3 Consolidation behavior (volumetric strain) of urethane foam in (a) transverse and (b) longitudinal directions

7 COMPRESSION BEHAVIOR OF HIGHER DENSITY FOAMS

The 3.1-pcf foam showed acceptable performance for long-term burial in the EMWMF landfill, except for compression resistance. BJC recognized this deficiency and decided that Argonne should investigate denser foam materials. Four new batches of foams were fabricated by NCFI and shipped to ANL. As before, the foam samples were cylindrical (about 8-in. dia and 4-ft length). These foams had the following designations as provided by NCFI:

- A: 63-122 (approx. density of 5 pcf)
- B: 63-35 (approx density of 7 pcf)
- C: 63-122 (approx. density of 5 pcf)
- D: 65-34-2 (same reactivity profile as current 21-011, approx. density of 4 pcf)

NCFI indicated that the above four foams were fabricated by mixing of two components: resin and polymeric isocyanate in a ratio of 1:1 by volume [5]. According to NCFI, higher density foams were fabricated by changing the proportion of the blowing agent, which in above foams was water. Other ingredients such as catalyst and surfactants were same. In addition, NCFI indicated that the compositional makeup of the higher density foams was same as the low density (3.1 pcf) originally supplied [5]. Per NCFI, difference between foams A and C was in the amount of catalyst added and it was minimal (on the order of a fraction of a percent).

7.1 BASELINE CHARACTERIZATION

The four new foam samples were reported to have higher density as compared to the one (3.1 pcf) used for the aging studies as discussed previously. Nevertheless, baseline characterization for density and compression was conducted on all four foams. In addition, for compressive strength, tests were conducted in the transverse (T) and longitudinal (L) directions in accord with the ASTM 1621 standard. Figure 7.1 shows the compressive strength of the four foams (designated A-D). Clearly, these foams have significantly higher strength than the original foam. Foam B was the best performer in both the transverse and longitudinal directions. The average compressive strengths of foam B in the longitudinal and transverse directions were 193 ± 7.4 psi and 116 ± 3 psi, respectively. Appendix 6 contains the raw data.

Figure 7.2 shows the compressive strength as a function density for foams A-D. Bars indicate the standard deviation. As expected, the compressive strength for all the foams depends on the density and increases with increasing density. Anisotropy is evident in the density data. Also, for the four foams, the measured density values were slightly lower than those designated by the foam manufacturer, NCFI.

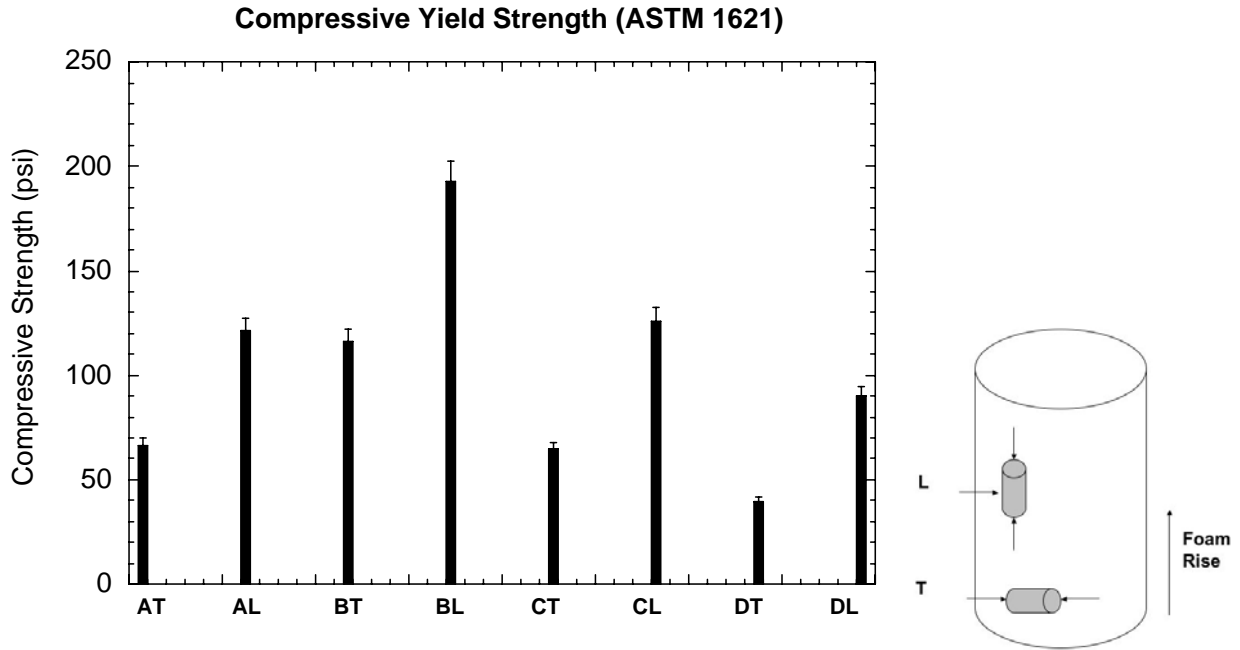


FIGURE 7.1 Compressive strength of foams tested for consolidation behavior

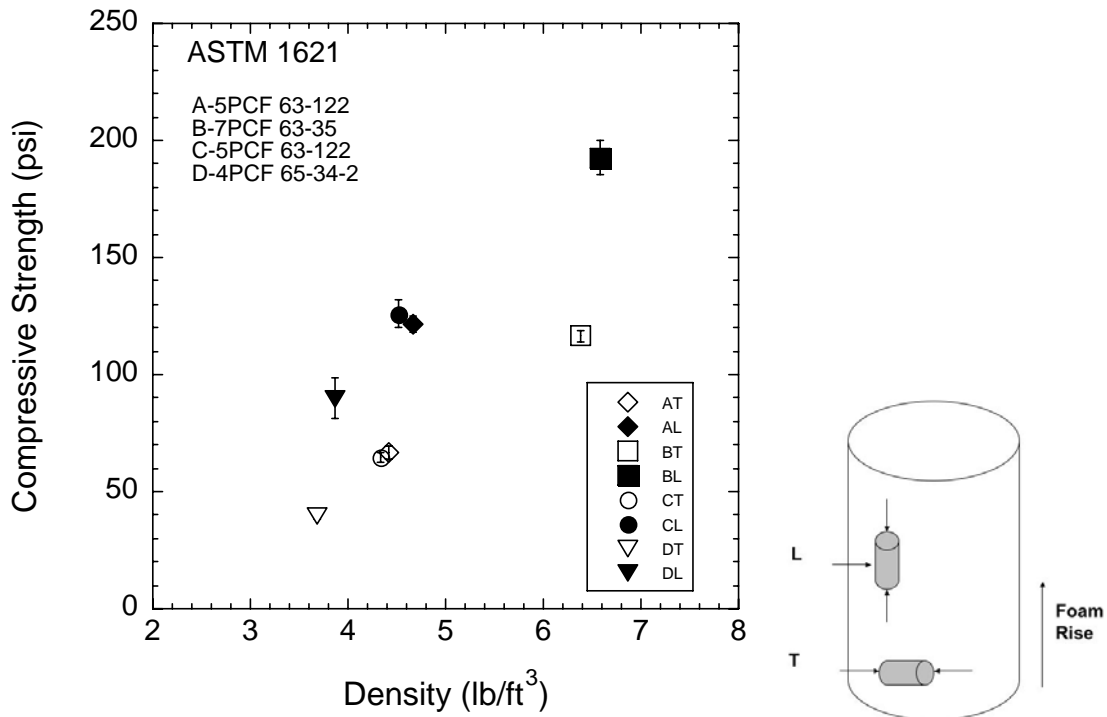


FIGURE 7.2 Compressive strength vs. density behavior of foams tested for consolidation behavior

7.2 COMPRESSION TESTING OF HIGHER DENSITY FOAMS

ASTM Standard D 2435-03 (Standard Test Method for One-Dimensional Consolidation Properties of Soils Using Incremental Loading) was followed for determining the compression characteristics of the higher density foams. In these tests, the samples were prepared and set up in the consolidometer as described before, and the deflection (or strain) was measured under a fixed stress after either (a) 30 min, followed by application of the next higher stress, or (b) 3 to 6 h, followed by application of the next higher stress. The compression (deflection) of the sample at different time periods was then recorded. This procedure was continued until no additional consolidation was observed at a particular stress in a several hour period. Data were represented as a function of strain and applied stress. Each of the four foams was tested in the transverse (T) and longitudinal (L) orientations. All of the samples were tested under dry laboratory conditions.

The stress-strain results for foams A-D are shown in Figs. 7.3(a-d). Initially, as normal stress increased, volumetric strain increased, but after a critical normal stress, a drastic change occurred in the volumetric strain. This behavior was observed with both the longitudinal- and transverse-cut samples. The large increase in volumetric strain could be due to the crushing of the foam cells. In general, for all the foams investigated, longitudinal-cut samples performed better (less consolidation) as compared to the transverse-cut samples. These results indicate that for many samples, the longer hold times at a particular stress decrease the stress under which initial crushing of the foam occurs.

In Figs. 7.3(a-d), the lines with arrowheads indicate 10% strain and 75 psi (5.4 tsf) stress, the allowable strain under the maximum EMWFM design load for the foam [6]. This stress corresponds to a maximum disposal depth of 90 ft based on a soil density of 120 pcf. Based on this preliminary screening and guidance from BJC, it was decided that foams C and D did not meet the criteria and were dropped from further investigation.

7.3 CREEP TESTING

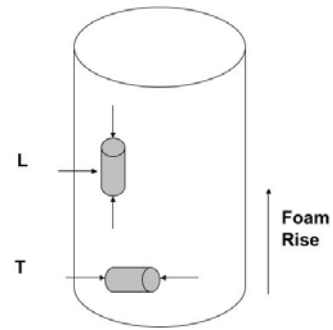
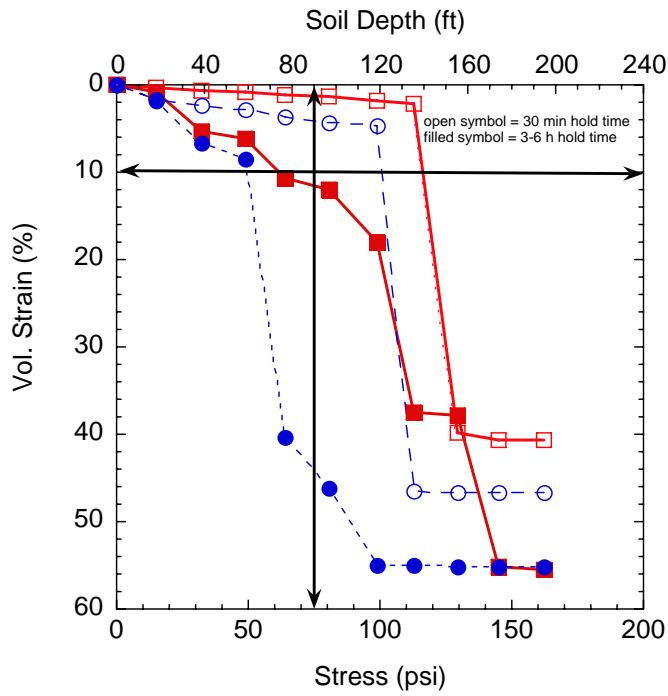
Because the foams are gas-filled cells, their long-term performance under load is of concern. Literature data on Confor polyurethane foam indicate that its creep behavior depends on the applied stresses [7]. At moderate stresses, the creep behavior shows an initial collapse of cells at 10% and then densification resulting in a strain of 60%. The creep process in Confor urethane foam has been related to the inhomogeneous distribution of strains at the localized foam cell level [7].

The curves in Fig. 7.3 show that the compressive behavior of the foams is time dependent. With longer hold times, at a particular stress, the crushing stresses or failure stresses decrease.

To establish the time-dependent compression (or creep) behavior, foams A and B were subjected to confined compression tests (as described above) in which a fixed stress was applied, and their deformation/strain was monitored as a function of time. Tests were conducted on

A - 5PCF 63-122
 Slowed Reactivity 50% cream/100% rise

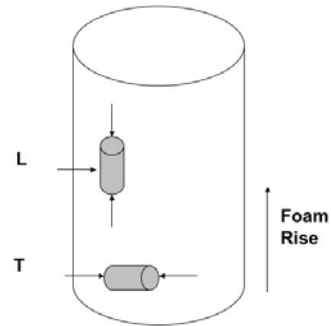
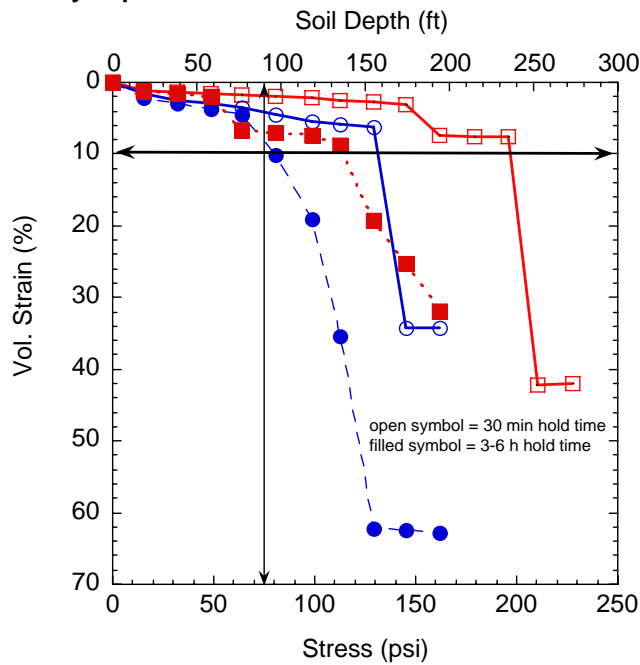
square = longitudinal cut
 circle = transverse cut



(a)

B - 7PCF 63-35
 Density in place

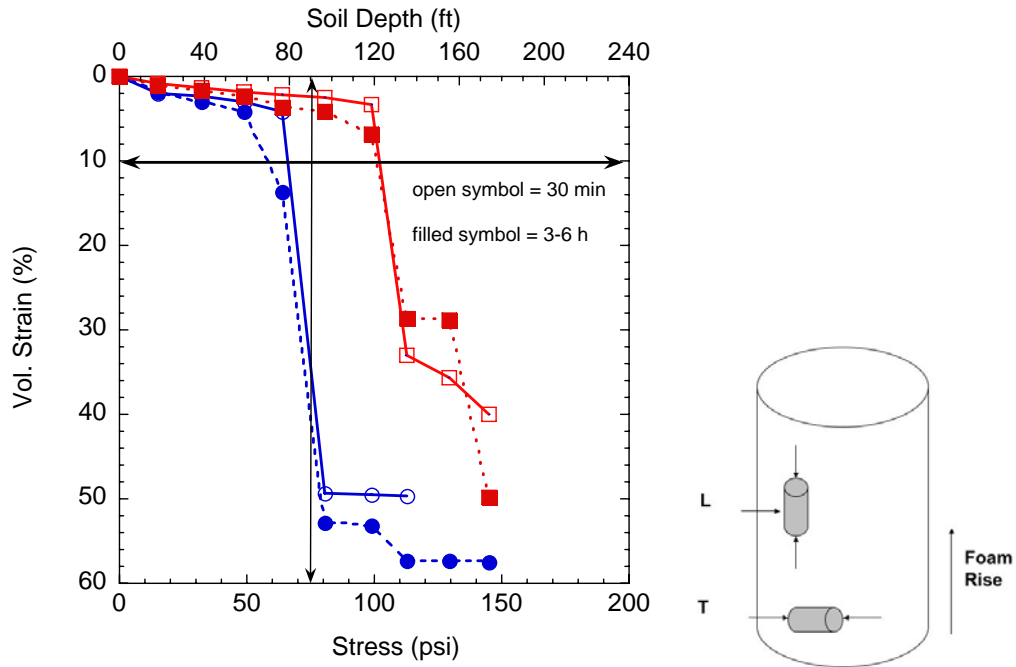
square = longitudinal cut
 circle = transverse cut



(b)

C - 5 PCF density in place
 formula 63-122
 same reactivity profile as current 21-011

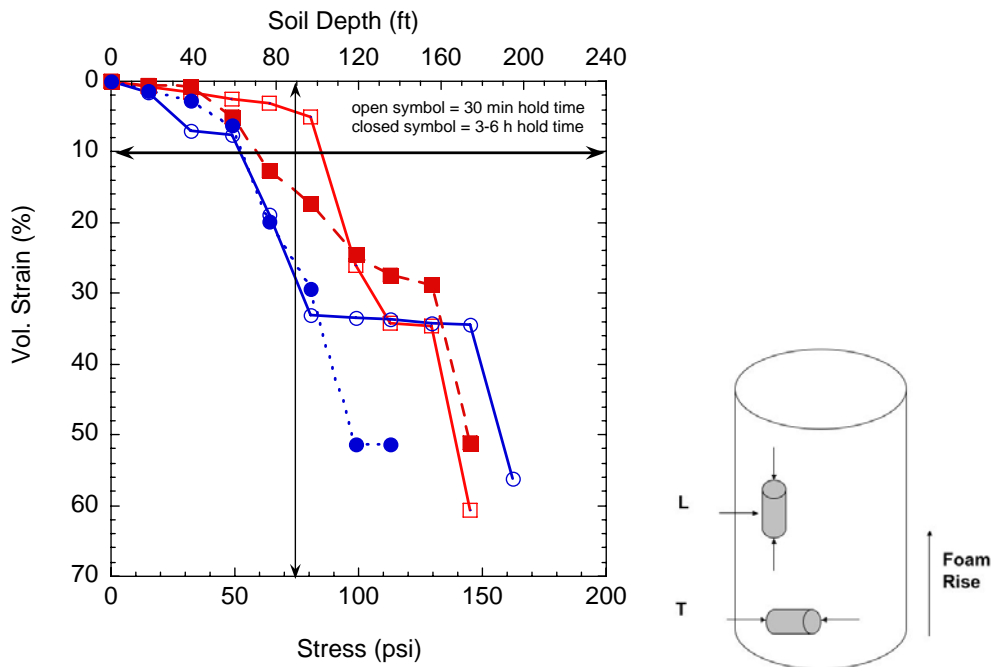
square = longitudinal cut
 circle = transverse cut



(c)

D - Approx 4PCF density in place
 Formula 65-34-2

square = longitudinal cut
 circle = transverse cut



(d)

FIGURE 7.3 Compression behaviors (volumetric strain) of urethane foams A, B, C, and D as a function of applied stress and hold times

samples machined in the transverse and longitudinal directions for the two foams. Because of the ORR application of the foam, only confined compressive properties were evaluated.

Two stresses were investigated for foams A (4.6 pcf) and B (6.6 pcf): 75 psi (5.4 tsf), comparable to 90 ft of overburden, representing the deepest possible burial in the landfill, and 64 psi (4.6 tsf), or 15 % less.

The 64 psi (4.6 tsf) tests were performed first. In these tests, the trimmed samples were set in the consolidometer as described above, and a single constant load was applied. Deflection (strain) was recorded at regular time increments, beginning at ½ min and doubling up to a day, after which daily increments were used. Figure 7.4 shows the strain as a function of time for foams A and B in their transverse and longitudinal directions. The tests were run until the load had been applied for about 400 h, or the foam crushed (as was the case for samples AT4 and AT5). Foam B performed significantly better in both directions. Raw data are presented in Appendix 6.

Based on the creep tests at 64 psi (4.6 tsf), only foam B samples were tested at 75 psi (5.4 tsf). These tests generally followed the methods from ASTM D-2990 (Standard Test Method for Tensile, Compressive, and Flexural Creep and Creep Rupture of Plastics) and guidance from BJC. It should be noted that this ASTM standard does not include foam materials and confined creep testing. Two samples from each orientation (samples BT5, BT6, BL5, and BL6) were tested for > 1000 h, with creep readings taken approximately daily. These samples were tested in a confined state.

Figure 7.5 shows the creep deformation of foam B in both directions, i.e., longitudinal and transverse. All the samples had a large initial deformation (3-6%). Subsequently, the deformation rate decreased. Samples BT5 and BL5 were tested for 1800-2000 h, and the cumulative strains for longitudinal and transverse directions were approximately 4.2% and 6.2%, respectively. For samples BT6 and BL6, tests were run for >1800 h, and the cumulative strains for longitudinal and transverse orientations were 6.2% and 7.8%, respectively. The differences in the two data sets reflect sample-to-sample variability. Furthermore, in both cases, transverse-cut samples deformed more than the longitudinal-cut samples. It appears that Foam B satisfies BJC's requirement of <10% strain over a 1000-h test [6]. Understanding the creep behavior, underlying mechanisms, and long-term creep prediction were beyond the scope of this study.

In summary, foam B (6.6 pcf) appears to satisfy the compressive characteristics required for EMWMF [6]. The foam deforms <10% at 75 psi for a hold time of at least 1800 h.

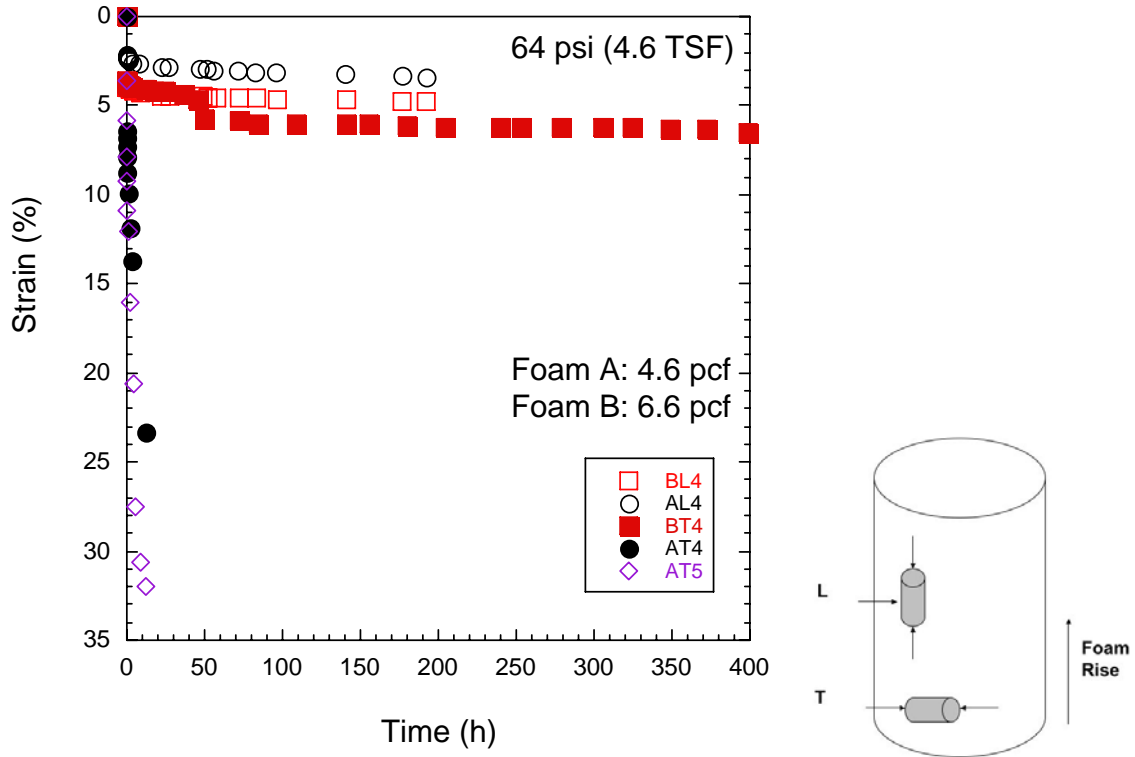


FIGURE 7.4 Compressive creep behaviors of foams A and B at a constant stress of 64 psi (4.6 tsf)

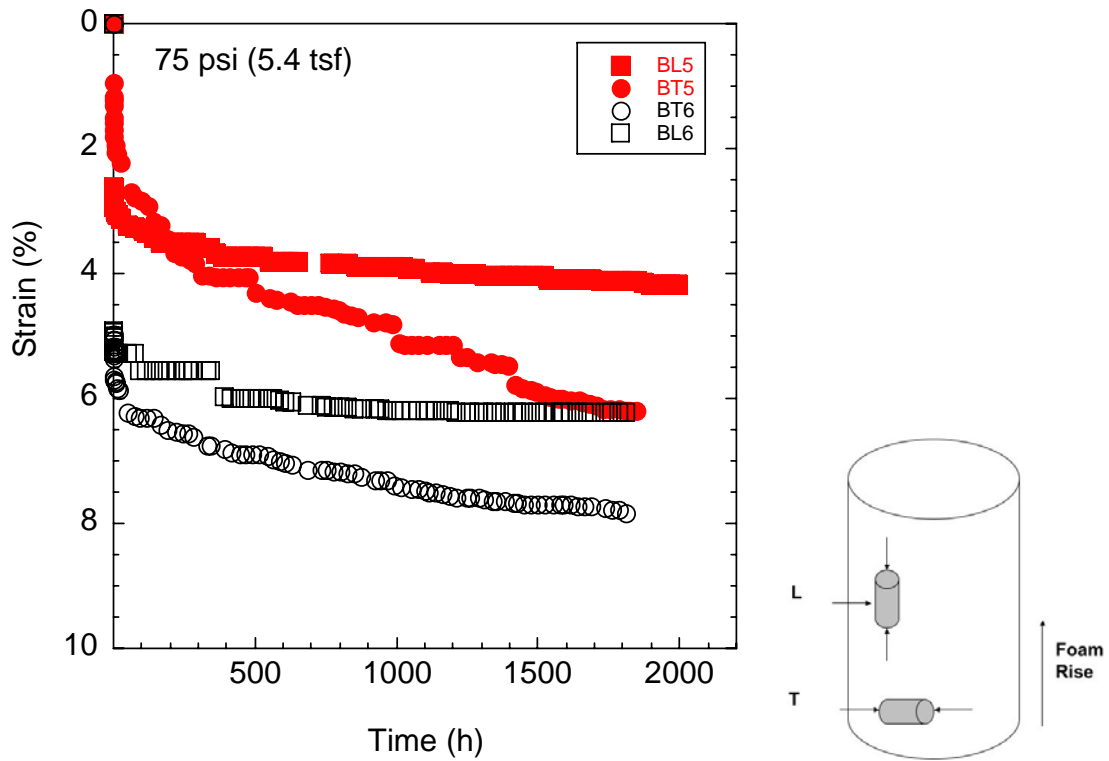


FIGURE 7.5 Consolidation of foam B (6.6 pcf) as a function of time at 75 psi (5.4 tsf)

8 BIODEGRADATION OF URETHANE FOAM

Polyurethane (PU) is widely used in many remediation applications, such as a physical barrier to prevent direct contact between hazardous compounds and the external environment. The resistance of the protective PU to microbial attacks is vital to prevent the release of hazardous compounds into the environment. Polyurethane damaged by microbial attacks can allow slow release of hazardous compounds to the environment (short-term release). If a significant portion of the PU is damaged by microbial attacks, the release of hazardous material into the environment could occur by diffusion (long-term release). The biodegradation of PU is due to utilization of PU as a carbon and/or nitrogen source by microorganisms. However, the fate and bioavailability of PU in the environment are not known very well. A better understanding of the bioavailability of PU is a key issue for the long-term integrity of the PU structure. On the other hand, assessing the environmental half-life of PU is difficult due to the need to measure many properties in the soil environment.

Furthermore, the lack of information on the environmental half-life of PU could limit its use in the remediation of polluted sites, such as those contaminated with radionuclides. Therefore, the environmental life of PU is a critical issue and needs to be investigated. Since PU is not a single, homogeneous material, the effects of chemical composition and physical properties on its degradation are very significant.

In this effort, the project team conducted laboratory experiments to determine the environmental half-life and biodegradation of PU in the laboratory. The main objectives were the following:

- Determine the bioavailability of PU as a carbon and/or nitrogen source under anaerobic conditions in batch, sequencing batch, and packed bed reactors using anaerobic inocula from soil and wastewater sludge.
- Determine the degree of PU deterioration by chemical and physical analysis and bioassays.
- In the event the PU samples used are bioavailable, determine the pseudo-first-order degradation rate constant of PU.

The research approach involved studying the following for PU biodegradation:

- Biodegradability of PU plugs (shake flask and continuous-flow reactor experiments): C source, N source, and C/N source.
- Change in the mechanical properties of PU plugs (tensile strength).
- Change in the weight of PU plugs.
- Change in the chemical structure of PU plugs (as determined by Fourier transform-infrared technique).

- Growth assay in the presence of PU plugs (bacterial count).
- Determination of degradation kinetics of PU.

8.1 LITERATURE REVIEW

The literature on PU biodegradation is limited and is often specific to the properties of the PU foam under consideration. This section presents a brief summary on PU biodegradation and its dependence on PU chemistry and structure. A more detailed review of the literature on PU structure, chemical composition, and degradation due to physical, chemical, and biological mechanisms is presented in Appendix 7. Polyurethanes are synthesized from three basic components: a diisocyanate, a polyglycol, and an extender, usually a low-molecular-weight diol, diamine, or water. Polyurethanes are produced using low-molecular-weight prepolymers, i.e., various block copolymers. The terminal hydroxyl group allows for alternating blocks, called “segments,” to be inserted into the PU chain. Blocks providing rigid crystalline phase and containing isocyanate and the chain extender are referred to as “hard segments.” Those yielding generally either a noncrystalline or low-crystallinity phase and containing polyester/polyether are called “soft segments.”

One of the factors that determine the properties of the polymer is the ratio of hard and soft segments. Generally, the hard segment contributes to hardness, tensile strength, impact resistance, stiffness, and modulus. The soft segment contributes to water absorption, elongation, elasticity, and softness. Modification of these segments might result in changes in the degree of tensile strength and elasticity. Hence, it is possible to produce versatile PU polymers whose properties can be easily modified by varying their molecular structures of soft segment and hard segment [8].

Physical, chemical, and/or biological degradation of PUs is possible. The chemical and physical degradation of polymers implies that microorganisms, macro-organisms, or enzymes are not present, and that the aging is totally dependent on physical, chemical, and/or mechanical influences. Microbial degradation can mainly be divided in two big blocks: the urethane bonds and the polyol segments because they are the major constituents of PU.

The first study of PU biodegradability was reported in 1966 by Ossefort and Testroet [9]. As soon as the properties of PUs are modified, the tensile strength and elasticity change, determining the accessibility to degrading enzyme systems [10,11]. It has been reported that polyester PUs are more biodegradable than polyether-type PUs [12]. However, comparing the different results given by each researcher is very difficult because the PU type and the microorganism type are different for each study. Many reports can be found on PU biodegradation in the laboratory under controlled conditions, especially on biodegradation of polyester PU by microorganisms (the main attention has been devoted to fungi) [13]. The literature results mostly come from lab studies, in many cases, providing additional nutrients to microorganisms. The successful cases of PU biodegradation suggest that it requires highly concentrated enzymes. No study has been published on the biodegradation of PU in the

environment. Yet, field studies are necessary in assessing the benefits and obstacles associated with the use of PU as insulator material for bioremediation applications in the environment.

8.2 MATERIALS AND METHODS

The PU bio-deterioration was assessed by bioavailability assay using batch shake flasks and soil reactors, as well as continuous-flow soil and sludge bioreactors. The microbial deterioration of PU was determined by measuring the physical properties (weight loss, tensile strength) of PU plugs before and after bioassays. Also determined was the chemical structure by Fourier transform infrared spectroscopy (FT-IR) and the growth of micro-organisms by microbial counts.

Material

The tested PU material was supplied by NCFI Polyurethanes Company (Mount Airy, NC). The chemical composition of the foam product can be summarized as follows (based on a fax report from the company):

- Polymeric MDI (50% by volume)
- Polyether polyol: 700 MW (molecular weight); 4,5 functional; propoxylated sucrose and glycerin (19% by volume)
- Polyester polyol: 350 MW; 2,2 functional; aromatic ester (10% by volume)
- Polyether polyol: 320 MW; 3 functional; propoxylated aromatic amine (7% by volume)

The remainder of the composition was made up of plasticizer, fire retardant, surfactant, catalysts, and blowing agents.

Preparation of PU Plugs

The solid blocks of PU were cut into dumb-bell-shaped plugs (4 in. × 1.4 in. × 0.7 in., or 10.2 cm × 3.5 cm × 1.8 cm) to increase the contact area with the microorganisms in the bioreactors. The PU plugs were pre-treated by washing once in ethanol and twice in distilled water. Then, the plugs were dried at 50°C (122°F) overnight to a constant weight after cooling under desiccation. This temperature was chosen to minimize the loss of volatile matter while drying of moisture.

Microbial Growth Media

The composition of the basal medium used is described by Nakajima-Kambe et al. [13], where glucose and/or ammonium nitrate are omitted when PU is supplied as a sole carbon and/or nitrogen source (Table 8.1), respectively.

Bioavailability Studies

A series of batch cultures was set up to screen the PU biodegradation ability of an anaerobic sludge inoculum and to monitor the degradation of PU. In batch growth assays, two plugs (4 in. × 1.4 in. × 0.7 in., or 10.2 cm × 3.5 cm × 1.8 cm) were placed in 1000 mL flasks containing 400 mL synthetic medium prepared according to the composition in Table 8.1 (~10 g per liter). Each shake flask was inoculated with 2.0 g of digester sludge from a local wastewater treatment plant. The sludge contained both hydrolytic and methanogenic microbial cultures maintained under anaerobic conditions. The PU bioavailability assay was performed in a defined basal medium in which PU and other alternative carbon and nitrogen compounds served as sources of carbon and/or nitrogen. Growth tests were performed under nine conditions as summarized below:

1. PU was sole source of carbon and nitrogen (ammonium nitrate and glucose omitted).
2. PU was sole source of carbon (an alternative nitrogen source, ammonium nitrate, was added; glucose omitted).
3. PU was sole source of nitrogen (an alternative carbon source, glucose-acetate, was added; ammonium nitrate omitted).
4. PU as well as added sources of carbon (glucose-succinate) and nitrogen (ammonium nitrate) was used.

TABLE 8.1 Composition of the basal medium (pH=7.2)

Component	Amount mg/L
KH ₂ PO ₄	2,000
K ₂ HPO ₄	7,000
NH ₄ NO ₃	1,000
Glucose	3,750
MgSO ₄ · 7 H ₂ O	100
ZnSO ₄ · 7 H ₂ O	1
CuSO ₄ · 7 H ₂ O	0.1
FeSO ₄ · 7 H ₂ O	10
MnSO ₄ · 7 H ₂ O	2

5. Only added nitrogen (ammonium nitrate) and carbon (glucose-succinate) sources were available (PU was not present) (positive control).
6. Nitrogen sources were not present, but alternative carbon (glucose-succinate) sources were added (negative control).
7. Carbon sources were not present, but alternative nitrogen (ammonium nitrate) sources were added (negative control).
8. Carbon and nitrogen sources were not present, but inoculum was present (negative control).
9. PU was the sole source of carbon and nitrogen, but no inoculum (negative control).

Flasks were purged for 5 min with 50 cm³/min of a 99.0% N₂ gas to remove dissolved oxygen and to maintain anaerobic conditions during the experiments. Before the analysis, flasks were initially connected to a trap system to relieve any excess gas pressure in the flasks and to trap off-gas. The flasks were shaken on a platform placed on a mechanical shaker. After the flasks were shaken for the required time, the cylindrical PU plugs were removed, and the flask contents were centrifuged for further analysis. The experiments were run for 2-6 weeks at room temperature (~25°C) with negative and positive controls.

Continuous Reactor Experiments

Two accelerated continuous-flow reactors were employed as follows:

1. A Sequencing Batch Reactor (SBR) was operated with suspended bacteria taken from an anaerobic digester using PU plugs as carbon and/or nitrogen source in the bioreactor.
2. An Upflow Packed Bed Reactor (UPBR) was operated with a bacterial suspension from the Oak Ridge (Tennessee) soil. The PU plugs served as packing material as well as carbon and/or nitrogen source.

The bioreactors were operated under anaerobic conditions and were allowed to develop anaerobic conditions before the addition of PU plugs by purging with N₂ gas. The bioreactors were made of two identical cylindrical flasks with a 2.5-L working volume and were operated under the same conditions. Thirteen PU plugs were placed in a wire basket inside each reactor. The SBR was operated with sequential 24-hour cycles at 2-day hydraulic retention time (HRT) and 30-day sludge retention time (SRT). The UPBR was operated in the same conditions with SBR, such as 2-day HRT and 30-day SRT. The basal medium used during the bioavailability studies was pumped through each of the reactors to maintain 2-day HRT.

Soil Burial Experiments

Soil burial experiments were conducted by placing the PU plugs buried in field soils in laboratory containers. Three sets of 10 replicate PU plugs were buried for 10 weeks in 4-in. (10-cm)-deep covered containers filled with the Oak Ridge (Tennessee) field soil to obtain statistically significant data. The dumb-bell-shape plugs were buried horizontally at a depth of 2 in. (5 cm) in soil to allow the development of anaerobic conditions to stimulate the environmental conditions in the field. Over the 10-week period, one plug was sacrificed each week to determine the extent of bio-deterioration from its physical and chemical properties.

Analysis

Physical examination of PU plugs can be considered an important criterion for investigating their bio-deterioration [11]. Physical changes in the structure of PU more likely occur before complete degradation of PU takes place. The degree of deterioration of a sampled PU plug each week was assessed by measuring changes in selected physical properties, including tensile strength and weight loss after appropriate sample cleaning procedures.

Weight Loss

PU degradation was monitored by measuring the weight of PU plugs before and after incubation in the soil containers. The PU plugs were taken out and washed with distilled water and ethanol to remove debris on the surface. Then, plugs were dried to constant weight overnight at 50°C (122°F) and weighed. The weight loss percentage was calculated as

$$\% \text{Weight loss} = \frac{m_o - m_t}{m_o} \times 100$$

where m_o is the initial weight of the plug, and m_t is the final weight of the plug after degradation.

Tensile Strength

Tensile strength is a measure of the force, generally given in pounds per square inch (psi), required to break the polymer plug. The tensile strength at the break point of a PU foam “dog-bone” plug was measured by ASTM D638 (Test Methods for Tensile Properties of Plastics, Philadelphia, Pennsylvania, pp. 401-404) using an Instron Universal Testing Instrument (Model 4465) at a crosshead speed of 0.1 in./min and a constant stressing rate of 100 lb_f/min. Other conditions included temperature of 23°C (73°F) and 50% relative humidity. The changes in tensile strength were determined from stress-strain curves. The sample size of the PU plug was 10.2 cm × 3.5 cm × 1.8 cm (4 in. × 1.4 in. × 0.7 in.) following ASTM guidelines. The average tensile strength values and standard deviation of untreated PU plugs for statistical purposes are

given in Table 8.2. The standard error is approximately 12% because of the heterogeneous physical structure of untreated PU plugs.

FT-IR Analysis

Before and after treatment, each PU foam plug was analyzed by Fourier transform infrared spectroscopy (Nexus FT-IR) equipped with a DTGS KBr detector (Thermo Nicolet, Madison, WI). Infrared spectra were collected every 1 mm along a diameter over the PU surface with a resolution of 4 cm^{-1} [14]. The FT-IR spectra were recorded over a range from 4000 cm^{-1} to 400 cm^{-1} . Of particular interest were the ranges of $3600\text{ to }2600\text{ cm}^{-1}$ and $1800\text{ to }700\text{ cm}^{-1}$, where the major absorption bands of PU are assigned [15]. The FT-IR spectrum of the PU plugs was determined before and after each treatment.

Growth Assay

The total number of anaerobic bacteria in the sample that have the ability to degrade and deteriorate PU plugs was determined by the Acridine Orange Direct Count (AODC) method [16] and expressed as number of cells per milliliter. Two milliliters of sample taken from the collected sample was stained with 0.2 mL of 0.1 % acridine orange. The stained bacterial mixture was incubated at room temperature for 1 or 2 min. Then, a treated filter paper (Osmonics, Polycarbonate Black 0.22-micron filter) was placed in a vacuum filter funnel, and the sample was filtered to obtain a better distribution of colonies on the filter paper. Next, the damp filter was placed on a glass microscope slide ($2\text{ cm} \times 5\text{ cm}$, $0.8\text{ in.} \times 2.0\text{ in.}$) for analysis. The number of bacteria per millimeter area was estimated from a count of at least 5-6 randomly chosen microscope fields. The results were expressed as number per milliliter.

TABLE 8.2 Tensile strength of untreated PU plugs

Sample	Size (in × in)	Load (lb _f)	Tensile Strength (psi)
1	0.495	11.10	36.68
	0.610		
2	0.495	9.60	38.87
	0.590		
3	0.490	11.74	40.19
	0.620		
4	0.505	13.66	41.68
	0.652		
5	0.495	10.04	32.68
	0.620		
		Average	38.02
		Std. dev.	3.54

8.3 RESULTS AND DISCUSSION

The ability of microorganisms to use PU as the sole carbon and energy source and/or the nitrogen source was investigated during the bioavailability studies. Sample taken from an anaerobic sludge digester treating municipal waste was used as inoculum during the experiments. Anaerobic sludge is a complex biological environment in which microbial diversity is high and can show potential degradation of PU under anaerobic conditions, if it is possible. Soil burial experiments were designed to investigate the degradation of PU in the Tennessee soil, where PU foam will be used to contain hazardous materials to be placed in dedicated landfills. Additionally, in this research, two different continuous-flow reactor systems were studied to determine the potential biodegradation of PU and the degradation rate constant if the PU is biodegradable using anaerobic sludge and field soil inocula in the laboratory. An UPBR and SBR were used to simulate accelerated biodegradation of PU in harsh environments and, hence, to estimate the long-term integrity of the material by using short-term experimental results. Experimental protocols followed ASTM D 5247-92 (Standard Test Method for Determining the Aerobic Biodegradability of Degradable Plastics by Specific Microorganisms), ASTM D5509-96 (Standard Practice for Exposing Plastics to a Simulated Compost Environment) and ASTM D5338-98 (Standard Test Method for Determining Aerobic Biodegradation of Plastics Materials under Controlled Composting Conditions).

Test Material

Since the PU-producing company did not give the exact chemical composition of the PU on a mass basis for proprietary reasons, we could not precisely determine the hard and soft segment content of the tested PU material. However, based on the chemicals used for the synthesis (see Section 8.2), the PU foam can be considered as rigid. It is well known that the blend of polyisocyanates (MDI) and polyols of higher functionality polyethers and aromatic polyester results in high cross-link density [17] in the PU foams. This high crosslink density can play a significant role in PU foam resistance to microbial attacks because the degradation of PU occurs first in the soft segment, i.e., amorphous region [18].

Bioavailability Studies

The PU bioavailability assay was performed in a defined basal medium in which the PU and other alternative carbon and nitrogen compounds served as sources of carbon and/or nitrogen. Table 8.3 shows the weight losses with incubation time of treatment in the shake flasks. No weight loss was observed during the 2-6 week accelerated tests of bioavailability. Each data point in Table 8.3 is an average measurement of two PU plugs inserted in a flask. The weight loss of PU foam plugs ranged from 0.46 to 2.4%, which can be considered statistically negligible based on the weight loss of control samples during the experiments and also weight loss for untreated PU foams used for QA/QC experiments (see attachment after references in Appendix 7).

TABLE 8.3 Weight loss during bioassay experiments*

Two weeks of bioassay

Treatment	% Weight Loss
Control(Untreated)	0.74
PU(+)/ C-/ N-	2.40
PU(+)/ C-/ N+	1.21
PU(+)/ C+/ N-	1.15
PU(+)/ C+/ N+	1.23

Four weeks of bioassay

Treatment	% Weight Loss
Control(Untreated)	0.42
PU(+)/ C-/ N-	1.11
PU(+)/ C-/ N+	0.63
PU(+)/ C+/ N-	0.75
PU(+)/ C+/ N+	0.46

Six weeks of bioassay

Treatment	% Weight Loss
Control(Untreated)	0.61
PU(+)/ C-/ N-	0.78
PU(+)/ C-/ N+	0.90
PU(+)/ C+/ N-	1.22
PU(+)/ C+/ N+	1.10

*Notes: PU + or – indicates presence or absence of PU plug in the assay. C + or – indicates presence or absence of supplementary carbon. N + or – indicates presence or absence of supplementary nitrogen.

The tensile strength of the treated PU plugs at break was used as the quantitative criterion for deterioration by the microorganisms under anaerobic conditions [19]. Degradation was assessed quantitatively by measuring changes in tensile strength at failure of dumb-bell-shaped PU plugs prepared according to ASTM D 638. The tensile strength of the plugs (Table 8.4) used as carbon and/or nitrogen sources during the bioavailability studies was the same as the tensile strength of untreated plugs (Table 8.2) (95% confidence limits). From tensile strength analysis of PU plugs, we concluded that no deterioration occurred on the surface of the PU foams during these bioassays. These results are important because it has been reported that mechanical failure of PU occurred before the weight loss [19, 20]; this finding suggests that weight loss measurement alone is not a reliable means to assess PU bio-deterioration. Our study showed no bio-deterioration of the PU plugs based on measurements of both weight loss and tensile strength.

FT-IR spectroscopy was used to monitor changes on the surface of PU foams due to microbial deterioration (Fig 8.1). FT-IR analysis of the PU plugs showed no change in the chemical signature of the PU foams and, hence, no deterioration on the surface of the PU foams due to the biological activity in the bioassays. These findings are important because degradation of PU is initiated at the surface of the PU foam and then penetrates into its solid structure [21]; as a result, the PU foam studied is further confirmed to be not susceptible to bio-deterioration such as might occur in a landfill.

Figure 8.2 shows the growth assay (AODC method) of the anaerobic bacteria during the 4 and 6 weeks of bioassay, respectively, for various samples. The growth assay showed no significant growth of the bacteria in the polyurethane-supplemented medium compared to positive and negative controls. The obtained growth for each bioassay is < 10 for each tested condition. From Fig. 8.2, it can also be concluded that the increase in bacteria population during the 4-week bioassay ranged from 2.8 to 8.9 times the initial concentration and 5.3 times for the negative control, which contained only inoculum in distilled water. The bacterial population increase during the 6-week bioassay ranged from 1.3 to 4.5 times the initial concentration and 2.4 times for the negative control containing inoculum in distilled water. The growth in negative controls was attributed to the used inoculum taken from the anaerobic digester containing high levels of nutrients that allow continued bacterial growth in these flasks.

From these experiments it can be concluded that bacteria **did not use** PU foam as either a carbon or nitrogen source under anaerobic conditions. Hence, the PU foam used in this study is probably not biodegradable under anaerobic conditions.

Soil Burial Experiments

Three sets of 10 replicate PU plugs were buried for 10 weeks in containers containing the Oak Ridge soil (Tennessee) to gather statistically significant data. The dumb-bell-shape plugs were buried horizontally at a depth of 2 in. (5 cm) in the soil. Tensile strength and weight loss measurements, along with FT-IR analysis, were performed on test plugs that had been removed weekly.

TABLE 8.4 Tensile strength of treated plugs during bioassay experiments**After two weeks of bioassay**

Treatment	Load (lb _f)	Tensile Strength (psi)
Control(Untreated)	11.23 ± 1.60	38.02 ± 3.54
PU(+)/ C-/ N-	12.64	39.09
PU(+)/ C-/ N+	13.11	37.04
PU(+)/ C+/ N-	12.57	35.18
PU(+)/ C+/ N+	12.46	34.97

After four weeks of bioassay

Treatment	Load (lb _f)	Tensile Strength (psi)
Control(Untreated)	11.23 ± 1.60	38.02 ± 3.54
PU(+)/ C-/ N-	13.61	37.26
PU(+)/ C-/ N+	14.05	37.83
PU(+)/ C+/ N-	14.37	40.14
PU(+)/ C+/ N+	14.13	38.10

After six weeks of bioassay

Treatment	Load (lb _f)	Tensile Strength (psi)
Control(Untreated)	11.23±1.60	38.02±3.54
PU(+)/ C-/ N-	13.50	41.24
PU(+)/ C-/ N+	13.67	40.56
PU(+)/ C+/ N-	13.28	39.31
PU(+)/ C+/ N+	12.77	39.26

Table 8.5 shows the cumulative weight loss in the PU plugs during the soil burial experiments. Dry weight analysis of 10-week treated samples showed no statistically significant weight loss, an average of 0.25% and standard deviation of ±0.28% within the 95% confidence interval. The data in Table 8.5 also show no distinct trend in the weight loss of the plugs with time. Thus, PU plugs do not appear to be affected by the potential biological activity in the soil.

Tensile strength was measured weekly in the removed test plugs, and the results for the three runs are shown in Table 8.6. The changes in the tensile strength of the PU plugs are not statistically significant at the 95% confidence limit.

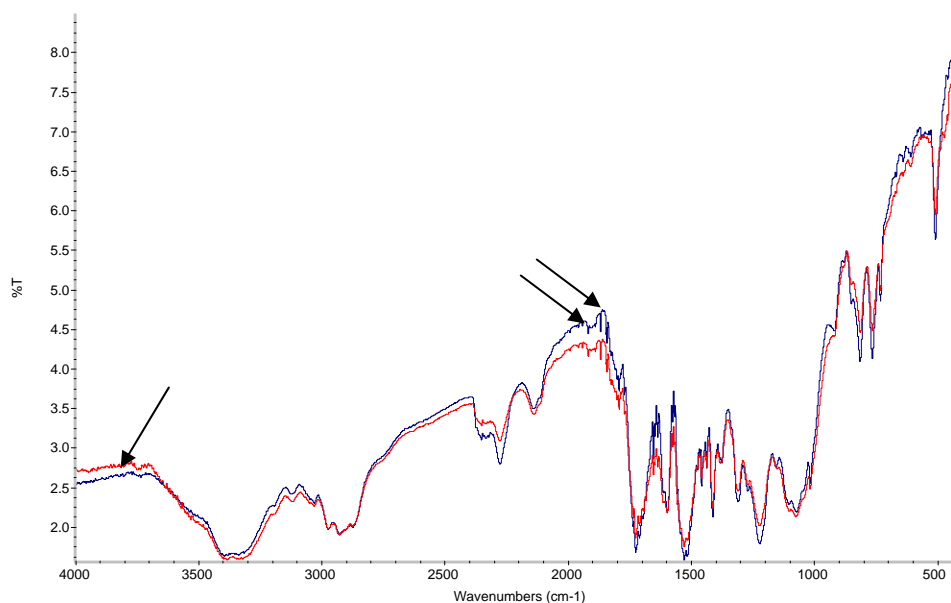


FIGURE 8.1 FT-IR spectrum of treated (single arrow) and untreated (double arrows) PU foams

Figure 8.3 shows the FT-IR spectrum of 10-week treated and untreated PU foam samples. The FT-IR signature of treated PU foams is the same as that of the control PU foam sample at the end of the 10 weeks. Similarly, no change in the FT-IR spectrum of the soil-buried samples was detected during the intermediate weeks of the 10-week experimental period. This finding indicates no deterioration of PU foam surface during the soil burial experiments.

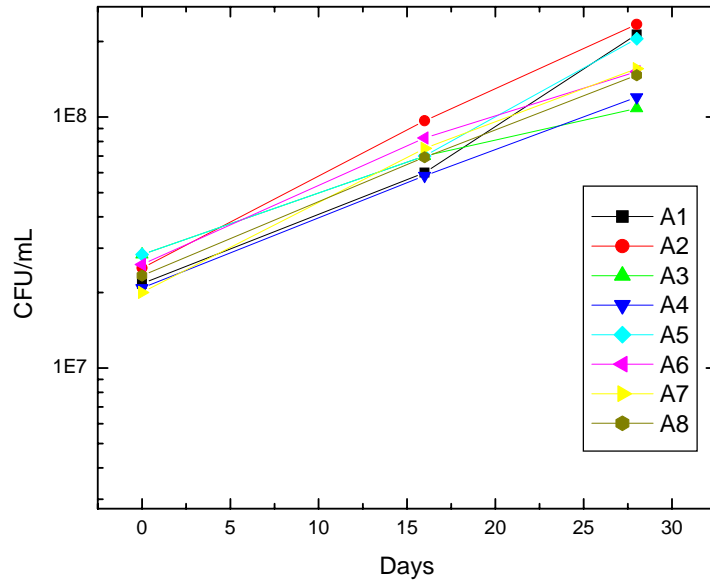
On the basis of the weight loss measurements, tensile strength measurements, and FT-IR spectra of the PU plugs buried in the soil and the control samples, no bio-deterioration of the PU foam occurred due to indigenous microbial activity in the field soil under anaerobic conditions.

8.4 CONCLUSIONS

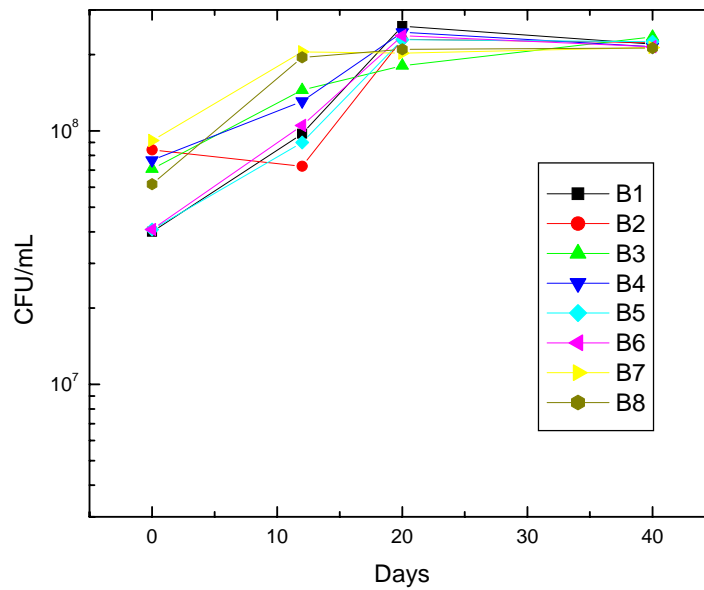
The results obtained within the time span of these investigations show no biodegradation of PU foam used in this study under anaerobic conditions based on the following experimental results:

- No change in the tensile strength of the PU plugs after biological treatment.
- No observed weight loss of PU plugs after biological treatment.
- No change in the FT-IR chemical signature of the PU plugs.
- No growth of anaerobic bacteria using PU as either the carbon or nitrogen source.

As a result of this investigation, the tested PU foam material could be considered as not biodegradable under anaerobic conditions. Based on literature, the blend of polyethylene and aromatic polyester is known to play a significant role in PU resistance to microbial attacks. The rigid foam used in this study is resistant to microbial attack due to its chemical and physical structure.



a) Bacterial growth during the 4 week of bioassay



b) Bacterial growth during the 6 week of bioassay

FIGURE 8.2 Growth assay of the anaerobic bacteria during the bioassay

TABLE 8.5 Cumulative weight loss during soil burial experiments

Treatment Time (week)	Weight Loss (%)		
	Run 1	Run 2	Run 3
Control	0.18	0.18	0.18
1	0.10	0.20	0.0
2	0.54	0.18	0.34
3	0.88	0.41	0.12
4	0.63	0.21	0.32
5	0.15	0.65	0.64
6	0.0	0.46	0.71
7	0.29	0.83	0.14
8	0.27	0.13	0.20
9	0.09	0.25	0.11
10	0.57	0.05	0.13

TABLE 8.6 Tensile strength of treated plugs during soil burial experiments

Run 1		
Treatment		
Time (week)	Load (lb _f)	Tensile Strength (psi)
Control	11.23±1.60	38.02±3.54
1	12.32	36.17
2	13.77	37.53
3	13.89	39.22
4	12.63	36.81
5	11.85	35.16
6	12.41	35.74
7	12.02	38.40
8	12.55	38.98
9	12.98	41.66
10	12.71	38.61

Run 2		
Treatment		
Time (week)	Load (lb _f)	Tensile Strength (psi)
Control	11.23±1.60	38.02±3.54
1	13.74	38.99
2	13.45	37.04
3	14.20	38.73
4	13.40	36.65
5	12.60	39.36
6	13.17	37.59
7	12.72	37.30
8	13.17	37.21
9	12.58	37.40
10	13.54	37.11

Run 3		
Treatment		
Time (week)	Load (lb _f)	Tensile Strength (psi)
Control	11.23±1.60	38.02±3.54
1	13.74	37.43
2	14.60	39.95
3	14.80	40.51
4	13.23	36.74
5	13.22	40.91
6	12.76	36.06
7	12.41	36.92
8	13.07	36.93
9	13.65	39.56
10	12.33	39.35

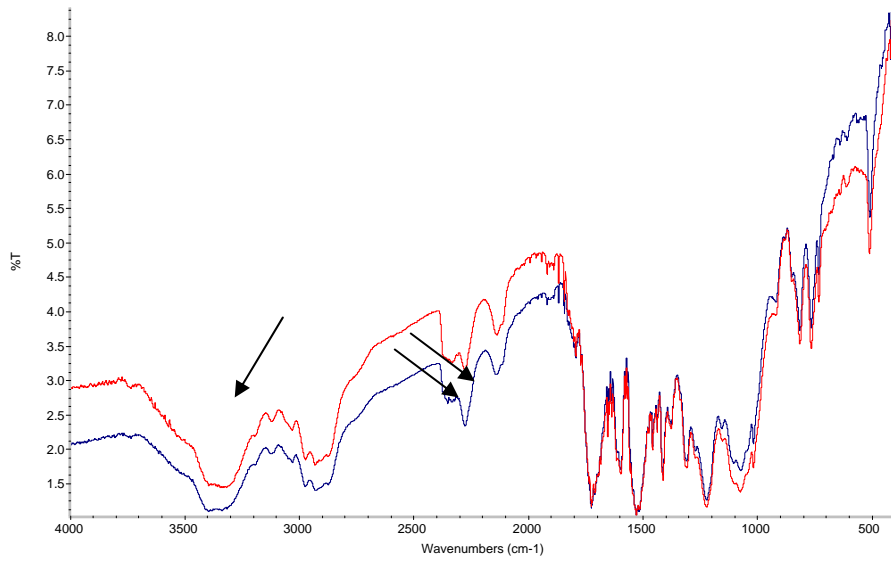


FIGURE 8.3 FT-IR spectrum of treated (single arrow) and untreated (double arrows) PU foams

9 RADIOLYTIC DEGRADATION OF URETHANE FOAM

An irradiation and testing campaign was conducted to ascertain the stability and durability of the foam with respect to the radiation emitted by the uranium that is expected to be present as a contaminant on the inner surfaces. The maximum level of contamination expected is 2 g of ^{235}U distributed uniformly on the inner surface over an 18-in. length of 8-in.-dia pipe. This study was conducted at Oak Ridge National Laboratory (ORNL).

Samples of the urethane foam were irradiated with the ORNL ^{60}Co irradiator to a dose equivalent to that expected to be accumulated in 1000 years for both alpha and gamma radiation from the uranium contamination. Most of the radiation dose from the uranium is expected to be in the form of alpha particles reaching only the outer foam layer. Therefore, the surface of the polyurethane foam will absorb a much higher dose than the bulk of the sample, and most of the radiation damage will be confined to the surface.

The penetrating gamma rays from ^{60}Co will reach the entire volume of the foam sample. To evaluate the radiation damage to the polyurethane surface, the entire sample was irradiated at the higher level of exposure typical of the surface. This very conservative approach gives a significant degree of confidence regarding the radiation stability of the polyurethane foam.

The physical properties of the urethane foam samples (microstructure, compressive strength, density, and porosity) were measured before and after irradiation. Additionally, gas generation from the foam was monitored during irradiation, and the head-space gases analyzed at the end. The properties measured included compressive strength, density, and porosity.

The overall conclusion from the irradiation and testing is that the foam did not suffer any significant degradation during the gamma irradiation equivalent to a "1000-year alpha and gamma dose" on the entire volume of the specimen and that gas generation was minimal.

Experimental details and results of this study have been published in a report entitled, "Radiolytic Degradation of Urethane Foam used for encapsulation of contaminated Components", (ORNL/TM-2006/15).

10 CORROSION OF STEEL PIPES

Before exposure of the foam to significant loading within the landfill, the surrounding PGE must first structurally degrade. A corrosion study of the steel pipes thus becomes important. Our corrosion study was conducted in the simulated environments that are expected to exist over time within the EMWMF and accelerated aging conditions.

10.1 MATERIAL AND EXPERIMENTAL PROCEDURE

An accelerated corrosion test, per ASTM standard, was conducted on an ASTM A53 carbon steel coupon provided by BJC and shown in Fig. 10.1. The composition of this material is similar to that of the ASTM A285 steel that replaced the original ASTM 70-42 designation for the actual converter plate steel. Sample coupons are 1 in. \times 1 in. (2.5 cm \times 2.5 cm) with a thickness of 0.3 in. (7 mm). However, the samples were not flat and had a small curvature. The thickness of the sample corresponds to that of the wall of some actual pipes for disposal.

ASTM Method G 31 (re-approved 2004) (Standard Practice for Laboratory Immersion Corrosion Testing of Metals) was closely followed during the tests. Corrosion tests were conducted by suspending the sample coupons by a plastic wire in the corrosion fluid contained in a plastic container (Fig. 10.2). This was done to avoid any secondary corrosion sources. The corrosion fluid simulates the leachate composition at the disposal site. BJC provided the typical leachate composition [22], from which the corrosion fluid profile in Table 10.1 was developed. The mean pH of the solution was 7.6. The major anions were chloride, bicarbonate, and sulfate, and the major cations were magnesium and sodium. The ratio of solution volume to sample surface area was 0.20 ml/mm².

Before placement in the corrosion cell, the sample was weighed (± 0.5 mg accuracy), and its geometric dimensions were measured. Test temperature was used as the corrosion rate accelerant. The test temperatures were room temperature, 60°C (140°F), and 80°C (176°F). Different samples (three sets in duplicate) were exposed to the corrosion fluid for 2 to 180 days at a specific temperature. As-received samples were cut into smaller pieces for corrosion tests. Nominal sample dimensions were 0.8 in. \times 1.0 in. \times 0.3 in. (20 mm \times 25 mm \times 7 mm).

Longer exposure times were explored if no discernible corrosion was observed. At the end of the test period, samples were removed, cleaned in acetone, brushed when needed, and carefully dried and measured for any changes in weight. The cleaning procedure is vital to reliable results and was followed as outlined in the ASTM G 31 standard. Weight loss as a function of time was plotted at a fixed test temperature.

The weight loss (ΔW) data as a function of time were used to determine the corrosion rate in accord with ASTM standard G31. The corrosion rate in units of mm/year was calculated from the following equation:

$$\text{Corrosion Rate (CR)} = \Delta W / A t \rho$$

where A is the sample surface area, t is the exposure time, and ρ is the density (7.9 g/cm^3) of the steel.

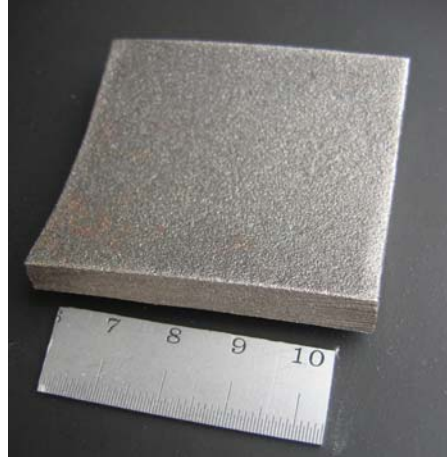


FIGURE 10.1 As-received ASTM A53 steel sample coupon



FIGURE 10.2 Corrosion samples in leachate solution.
Note the corrosion product at the bottom

TABLE 10.1 Compositional make-up of corrosion fluid

Species	Amount
Deionized water	2000 ml
NaHCO ₃	443.4 mg
MgSO ₄	313 mg
MgCl ₂ .H ₂ O	75.4 mg

10.2 CORROSION STUDY RESULTS

10.2.1 Corrosion in Leachate Solution

Figure 10.3 shows the corrosion rates of as-cut and polished sample coupons during the testing at room temperature. The arrows indicate the start of weight monitoring for the particular sample. In all cases, the corrosion rate is initially high and then reaches a steady state. Based on 180 days of testing, the corrosion rate is about 0.065-0.07 mm/year for as-cut and polished samples directly suspended in the leachate.

Figures 10.4 and 10.5 show the corrosion rates for as-cut and polished samples tested at 60°C (140°F) and 80°C (176°F), respectively. Based on 180 days of testing, the corrosion rate is about 0.130 mm/year for samples directly suspended in the leachate at 60°C (140°F), double that of the room-temperature tested samples. For samples tested at 80°C (176°F), the corrosion rate, within the scatter in data, is 0.05-0.1 mm/year, close to that of the room-temperature tested samples. At elevated temperatures, passivation of the samples may have led to the unexpectedly lower corrosion rates. The mechanism for reduced corrosion rates at elevated temperatures was not investigated.

10.2.2 Corrosion in Soil Mixed with Leachate (open condition)

Figure 10.6 shows the corrosion rates for samples that were placed directly in contact with soil from Oak Ridge, Tennessee. The pH values of Tennessee soil were determined from the Soil Survey Laboratory Information Manual (USDA, 1995) using 1 soil:1 H₂O (one part soil to one part distilled water by weight) pH of the soil sample that ranged from 6.47-6.76. The soil was mixed with the leachate solution, such that the proportion of leachate was about 10% by weight (20 ml solution/200 g soil). The sample was completely covered by the soil. The container was then covered with aluminum foil (Fig. 10.7). There was some drying of soil as the test ensued. Therefore, periodically, leachate solution was added to compensate for the drying. Tests were conducted at 23°C (73°F), 60°C (140°F), and 80°C (176°F). The corrosion rate initially was high and then reached a steady state. For the 23°C (73°F) tested sample, the

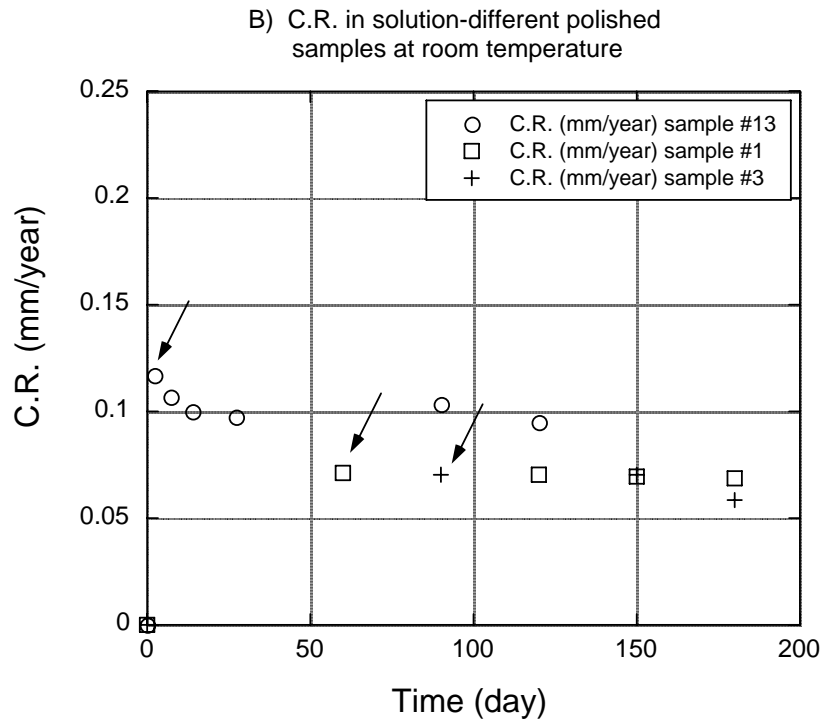
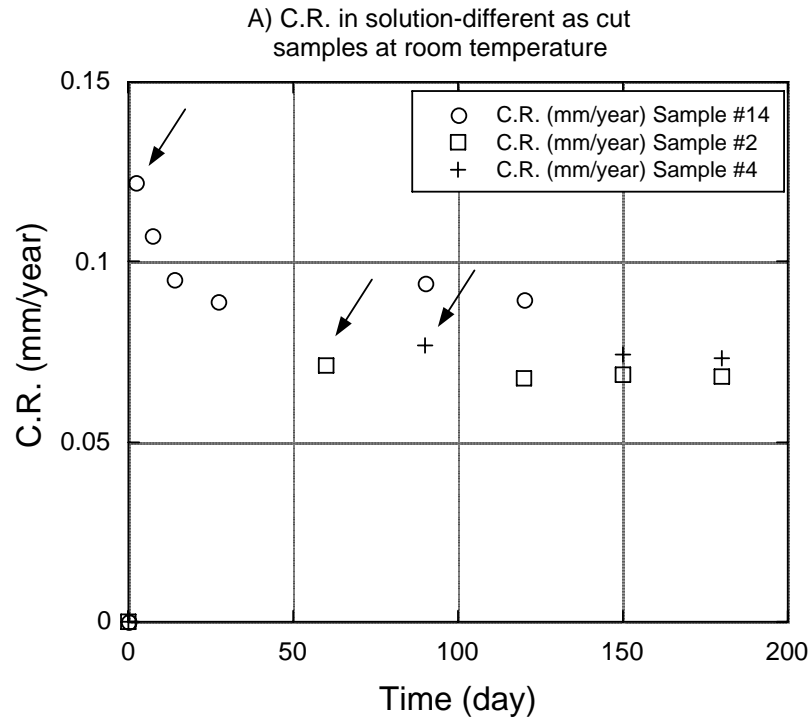


FIGURE 10.3 Corrosion rates (C.R.) of (a) as-cut and (b) polished samples directly suspended in solution and tested at room temperature

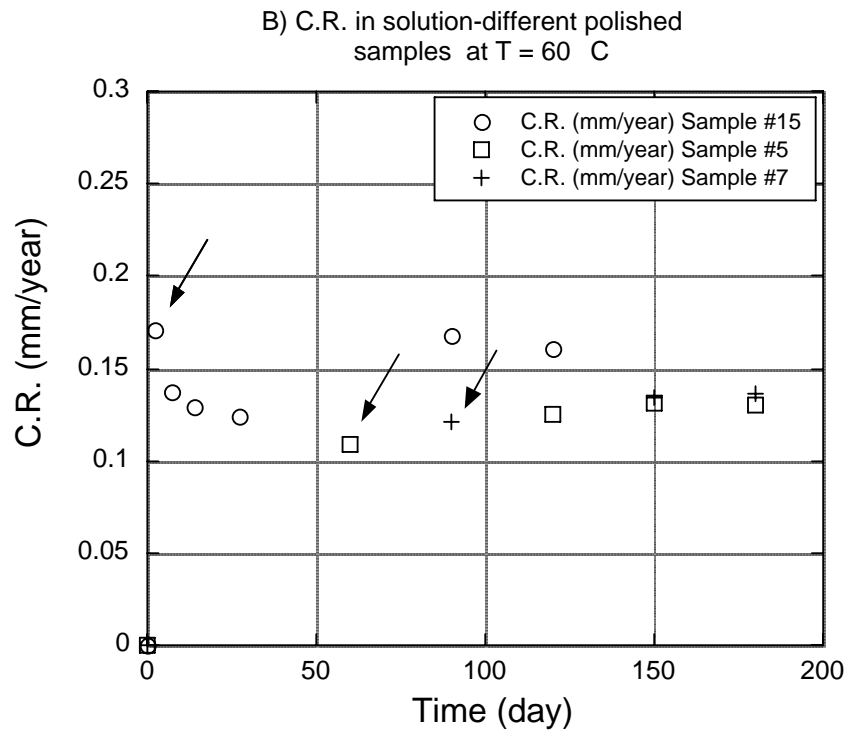
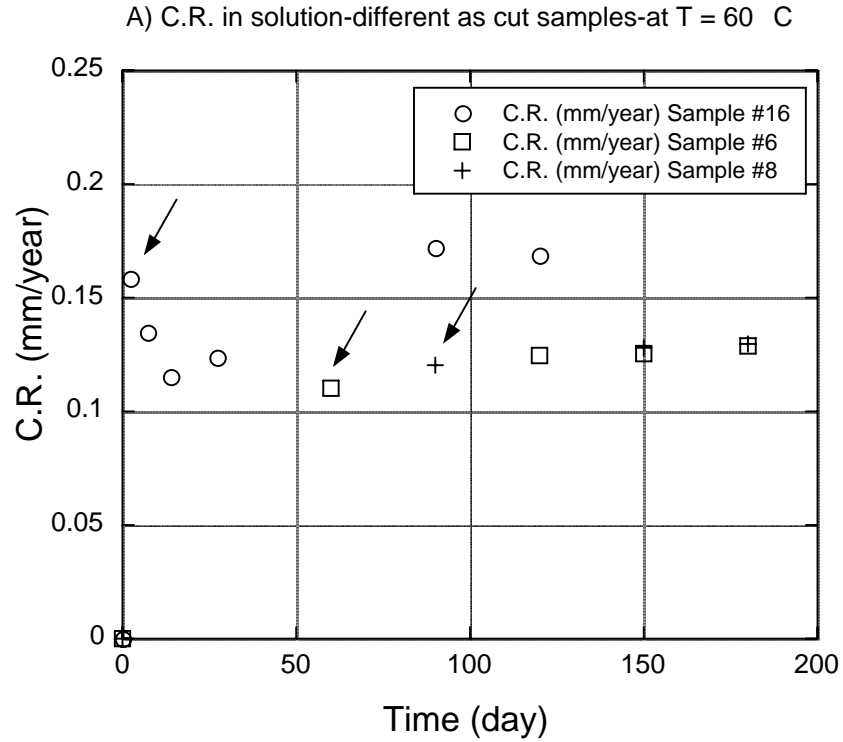


FIGURE 10.4 Corrosion rates of (a) as-cut and (b) polished samples directly suspended in solution and tested at 60°C (140°F)

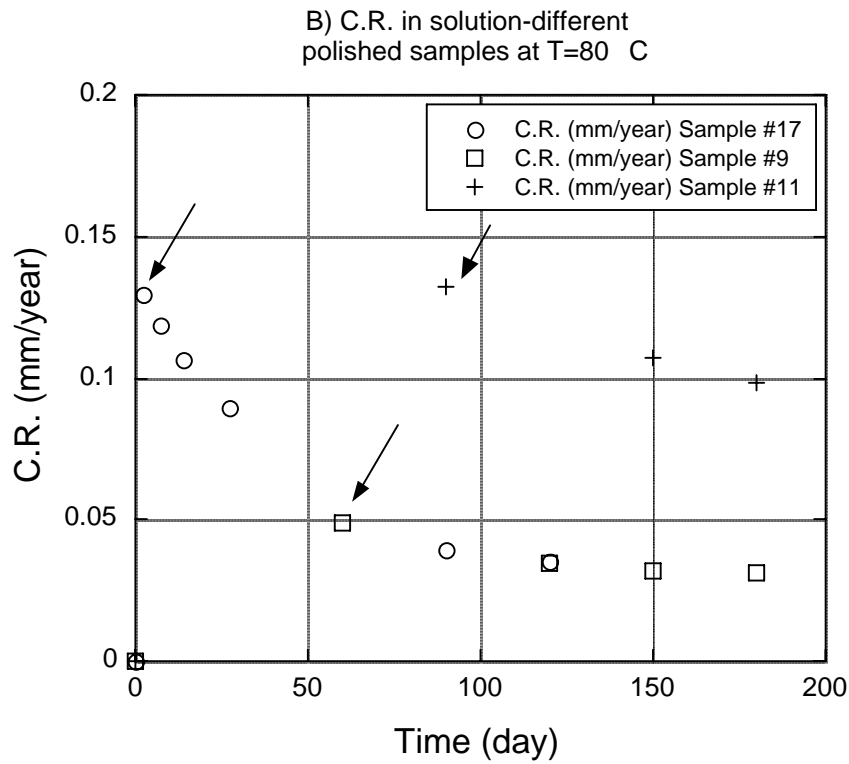
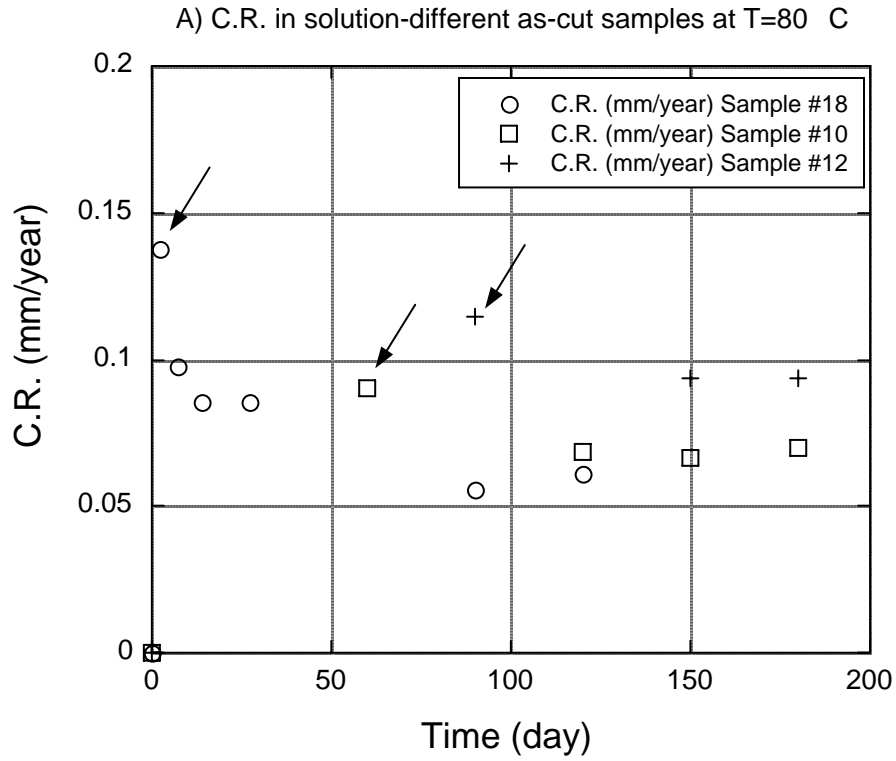


FIGURE 10.5 Corrosion rates of (a) as-cut and (b) polished samples directly suspended in solution and tested at 80°C (176°F)

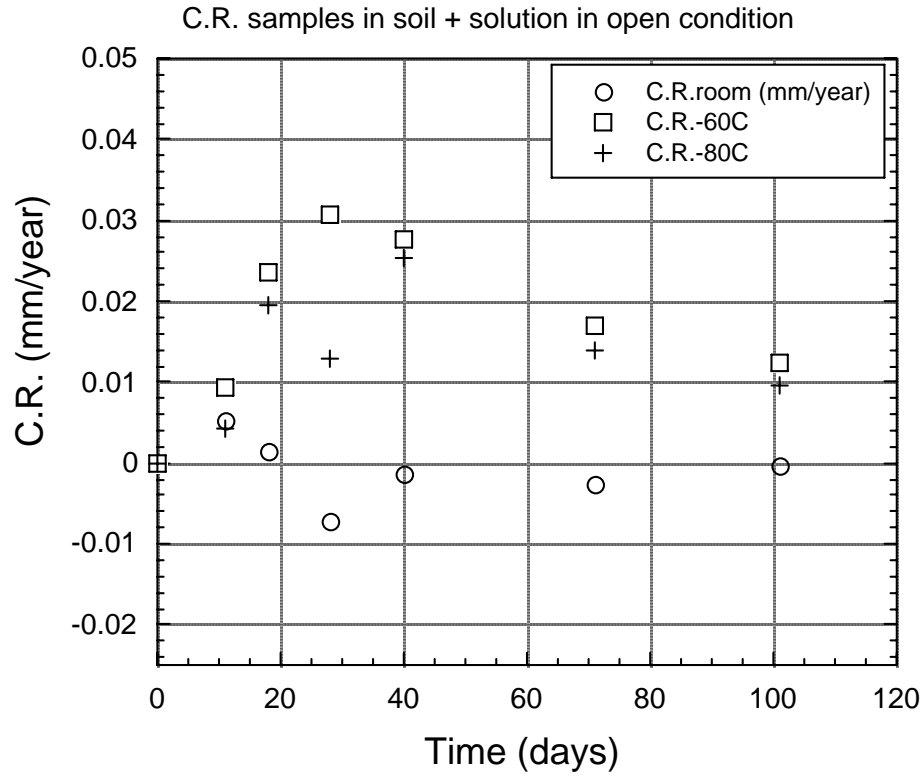


FIGURE 10.6 Corrosion rates of samples placed in soil mixed with leachate (open condition) and tested at 23°C (73°F), 60°C (140°F), and 80°C (176°F)



FIGURE 10.7 Corrosion samples in Oak Ridge soil under open condition

corrosion rate was almost negligible for the 101 days of testing. For the 60°C (140°F) and 80°C (176°F) tested samples, corrosion rates were approximately 0.01-0.015 mm/year. These rates are significantly lower than those observed when samples are directly suspended in the leachate.

10.2.3 Corrosion in Soil Mixed with no Leachate (sealed condition)

Figure 10.8 shows the corrosion rates for samples that were placed directly in contact with soil from Oak Ridge. The container was completely sealed so that no evaporation took place (Fig. 10.9). The as-received soil was quite wet, and no leachate solution was added in these experiments. The sample was completely covered by the soil. Tests were again conducted at 23°C (73°F), 60°C (140°F), and 80°C (176°F), and the corrosion rate, initially high, reached a steady state. For the 23°C (73°F) tested sample, the corrosion rate was about 0.02 mm/yr for the 63 days of testing. For the same period, the 60°C (140°F) tested samples reached a corrosion rate of 0.04 mm/year. However, for 80°C (176°F) tested samples, the corrosion rate was almost negligible for the 63 days. As expected, these corrosion rates are intermediate to the tests where the samples were immersed completely in leachate solution, and where the samples were placed in soil (with leachate solution) but not sealed.

10.2.4 Corrosion in Soil Mixed with Leachate (sealed and open conditions)

To guarantee a constant concentration of ions in the soil from the leachate solution, analogous tests were repeated at room temperature in open and sealed conditions. The soil was mixed with the leachate solution such that the proportion of leachate was about 10% by weight (20 ml solution/200 g soil) initially, but then deionized water was added to compensate for drying (only needed in open conditions). The samples were completely covered by the soil. Despite the initial scatter in data, corrosion rates tended to a steady value. For the open condition, after 43 days of testing, the corrosion rate ranged from -0.01 mm/year to +0.01 mm/year (Fig. 10.10). For sealed conditions, the corrosion rates (Fig. 10.11) ranged from -0.03 mm/year to +0.03 mm/year for the same period. As expected, these values are intermediate to the situation where the samples were immersed completely in leachate solution, and where the samples were placed in soil (with leachate solution) but not sealed.

Figures 10.12(a-c) show corroded steel samples after 90-day exposure in leachate solution at room temperature, 60°C (140°F), and 80°C (176°F), respectively. Clearly, the degree of corrosion is different in the three samples. Corrosion appears to be over a large area and not localized.

10.2.5 Corrosion in Anaerobic Soil

Figure 10.13 shows the corrosion rates for samples that were buried for 40 days in 4-in. (10-cm)-deep covered containers filled with the Oak Ridge (Tennessee) field soil. Samples were placed at a depth of 2 in. (5 cm) of soil to allow the development of anaerobic conditions that

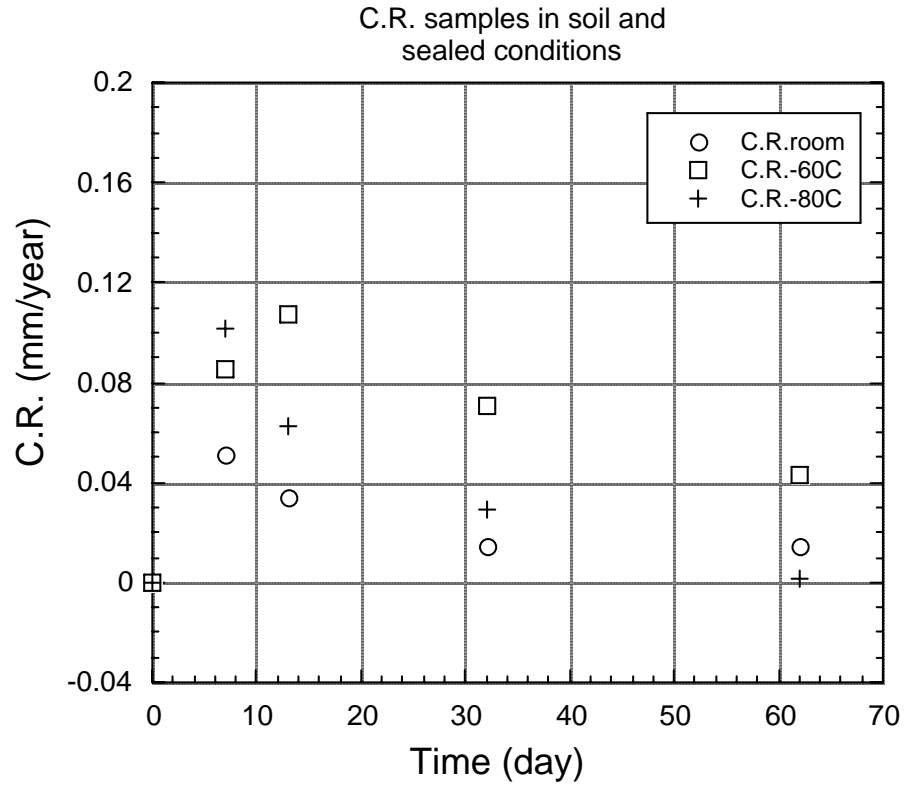


FIGURE 10.8 Corrosion rates for samples placed in soil, in sealed condition, and tested at 23°C (73°F), 60°C (140°F), and 80°C (176°F)



FIGURE 10.9 Corrosion samples in Oak Ridge soil in sealed condition

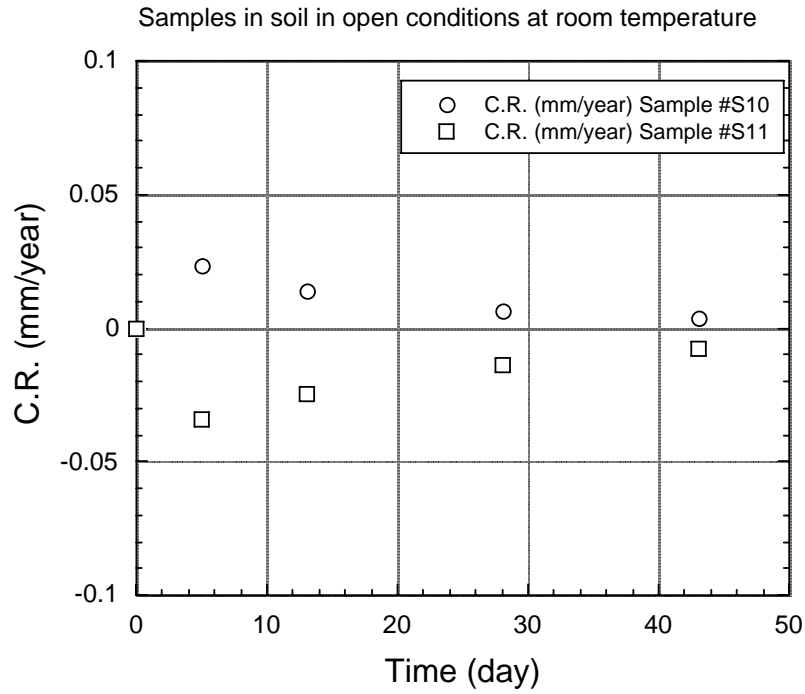


FIGURE 10.10 Corrosion rates of samples placed in soil, in open condition, and tested at room temperature

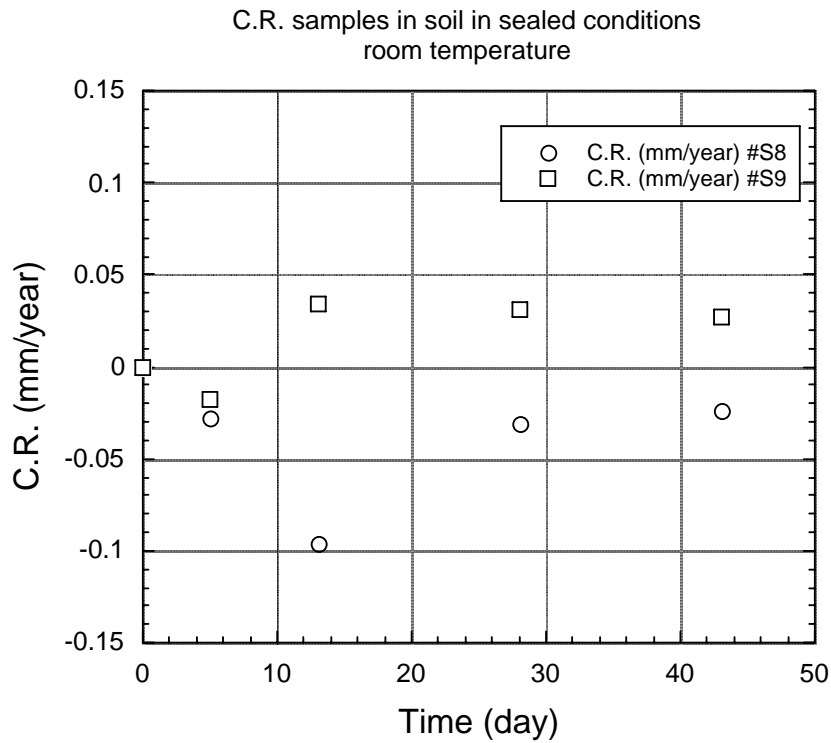


FIGURE 10.11 Corrosion rates of samples placed in soil, in sealed condition, and tested at room temperature



(a)



(b)



(c)

FIGURE 10.12 Steel samples suspended in leachate solution for 90 days at (a) 23°C (73°F), (b) 60°C (140°F), and (c) 80°C (176°F)

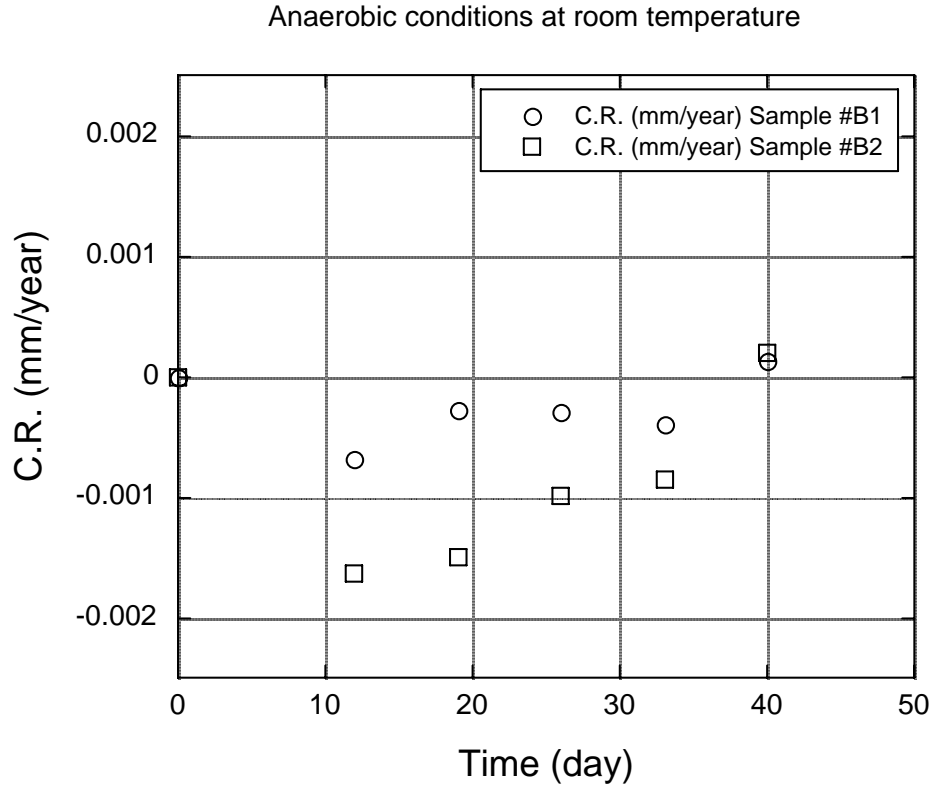


FIGURE 10.13 Corrosion rates of samples placed in Oak Ridge soil, in anaerobic condition, and tested at room temperature

would simulate the environmental conditions in the field when the landfill is capped. As shown in the figure, the corrosion rate is negligible for the 40-day period.

10.3 SUMMARY

Table 10.2 summarizes the steady-state corrosion rates of steel determined under various test scenarios. These data will allow BJC to determine useful lifetimes of the steel PGE under various environmental conditions that may exist within the EMWMF over time.

TABLE 10.2 Summary of corrosion rates in various test conditions

		Test Period (days)	Temperature, °C		
			23	60	80
Surrogate leachate solution		175	0.05-0.075	0.1-0.15	0.04-0.10
Soil w/o surrogate leachate	Closed container	63	0.02	0.04	~0
	Open to atmosphere	101	~0	~0.01	0.015
Soil spiked w/ surrogate leachate	Closed container	43	±0.03		
	Anaerobic condition	40	~0		
Dry soil					
All units reported in mm/yr					

11 SUMMARY

This detailed investigation determined the aging behavior of commercial urethane foam that potentially will be used for infiltrating contaminated PGE before it is sent to EMWFM in ORR for disposal. Various properties that could lead to degradation such as mechanical stresses, heat, moisture, temperature cycling, biodegradation, and radiation exposure were studied. In addition, the corrosion behavior of the EMWFM steel pipes was studied in various disposal scenarios. The data for steel corrosion rate will assist EMWFM personnel in establishing the durability of steel structures and in assessing the potential of subsidence due to structural collapse. Consequently, they could be used in assessing the design life of the EMWFM.

The main conclusions from this study are as follows:

- Baseline mechanical property characterization of the as-received urethane foam (density of 3.1 pcf) showed that unconfined compressive strengths were anisotropic. Compressive strengths were 50 psi in the direction of foam rise (longitudinal) and 31 psi in the direction perpendicular to foam rise (transverse).
- Compressive strength of urethane foam degrades with test temperature. Strength dropped by 40% at 90°C (194°F) to 19 psi from a room temperature value of 31 psi.
- Thermal aging of the as-received foam (3.1 pcf), in both air and water environments, did not show any mechanical degradation (as characterized by compressive strengths) when exposed to temperatures as high as 90°C (194°F) and for periods as long as 60 days. However, the density of the material decreased with long-term aging.
- Dry and wet freeze-thaw cycling did not degrade the compressive strength of the urethane foam.
- Urethane foam did not biodegrade under anaerobic conditions. The rigid foam (3.1 pcf) used in this study is resistant to microbial attack due to its chemical and physical structure.
- Irradiation of the urethane foam (3.1 pcf) resulted in no significant degradation of the foam, and the gas generation was minimal during a gamma irradiation to a “1000-year alpha and gamma” dose on the entire sample volume.
- Confined compression tests conducted on 3.1 pcf density foam failed the compressibility requirement (<10% deformation at 75 psi) for overburden loads.

- Higher density foams (4-7 pcf) showed improved response in confined compression tests. However, foam B (6.6 pcf) performed best in both directions, i.e., parallel and perpendicular to the foam rise.
- In long-term testing (1000 h) of foam B under a fixed compressive stress of 75 psi (equivalent to 90-ft soil depth), the maximum deformation was ~ 8%. Longer term testing on a larger sample size is recommended.
- Corrosion tests on the ASTM A51 steel were conducted under four conditions: (a) sample suspended in leachate, (b) sample buried in soil mixed with leachate and soil open to air, (c) sample buried in soil mixed with leachate in a sealed container, and (d) sample buried in soil to create anaerobic conditions. Corrosion rates, at room temperature, for the above test conditions were 0.065 mm/yr, negligible, 0.03 mm/yr, and negligible, respectively.

12 REFERENCES

1. Bechtel Jacobs Corp, email communication, June 13, 2006.
2. S. L. De Gisi and T. E. Neet, "Predicting the Compressive Properties of Rigid Urethane Foam", *J. Appl. Poly. Sci.*, Vol. 20, No. 8, pp. 2011 (1976).
3. www.pipingtech.com/products/preis/poly.pdf
4. Handbook of Polymer Degradation eds. S. H. Hamid, M. B. Amin, and A. G. Maadhah, Marcel Dekker, Inc., New York, pp. 309 (1992).
5. Letter communication dated 6/13/06 by North Carolina Foam Industries to Bechtel Jacobs Company.
6. Bechtel Jacobs Corp., email communication, June 1, 2006.
7. O. L. Davies and N. J. Mills, "The Rate Dependence of Confor Polyurethane Foams," *Cellular Polymers*, Vol. 18, No. 2, (1999).
8. X. Zhang, R. Xu, Z. Wu, and C. Zhou, "The synthesis and characterization of polyurethane/clay nanocomposites," *Polymer International* 52: 790-794 (2003).
9. Z. T. Ossefort and F. B. Testroet, "Hydrolytic stability of urethane elastomers," *Rubber Chemistry and Technology* 39: 1308-1327 (1966).
10. R. A. Pathirana and K. J. Seal, "Studies on polyurethane deteriorating fungi: Part 3, Physico-mechanical and weight changes during fungal deterioration," *International Biodeterioration* 21: 41-49 (1985).
11. G. T. Howard and N. P. Hilliard, "Use of Coomassie blue-polyurethane interaction in screening of polyurethanase proteins and polyurethanolytic bacteria," *International Biodeterioration & Biodegradation* 43: 23-30 (1999).
12. R. T. Darby and A. M. Kaplan, "Fungal susceptibility of polyurethanes," *Applied Microbiology* 16: 900-905 (1968).
13. T. Nakajima-Kambe, Y. Shigeno-Akutsu, N. Nomura, F. Onuma, and T. Nakahara, "Isolation and characterization of a bacterium which utilizes polyester polyurethane as a sole carbon and nitrogen source," *FEMS Microbiology Letters* 129: 39-42 (1995).
14. M. J. Wiggins, J. M. Anderson, and A. Hiltner, "Biodegradation of polyurethane under fatigue loading," *Journal of Biomedical Material Research* 65A: 524-535 (2003).

15. C. Guignot, N. Betx, B. Legendre, A. Le Moel, and N. Yagoubi, "Influence of filming process on macromolecular structure and organization of a medical segmented polyurethane," *Journal of Applied Polymer Science* 85: 1970-1979 (2002).
16. J. E. Hobbie, R. J. Daley, and S. Jasper, "Use of nucleopore for counting bacteria by fluorescence microscopy," *Applied Environmental Microbiology* 33: 1225-1228 (1977).
17. K. C. Frisch, "High performance polyurethanes," in *Macromolecular Design of Polymeric Materials*, Eds., Hatada, E., Kitaiyama, N., and Vogl, O., New York: Marcel Dekker, Inc., pp. 523-560 (1997).
18. A.-C. Albertsson and S. Karlsson, "Controlled degradation by artificial and biological processes," in *Macromolecular Design of Polymeric Materials*, Eds., Hatada, E., Kitaiyama, N., and Vogl, O., New York: Marcel Dekker, Inc., pp. 793-803 (1997).
19. P. J. Whitney, H. Clare, A. J. Graffham, and S. J. Graffham, "The environmental degradation of thin plastic films," *International Biodeterioration & Biodegradation* 31: 179-198 (1993).
20. W. K. Lee, J. H. Ryou, and C. S. Ha, "Retardation of enzymatic degradation," *Surface Science* 542: 235-243 (2003).
21. T. Nakajima-Kambe, Y. Shigeno-Akutsu, N. Nomura, F. Onuma, and T. Nakahara, "Microbial degradation of polyurethane, polyester polyurethanes and polyether polyurethanes," *Applied Microbiology Biotechnology* 51: 134-140 (1999).
22. EMWMF Leachate Analysis provided to ANL by J. Gadd (BJC) via email June 2005.

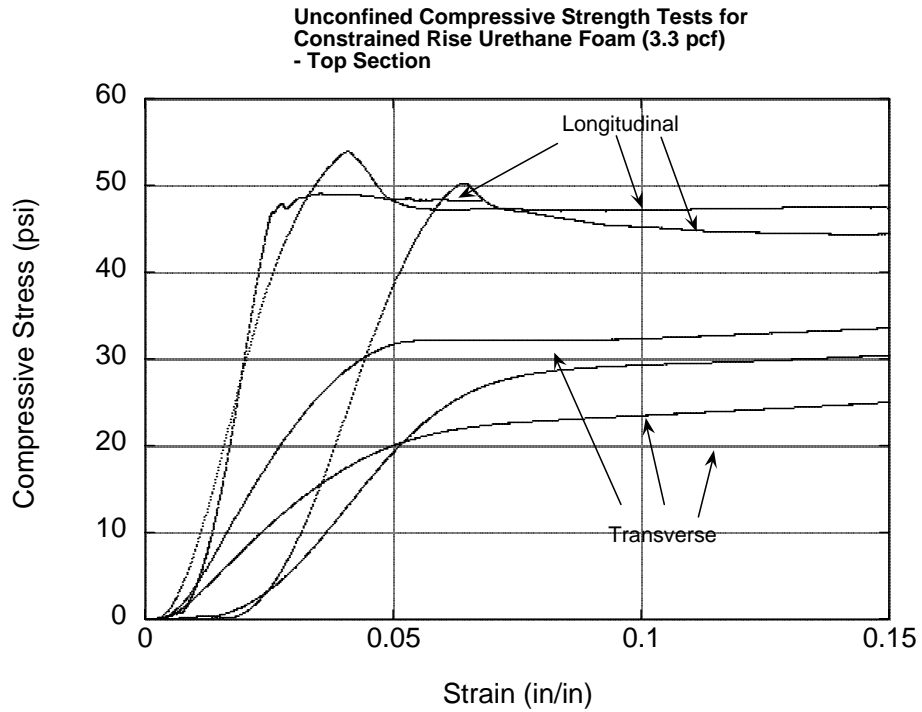
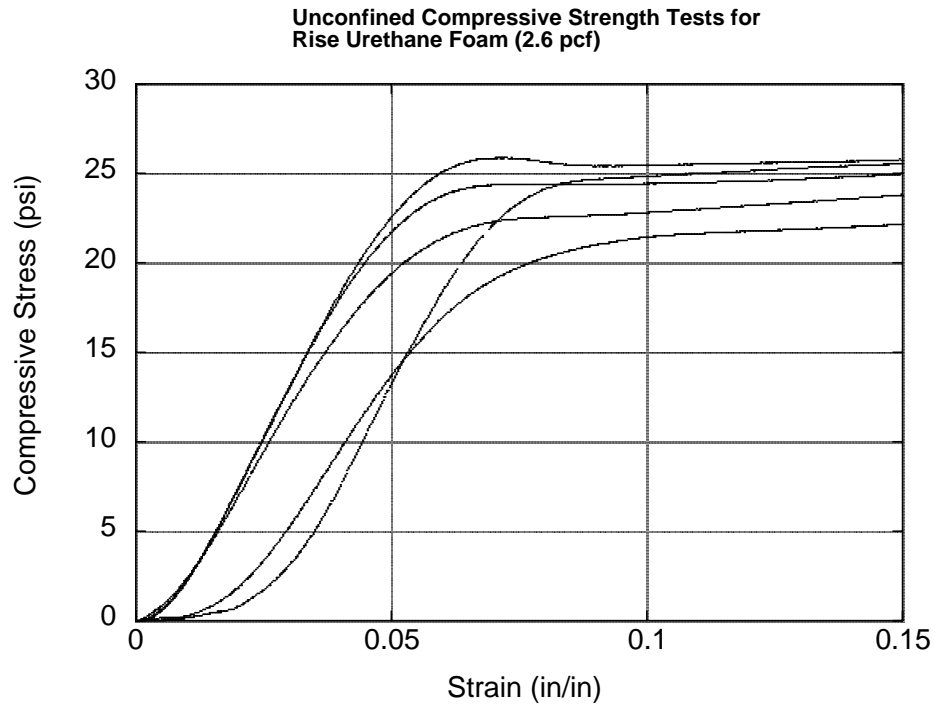
APPENDIX 1:

TEST DATA FOR AS-RECEIVED URETHANE FOAM SAMPLES

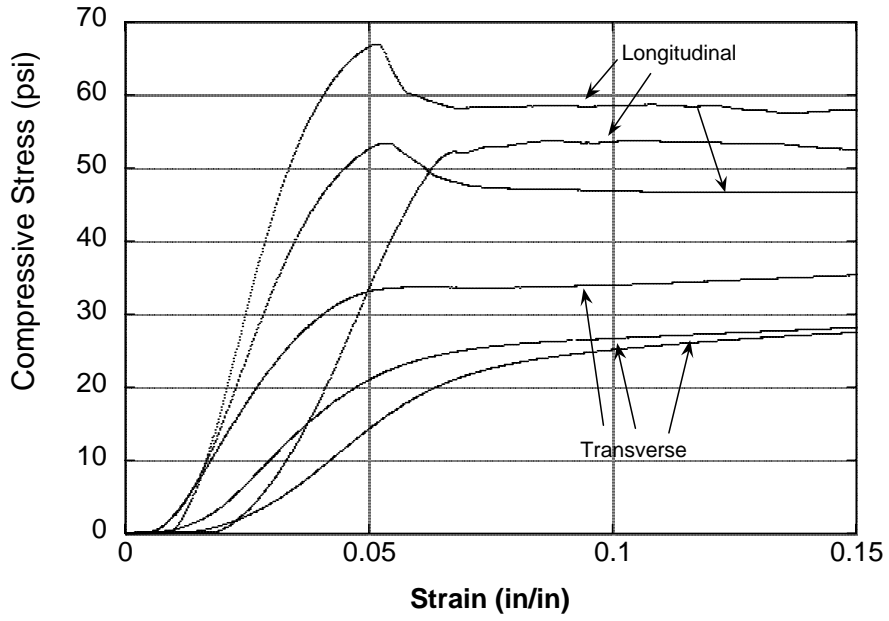
1.1 Density and unconfined compressive strengths

Sample ID	Length (cm)	Dia (cm)	Weight (g) (g)	Density (g/cm ³)	Density (pcf)	Max load (lbs)	Yield Load (lbs)	Yield Strength (psi)
Free rise								
#1	6.089	6.132	7.4889	0.0417	2.5990	118.73	116.60	25.08
#2	6.115	6.135	7.4191	0.0410	2.5611	117.86	115.70	24.86
#3	6.090	6.132	7.8356	0.0436	2.7189	110.58	105.10	22.60
*4	5.895	6.341	7.6327	0.0410	2.5582	110.42	106.30	21.37
*5	6.072	6.132	7.7047	0.0430	2.6814	115.71	111.90	24.06
Top-Longitudinal	Top-Longitudinal							
TL-1	6.143	6.102	8.4137	0.0468	2.9224	244.26	244.26	53.04
TL-2	6.176	6.108	8.4144	0.0465	2.9013	222.26	222.26	48.17
TL-3	6.197	6.124	8.9102	0.0488	3.0463	229.29	229.29	49.44
Top-Transverse	Top-Transverse							
TT-1	6.120	6.150	9.1632	0.0504	3.1446	142.36	136.80	29.24
TT2	6.214	6.159	9.3116	0.0503	3.1389	156.55	150.00	31.98
TT-3	6.137	6.147	9.0549	0.0497	3.1021	117.30	108.80	23.28
Middle-Longitudinal	Middle-Longitudinal							
ML1	6.185	6.116	8.6531	0.0476	2.9711	304.66	304.66	65.85
ML2	6.163	6.131	8.9029	0.0489	3.0533	245.97	245.97	52.91
ML3	6.097	6.138	8.5740	0.0475	2.9657	245.08	245.08	52.60
Middle-Transverse	Middle-Transverse							
MT1	6.085	6.176	8.7782	0.0482	3.0047	129.00	122.86	26.04
MT2	6.255	6.151	9.3085	0.0501	3.1254	164.67	157.20	33.60
MT3	6.187	6.146	9.4310	0.0514	3.2057	131.55	124.90	26.73
Bottom-Longitudinal	Bottom-Longitudinal							
BL1	6.190	6.148	8.5651	0.0466	2.9082	232.38	232.38	49.70
BL2	6.173	6.138	8.6039	0.0471	2.9388	235.38	235.38	50.51
BL3	6.165	6.109	8.6086	0.0476	2.9727	336.76	336.76	72.96
Bottom-Transverse	Bottom-Transverse							
BT1	6.153	6.152	9.2039	0.0503	3.1403	162.70	156.50	33.44
BT2	6.172	6.183	9.4564	0.0510	3.1843	144.14	134.70	28.49
BT3	6.123	6.150	9.2327	0.0508	3.1680	134.30	124.90	26.70

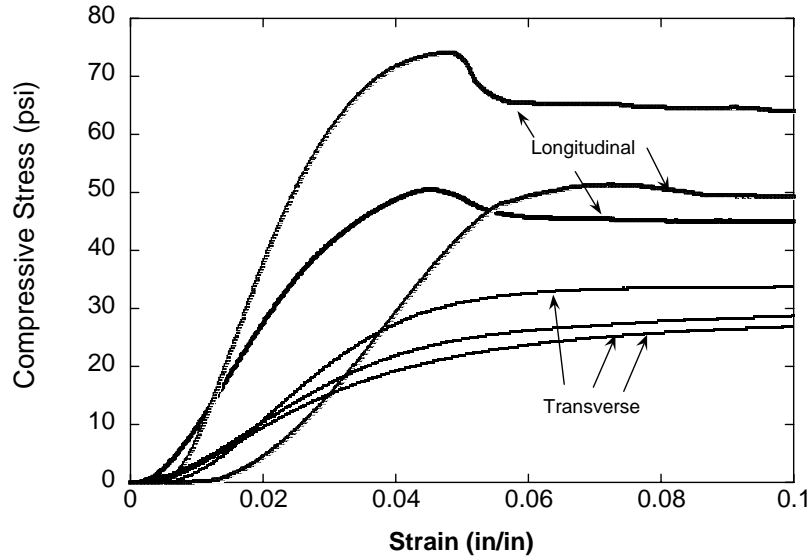
1.2 Stress-strain plots from compression testing

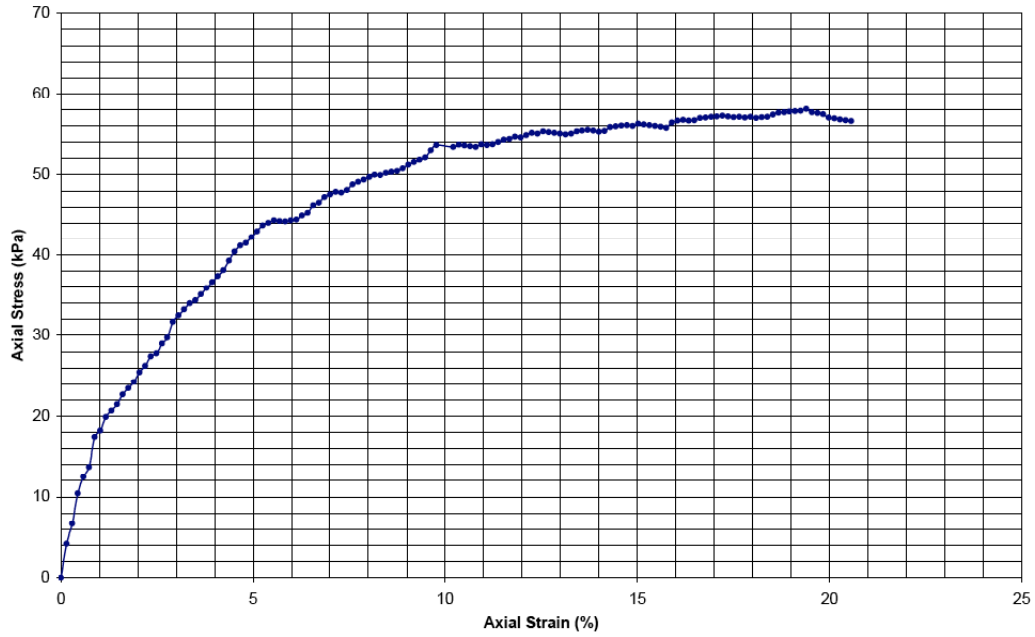
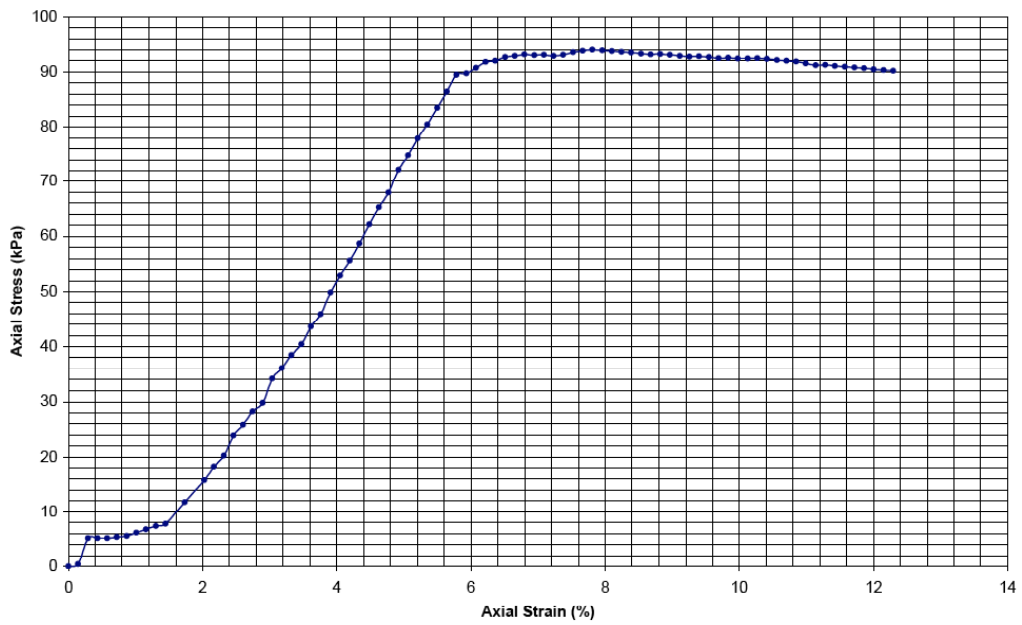


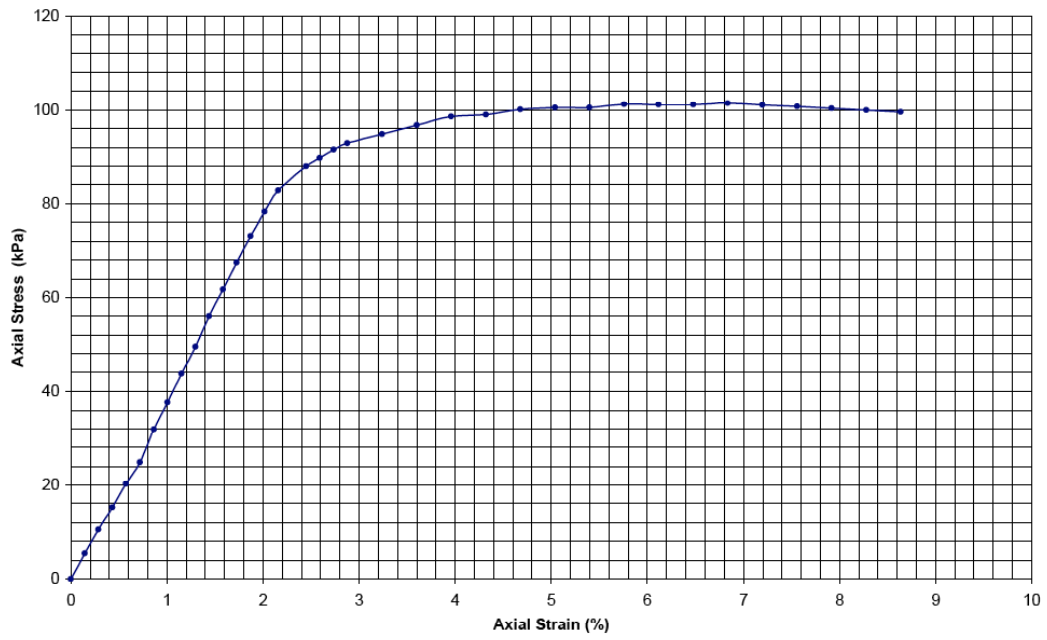
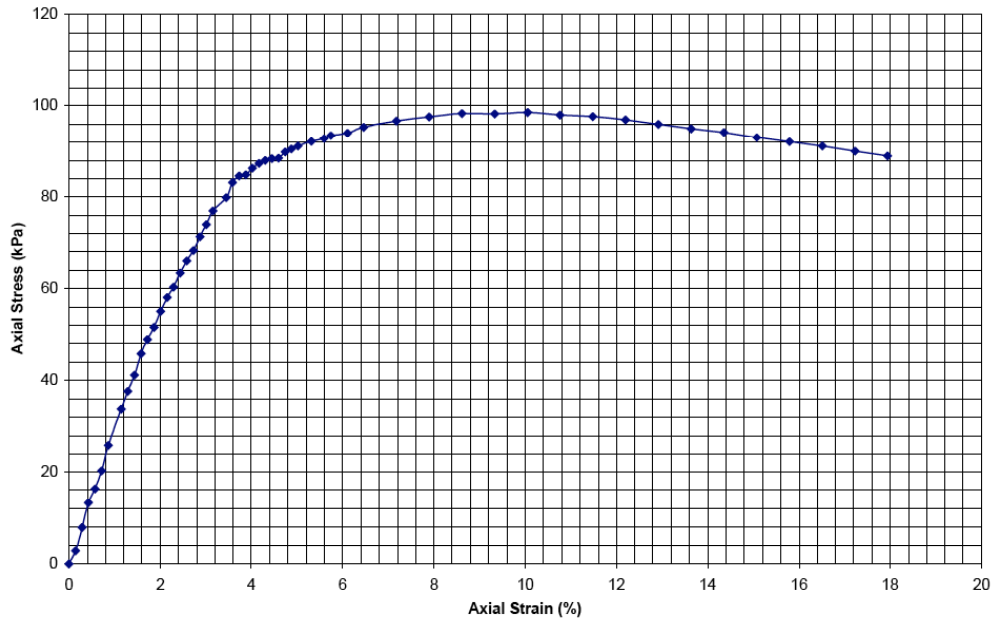
Unconfined Compressive Strength Tests for
Constrained Rise Urethane Foam (3.3 pcf)
- Middle Section

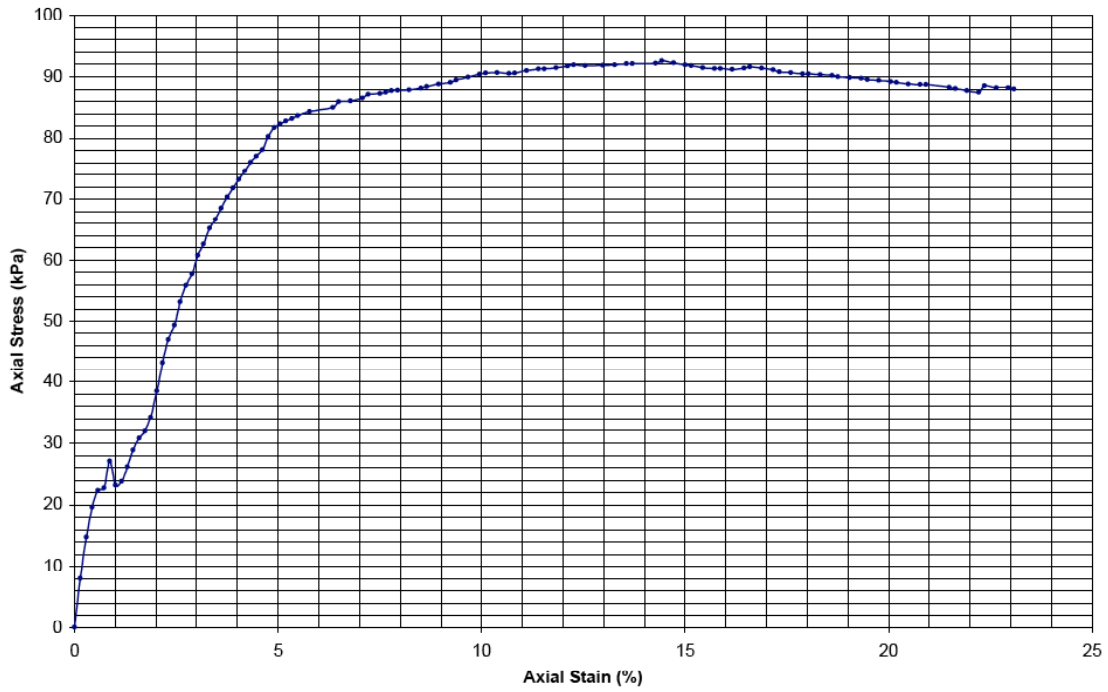
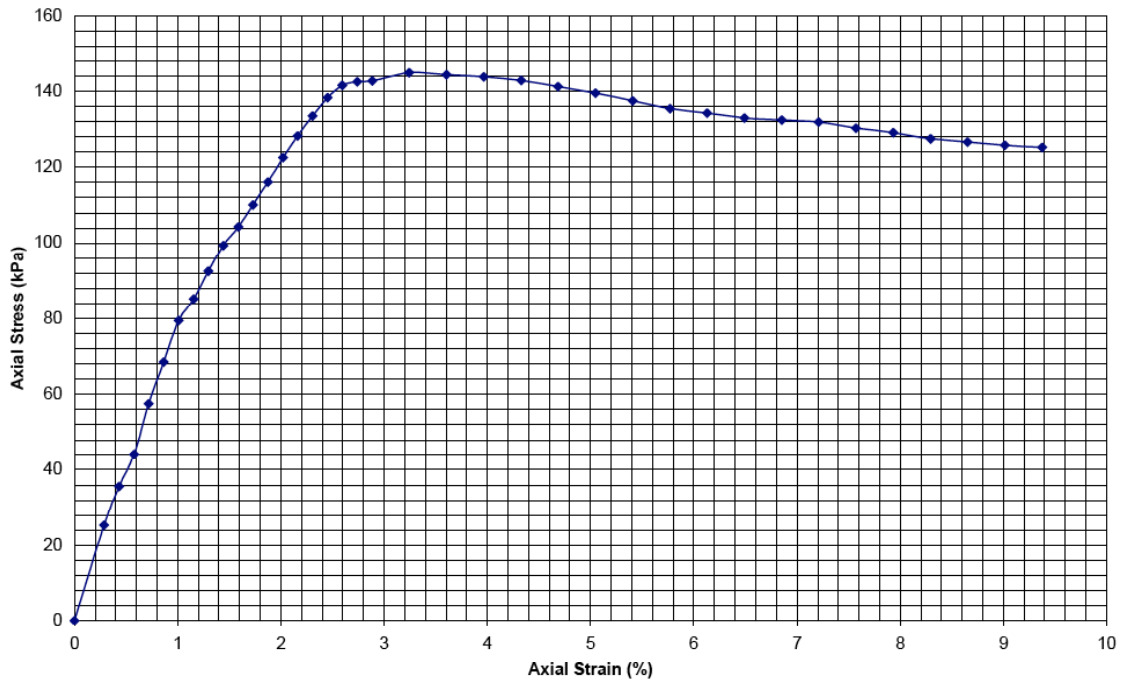


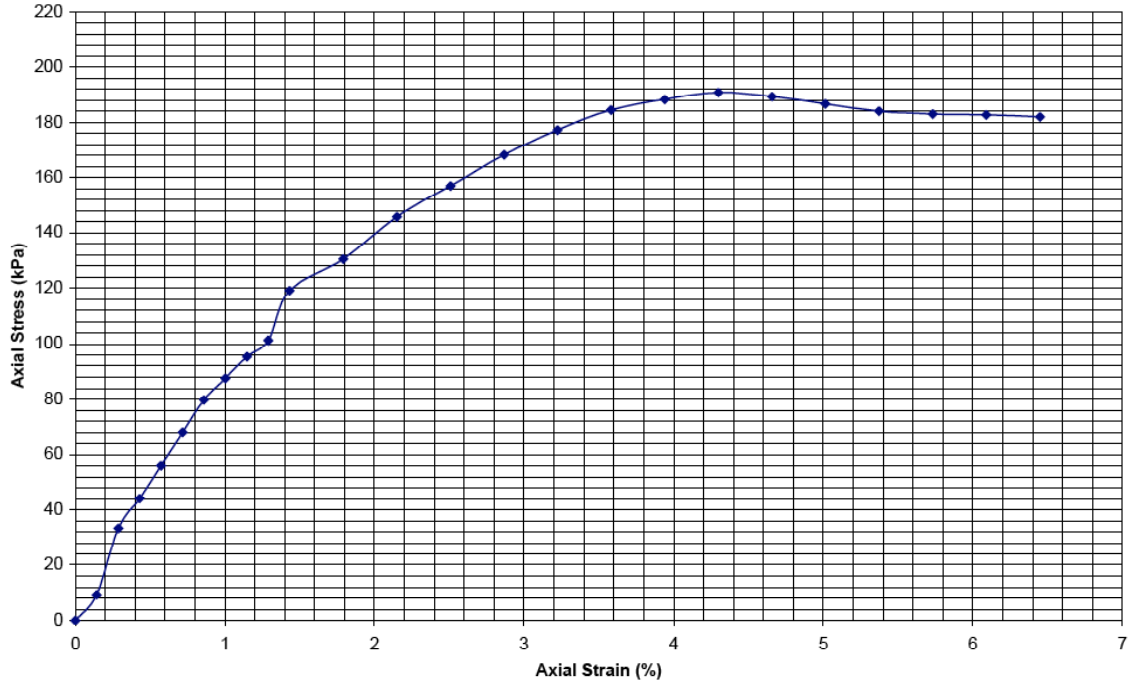
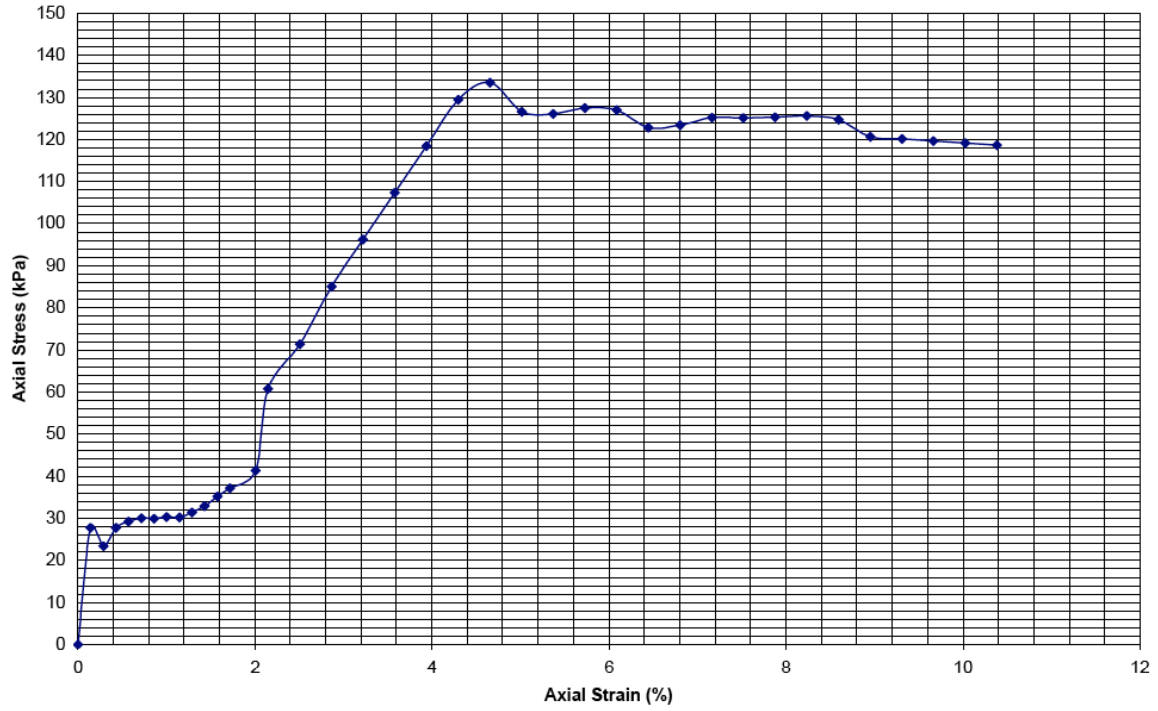
Unconfined Compressive Strength Tests for
Constrained Rise Urethane Foam (3.3 pcf)
- Bottom Section



APPENDIX 2:**TRIAXIAL TEST DATA ON LONGITUDINAL (V) AND
TRANSVERSE (H) CUT URETHANE FOAM (3.1 PCF)****Sample H1 - Confining Pressure 206.8 kPa (30 PSI)****Sample H2 - Confining Pressure 137.9 kPa (20 PSI)**

Sample H6 - Confining Pressure 68.9 kPa (10PSI)**Sample V1 - Confining Pressure 413.7 kPa (60 PSI)**

Sample V2 - Confining Pressure 275.8 kPa (40 PSI)**Sample V3 - Confining Pressure 137.9 kPa (20 PSI)**

Sample V4 - Confining Pressure 137.9 kPa (20 PSI)**Sample V5 - Confining Pressure 137.9 kPa (20PSI)**

APPENDIX 3:**EFFECT OF TEMPERATURE ON URETHANE FOAM COMPRESSION STRENGTH**

Sample	Test Temp (°F)	Dia. (in)	H (in)	Sample weight (g)	Failure Load (lb)	Failure Stress (psi)
1	158	2.24	2.36	7.4158	94	23.8
2	158	2.24	2.40	6.9185	92	23.7
3	158	2.25	2.35	7.3633	77	21.8
4	158	2.19	2.34	7.1387	96	25.6
5	158	2.24	2.38	7.5057	99	25.1
6	194	2.19	2.37	6.8520	66	17.5
7	194	2.24	2.37	7.5126	78	19.8
8	194	2.24	2.36	7.0607	81	20.5
9	194	2.20	2.38	7.4213	79	20.7
10	194	2.22	2.33	6.4271	69	17.9

APPENDIX 4:
THERMAL AGING TEST RESULTS

4A) Dry aging

Sample ID Key: Sample #-Days-Air (A)-Test Temp (°C)

Sample ID	Dia (cm)					Height (cm)					Wt. (g)	% wt. change	Density g/cc	%Density Change	Avg. % Density	SD
	D1 (cm)	D2 (cm)	D3 (cm)	Davg (cm)	SD	H1 (cm)	H2 (cm)	Havg (cm)	SD							
16-1-A-70	5.600	5.642	5.640	5.627	0.0237	6.090	6.100	6.095	0.0050	7.4393		0.0491				
	5.590	5.620	5.732	5.647	0.0748	6.125	6.088	6.107	0.0185	7.4259	-0.1801	0.0486	-1.0726			
17-1-A-70	5.505	5.630	5.574	5.570	0.0626	6.005	6.015	6.010	0.0050	6.9742		0.0477				
	5.506	5.615	5.617	5.579	0.0635	6.015	6.003	6.009	0.0060	6.9588	-0.2208	0.0474	-0.5497	0.0128	1.45	
18-1-A-70	5.528	5.619	5.690	5.612	0.0812	5.990	6.000	5.995	0.0050	7.4650		0.0504				
	5.545	5.584	5.545	5.558	0.0225	5.996	6.004	6.000	0.0040	7.4489	-0.2157	0.0512	1.6600			
19-1-A-90	5.606	5.636	5.600	5.614	0.0193	6.015	6.001	6.008	0.0070	7.0267		0.0473				
	5.628	5.615	5.610	5.618	0.0093	6.018	6.030	6.024	0.0060	7.0086	-0.2576	0.0470	-0.6523			
20-1-A-90	5.660	5.795	5.716	5.724	0.0678	5.960	5.958	5.959	0.0010	7.4294		0.0485				
	5.651	5.750	5.730	5.710	0.0523	5.983	5.956	5.970	0.0135	7.4200	-0.1265	0.0486	0.1639	-0.165	0.43	
21-1-A-90	5.598	5.645	5.620	5.621	0.0235	5.955	5.945	5.950	0.0050	6.6200		0.0449				
	5.580	5.610	5.650	5.613	0.0351	5.955	5.960	5.958	0.0025	6.6099	-0.1526	0.0449	-0.0057			

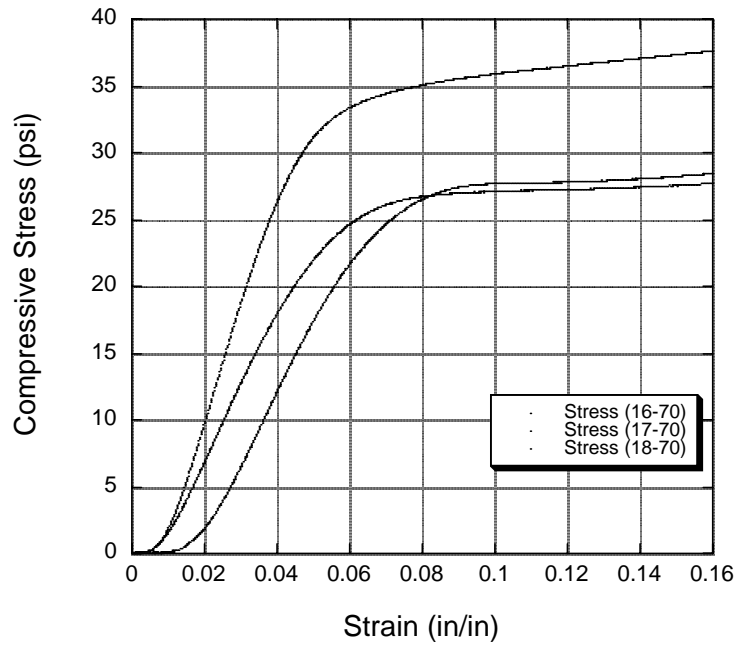
Sample ID	Dia (cm)					Height (cm)					Wt. (g)	% wt. change	Density g/cc	%Density Change	Avg. % Density	SD
	D1 (cm)	D2 (cm)	D3 (cm)	Davg (cm)	SD	H1 (cm)	H2 (cm)	H3 (cm)	Havg (cm)	SD						
S2D-7-A-70	6.144	6.145	6.150	6.146	0.0032	6.065	6.022	6.050	6.046	0.0218	10.2980		0.0574			
	6.155	6.144	6.170	6.156	0.0131	6.085	6.048	6.070	6.068	0.0186	10.2110	-0.8448	0.0566	-1.5250		
S2F-7-A-70	6.157	6.150	6.142	6.150	0.0075	6.074	6.072	6.070	6.072	0.0020	10.6221		0.0589			
	6.152	6.171	6.184	6.169	0.0161	6.082	6.075	6.065	6.074	0.0085	10.5425	-0.7494	0.0581	-1.4030	-1.689	0.394
S2H-7-A-70	6.118	6.160	6.101	6.126	0.0304	6.138	6.102	6.106	6.115	0.0197	10.7668		0.0598			
	6.150	6.184	6.175	6.170	0.0176	6.116	6.112	6.123	6.117	0.0056	10.6891	-0.7217	0.0585	-2.1380		
S2E-7-A-90	6.135	6.145	6.136	6.139	0.0055	6.113	6.170	6.121	6.135	0.0309	10.3702		0.0571			
	6.147	6.180	6.160	6.162	0.0166	6.118	6.136	6.135	6.130	0.0101	10.2731	-0.9363	0.0562	-1.6156		
S2G-7-A-90	6.165	6.152	6.144	6.154	0.0106	6.107	6.139	6.150	6.132	0.0223	10.4382		0.0573			
	6.145	6.151	6.172	6.156	0.0142	6.166	6.175	6.140	6.160	0.0182	10.3443	-0.8996	0.0564	-1.4301	-1.73	0.373
S2I-7-A-90	6.142	6.125	6.114	6.127	0.0141	6.086	6.085	6.090	6.087	0.0026	10.1849		0.0568			
	6.158	6.176	6.135	6.156	0.0206	6.125	6.100	6.105	6.110	0.0132	10.0997	-0.8365	0.0556	-2.1490		

Sample ID	Dia (cm)					Height (cm)					Wt. (g)	% wt. change	Density g/cc	%Density Change	Avg. % Density	SD
	D1 (cm)	D2 (cm)	D3 (cm)	Davg (cm)	SD	H1 (cm)	H2 (cm)	H3 (cm)	Havg (cm)	SD						
S1N-14-A-70	6.174	6.154	6.152	6.160	0.0122	6.076	6.070	6.057	6.068	0.0097	10.129		0.0560			
	6.15	6.16	6.155	6.155	0.0050	6.055	6.058	6.052	6.055	0.0030	10.094	-0.3377	0.0561	0.0332		
S2B-14-A-70	6.144	6.16	6.157	6.154	0.0085	6.103	6.110	6.073	6.095	0.0197	10.594		0.0585			
	6.15	6.179	6.158	6.162	0.0150	6.070	6.092	6.070	6.077	0.0127	10.543	-0.4739	0.0582	-0.4597	-0.201	0.247
SiL-14-A-70	6.16	6.163	6.153	6.159	0.0051	6.120	6.145	6.150	6.138	0.0161	10.286		0.0563			
	6.136	6.175	6.145	6.152	0.0204	6.135	6.134	6.145	6.138	0.0061	10.245	-0.3986	0.0562	-0.1772		
S1M-14-A-90	6.16	6.158	6.145	6.154	0.0081	6.111	6.112	6.102	6.108	0.0055	9.9619		0.0549			
	6.13	6.15	6.14	6.140	0.0100	6.204	6.194	6.232	6.210	0.0197	9.9205	-0.4156	0.0540	-1.5881		
S2A-14-A-90	6.175	6.167	6.149	6.164	0.0133	6.045	6.050	6.050	6.048	0.0029	10.591		0.0587			
	6.166	6.134	6.134	6.145	0.0185	6.087	6.100	6.100	6.096	0.0075	10.53	-0.5722	0.0583	-0.7332	-0.96	0.55
S2C-14-A-90	6.133	6.126	6.155	6.138	0.0151	6.041	6.066	6.040	6.049	0.0147	10.489		0.0586			
	6.133	6.155	6.14	6.143	0.0112	6.065	6.022	6.050	6.046	0.0218	10.44	-0.4671	0.0583	-0.5635		

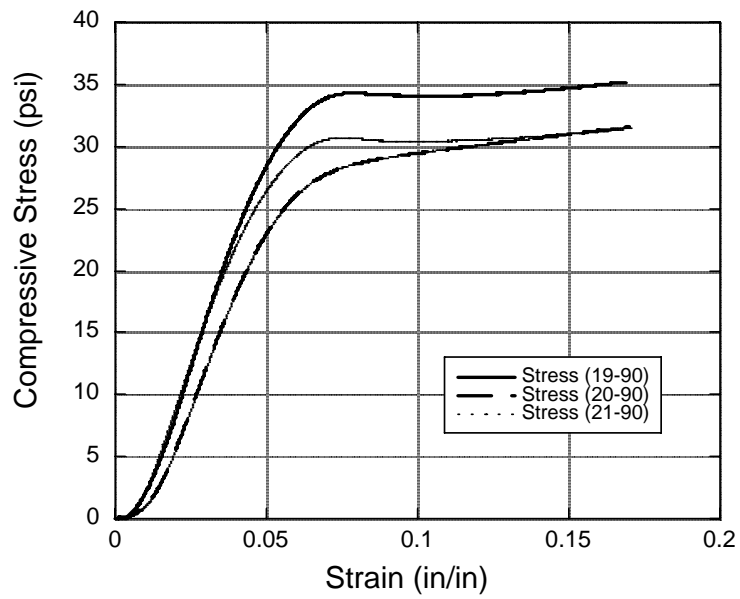
Sample ID	Dia (cm)					Height (cm)					Wt. (g)	% wt. change	Density g/cc	%Density Change	Avg. % Den. Change	SD
	D1 (cm)	D2 (cm)	D3 (cm)	Davg (cm)	SD	H1 (cm)	H2 (cm)	H3 (cm)	Havg (cm)	SD						
31-30-A-70	5.627	5.644	5.656	5.642	0.01457	6.004	5.994		5.999	0.0071	7.3363		0.0489			
	5.65	5.631	5.667	5.649	0.01801	6.069	6.059		6.064	0.0071	7.3214	-0.2031	0.0482	-1.5173		
32-30-A-70	5.715	5.725	5.651	5.697	0.04015	6.005	6.420		6.213	0.2934	7.0432		0.0445			
	5.708	5.64	5.61	5.653	0.05021	6.036	6.055		6.046	0.0134	7.0353	-0.1122	0.0464	4.2635	-0.201	0.247
33-30-A-70	5.535	5.758	5.605	5.633	0.11405	5.985	6.002		5.994	0.0120	7.5282		0.0504			
	5.592	5.7	5.614	5.635	0.05707	6.005	6.013		6.009	0.0057	7.5155	-0.1687	0.0502	-0.5204		
34-30-A-90	5.603	5.578	5.575	5.585	0.01537	5.970	5.978		5.974	0.0057	7.1074		0.0486			
	5.645	5.652	5.533	5.61	0.06678	6.064	6.064		6.064	0.0000	7.0575	-0.7021	0.0471	-3.0342		
35-30-A-90	5.496	5.64	5.636	5.591	0.08201	5.925	5.955		5.940	0.0212	7.1684		0.0492			
	5.623	5.592	5.596	5.604	0.01686	6.040	6.060		6.050	0.0141	7.1361	-0.4506	0.0479	-2.7135	-0.96	0.55
36-30-A-90	5.582	5.73	5.694	5.669	0.07718	6.011	6.020		6.016	0.0064	7.5136		0.0495			
	5.615	5.765	5.665	5.682	0.07638	6.066	6.060		6.063	0.0042	7.4827	-0.4113	0.0487	-1.6431		

Sample ID	Dia (cm)					Height (cm)										
	D1 (cm)	D2 (cm)	D3 (cm)	Davg (cm)	SD	H1 (cm)	H2 (cm)	H3 (cm)	Havg (cm)	SD	Wt. (g)	% wt. change	Density g/cc	%Density Change	Avg. % Den. Change	SD
T2-60-A-70	6.067	6.110	6.103	6.093	0.0231	6.075	6.093	6.07	6.079	0.0121	8.3733		0.0473			
	6.162	6.170	6.166	6.166	0.0040	6.105	6.102	6.107	6.105	0.0025	8.3273	-0.5494	0.0457	-3.2826		
BC2-60-A-70	6.136	6.120	6.143	6.133	0.0118	6.1	6.102	6.11	6.104	0.0053	10.2143		0.0567			
	6.154	6.185	6.168	6.169	0.0155	6.142	6.14	6.155	6.146	0.0081	10.1307	-0.8185	0.0552	-2.6373	-0.201	0.247
TC2-60-A-70	6.112	6.110	6.100	6.107	0.0064	6.095	6.101	6.13	6.109	0.0187	8.5842		0.0480			
	6.130	6.142	6.142	6.138	0.0069	6.165	6.17	6.185	6.173	0.0104	8.5368	-0.5522	0.0468	-2.5748		
T3-60-A-90	6.098	6.105	6.095	6.099	0.0051	6.07	6.07	6.05	6.063	0.0115	8.1963		0.0463			
	6.165	6.175	6.165	6.168	0.0058	6.122	6.127	6.13	6.126	0.0040	8.0988	-1.1896	0.0443	-4.3813		
BC3-60-A-90	6.118	6.132	6.080	6.110	0.0269	6.105	6.1	6.091	6.099	0.0071	8.6263		0.0483			
	6.134	6.168	6.155	6.152	0.0172	6.354	6.345	6.325	6.341	0.0148	8.5432	-0.9633	0.0453	-6.0595	-0.96	0.55
TC3-60-A-90	6.085	6.120	6.098	6.101	0.0177	6.146	6.179	6.16	6.162	0.0166	8.6728		0.0482			
	6.159	6.145	6.165	6.156	0.0103	6.304	6.315	6.301	6.307	0.0074	8.5651	-1.2418	0.0456	-5.2391		

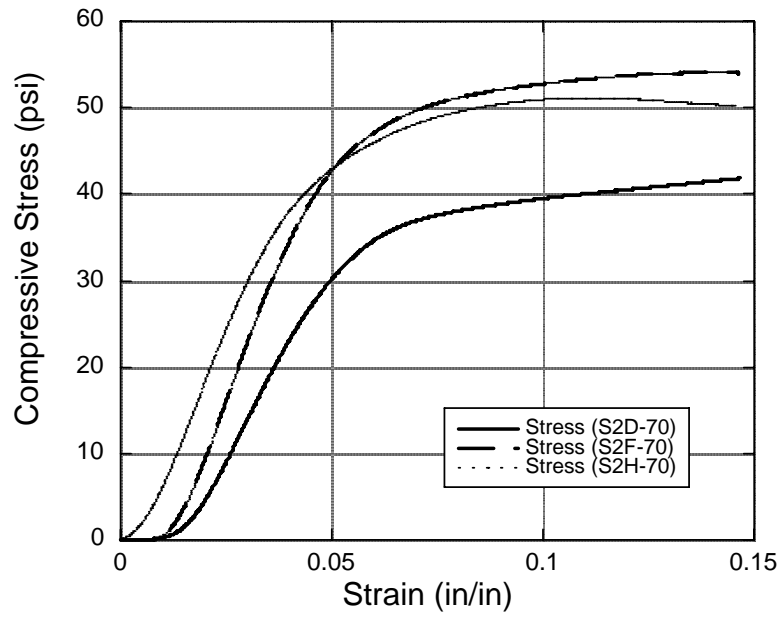
1 day Air aging at 70°C



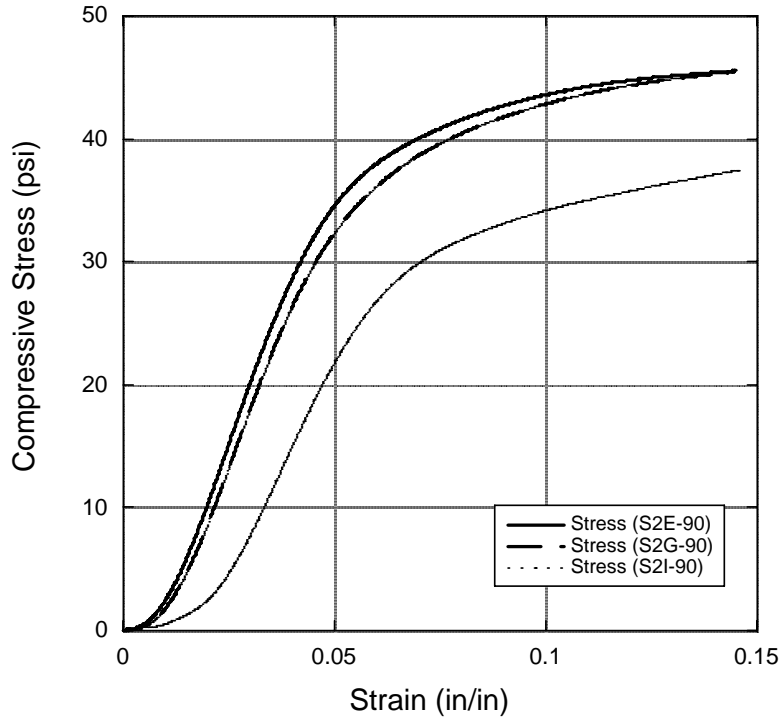
1 day Air Aging 90°C

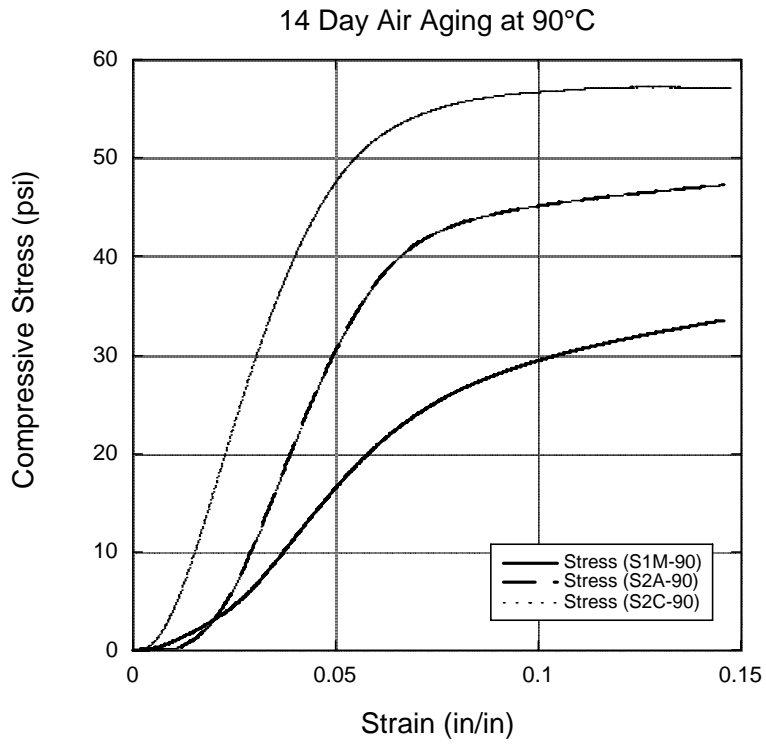
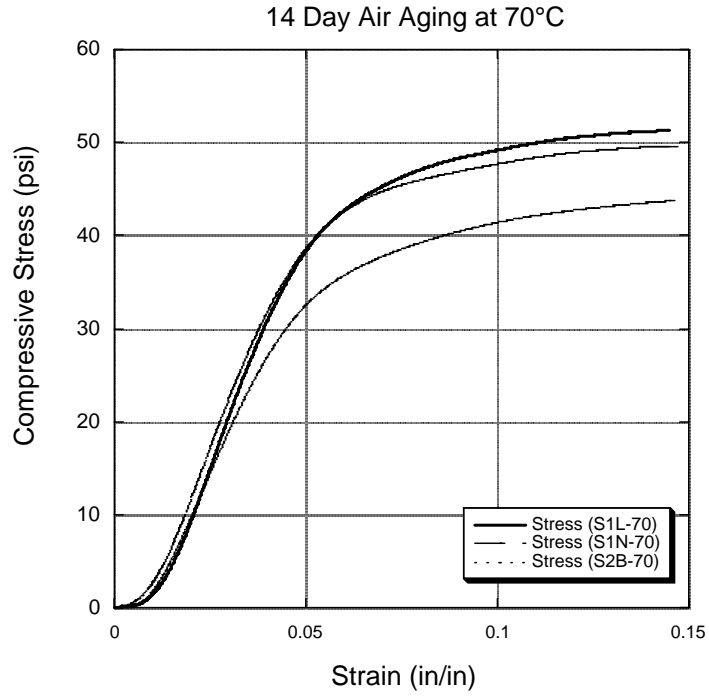


7 day Air Aging at 70°C

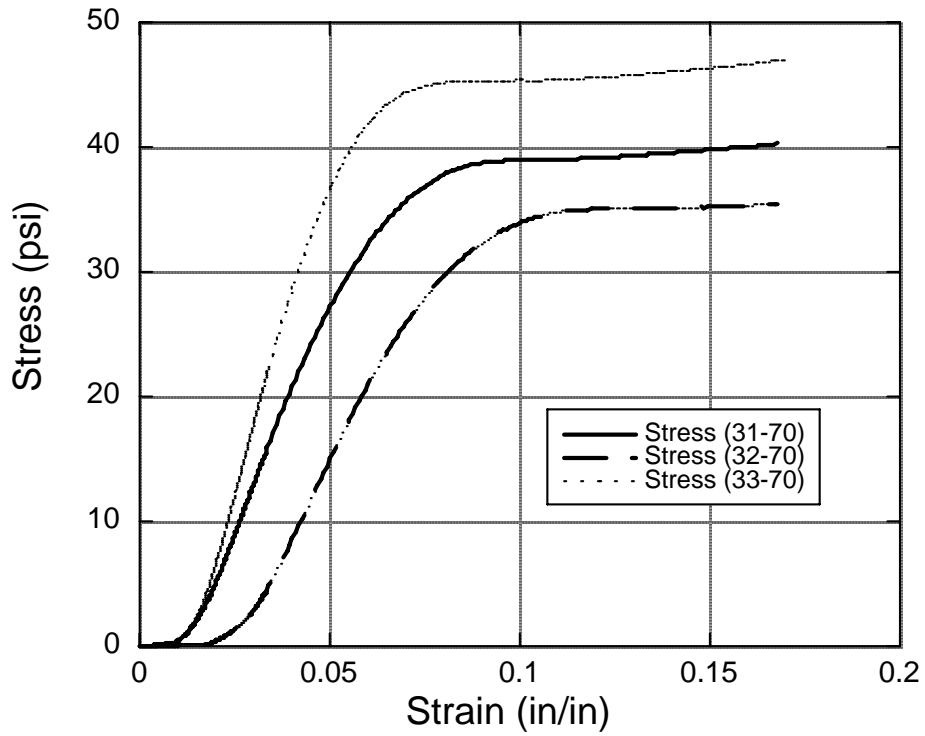


7 Day Air Aging at 90°C

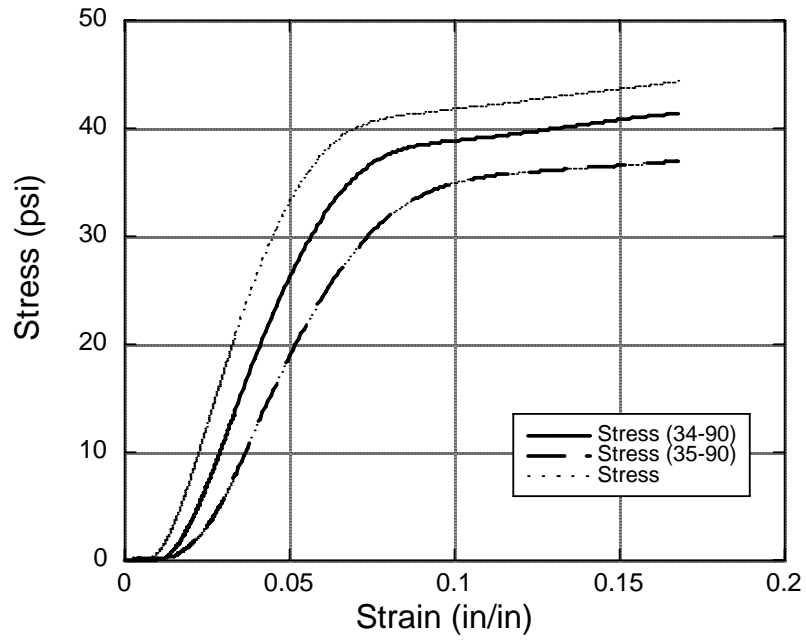




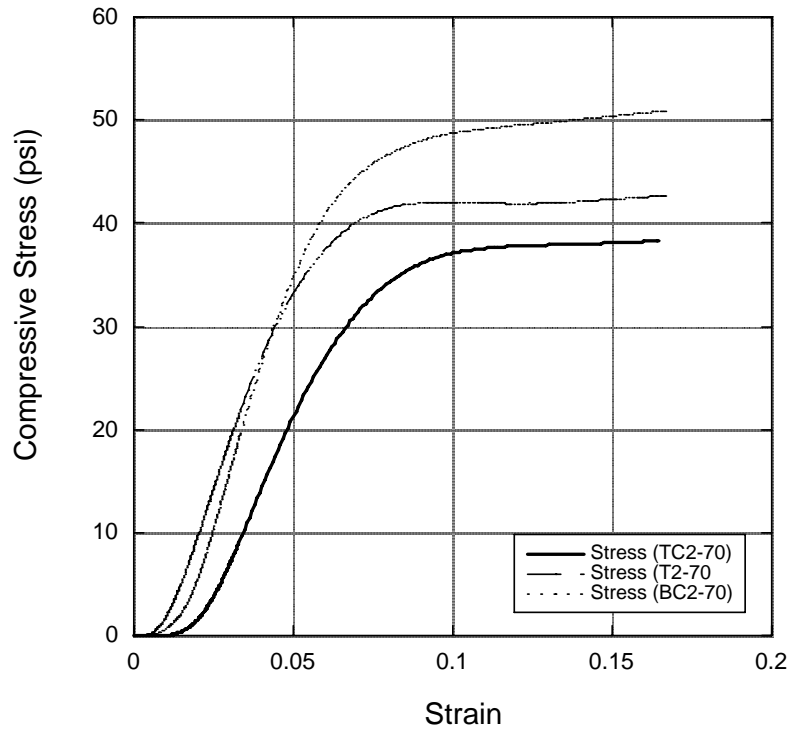
30 Day Air Aging at 70°C



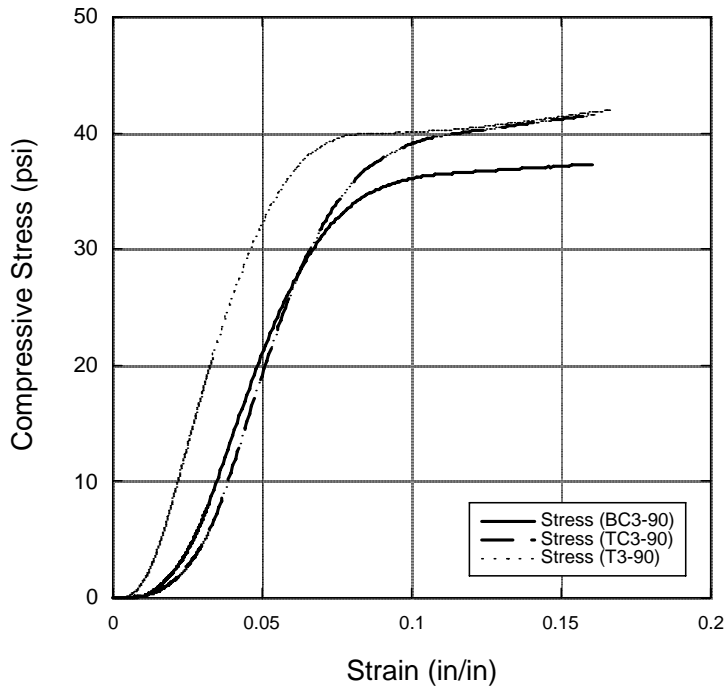
30 Day Air Aging at 90°C



60 day Air aging at 70°C



60 day Air Aging 90°C



4B) Water Aging

Sample ID	Dia (cm)			Dia Avg. SD (cm)		Height (cm)		Ht. Avg. SD (cm)			Weight (g)	% Wt. Change	Density (g/cc)	% Density Change	Avg. Change	SD
1 day water exposure and 5 day drying in air																
7-1-W-R	5.59	5.62	5.455	5.555	0.088	6.085	6.075	6.08	0.005	6.862		0.0466				
	5.53	5.595	5.685	5.603	0.078	6.05	6.068	6.059	0.009	6.88	0.262	0.0461	-1.118			
8-1-W-R	5.617	5.75	5.606	5.658	0.080	5.965	5.98	5.9725	0.0075	7.684		0.0512				
	5.605	5.744	5.659	5.669	0.070	5.965	5.949	5.957	0.008	7.698	0.182	0.0512	0.030	0.61	2.08	
9-1-W-R	5.502	5.63	5.605	5.579	0.068	5.98	5.945	5.9625	0.0175	10.71		0.0735				
	5.505	5.51	5.48	5.498	0.016	5.997	5.945	5.971	0.026	10.72	0.122	0.0757	2.935			
10-1-W-70	5.505	5.614	5.655	5.591	0.078	6.09	6.077	6.0835	0.0065	7.372		0.0494				
	5.505	5.583	5.685	5.591	0.090	6.053	6.051	6.052	0.001	7.427	0.742	0.0500	1.278			
11-1-W-70	5.502	5.622	5.478	5.534	0.077	6.016	6.032	6.024	0.008	6.468		0.0447				
	5.545	5.614	5.422	5.527	0.097	5.992	5.992	5.992	0	7.515	16.187	0.0523	17.104	1.49	0.31	
12-1-W-70	5.6	5.56	5.73	5.630	0.089	5.965	5.955	5.96	0.005	7.04		0.0475				
	5.588	5.73	5.571	5.630	0.087	5.904	5.907	5.9055	0.0015	7.094	0.767	0.0483	1.709			
13-1-W-90	5.505	5.615	5.55	5.557	0.055	6.063	6.045	6.054	0.009	6.727		0.0458				
	5.658	5.554	5.615	5.609	0.052	6.22	6.223	6.2215	0.0015	6.74	0.193	0.0439	-4.315			
14-1-W-90	5.555	5.7	5.62	5.625	0.073	6.045	6.046	6.0455	0.0005	6.941		0.0462				
	5.685	5.679	5.59	5.651	0.053	6.242	6.227	6.2345	0.0075	6.959	0.258	0.0445	-3.685	-4.4	0.71	
15-1-W-90	5.649	5.489	5.614	5.584	0.084	6.072	6.09	6.081	0.009	7.085		0.0476				
	5.8	5.666	5.48	5.649	0.161	6.229	6.293	6.261	0.032	7.084	-0.013	0.0452	-5.098			

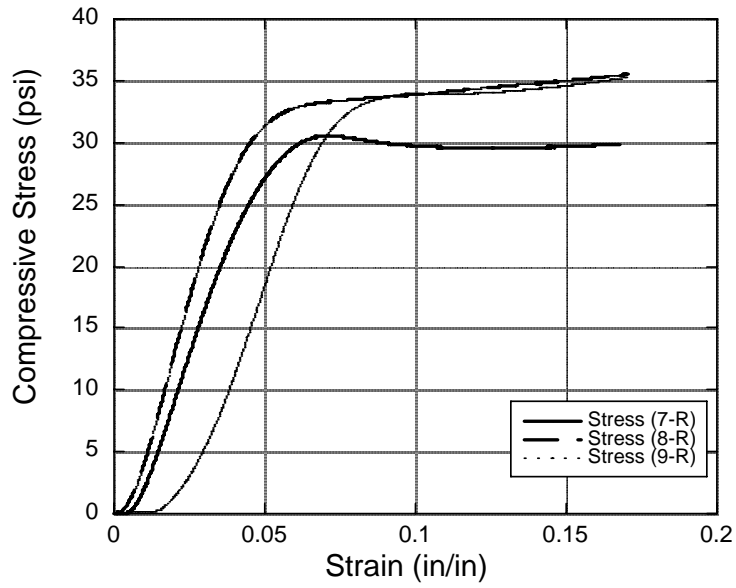
Sample ID	Dia (cm)				Height (cm)											Yield Stress (psi)			
	D1	D2	D3	Davg	SD	H1	H2	H3	Havg	SD	Wt. (g)	% wt. change	Density g/cc	%Density Change	Avg. Den. Change	% Change	SD	Yield Stress (psi)	
7 day water exposure and 5 day drying in air																			
S2J-7-W-R	6.167	6.145	6.080	6.131	0.0452	6.092	6.085	6.065	6.081	0.0140	10.1368		0.0565						
	6.131	6.140	6.124	6.132	0.0080	6.070	6.071	6.070	6.070	0.0006	10.0979	-0.3838	0.0564	-0.2467					41.8
1-7-W-R	5.620	5.730	5.710	5.687	0.0586	5.955	5.965	5.950	5.957	0.0076	7.5102		0.0497						
	5.675	5.723	5.675	5.691	0.0277	5.937	5.928	5.950	5.933	0.0064	7.5123	0.0280	0.0498	0.2825	0.371	0.66			35.88
4-7-W-R	5.510	5.490	5.675	5.558	0.1015	6.070	6.060	6.062	6.064	0.0053	6.6309		0.0451						
	5.499	5.690	5.440	5.543	0.1307	6.040	6.049	6.062	6.045	0.0064	6.6441	0.1991	0.0456	1.0792					28
2-7-W-70	5.480	5.665	5.695	5.613	0.1164	6.025	6.020	6.020	6.023	0.0035	7.3009		0.0490						
	5.690	5.640	5.617	5.649	0.0373	6.450	6.650	6.020	6.550	0.1414	7.3201	0.2630	0.0446	-8.9721					34.3
5-7-W-70	5.540	5.560	5.675	5.592	0.0729	5.970	5.955	5.970	5.963	0.0087	7.1295		0.0487						
	5.487	5.590	5.663	5.580	0.0884	5.940	5.936	5.970	5.938	0.0028	7.1318	0.0323	0.0491	0.8655	-3.196	5.14			34.3
S2K-7-W-70	6.133	6.160	6.155	6.149	0.0144	6.040	6.025	6.065	6.043	0.0202	10.2944		0.0574						
	6.120	6.100	6.130	6.117	0.0153	6.238	6.155	6.175	6.189	0.0433	10.2766	-0.1729	0.0565	-1.4838					35.6
S2L-7-W-90	6.155	6.122	6.100	6.126	0.0277	6.055	6.068	6.055	6.059	0.0075	10.6023		0.0594						
	6.332	6.300	6.262	6.298	0.0350	6.546	6.540	6.055	6.543	0.0042	10.4266	-1.6572	0.0512	-13.8427					44
6-7-W-90	5.585	5.675	5.704	5.655	0.0621	5.942	5.960	5.950	5.951	0.0090	7.2695		0.0487						
	5.977	5.653	5.735	5.788	0.1685	6.385	6.427	6.385	6.399	0.0242	7.0849	-2.5394	0.0421	-13.5053	-14.7	1.05			23.4
3-7-W-90	5.455	5.595	5.565	5.538	0.0737	6.050	6.040	6.055	6.048	0.0076	7.0203		0.0482						
	5.976	5.720	5.723	5.806	0.1469	6.405	6.407	6.055	6.406	0.0014	6.9075	-1.6068	0.0407	-15.4783					26.2

Sample ID	Dia (cm)					Height (cm)					Wt. (g)	% wt. change	Density g/cc	%Density Change	Avg. % Den. Change	SD
	D1 (cm)	D2 (cm)	D3 (cm)	Davg (cm)	SD (cm)	H1 (cm)	H2 (cm)	H3 (cm)	Havg (cm)	SD (cm)						
S1A-14-W-R	6.107	6.13	6.132	6.123	0.0139	6.096	6.056	6.085	6.079	0.0207	10.036		0.0561			
	6.18	6.16	6.15	6.163	0.0153	6.090	6.086	6.075	6.084	0.0078	10.044	0.0717	0.0554	-1.3095		
S1E-14-W-R	6.127	6.145	6.143	6.138	0.0099	6.076	6.076	6.086	6.079	0.0058	10.023		0.0557			
	6.175	6.195	6.175	6.182	0.0115	6.076	6.062	6.095	6.078	0.0166	10.132	1.0905	0.0556	-0.2945	-0.66	0.57
S1G-14-W-R	6.15	6.14	6.15	6.147	0.0058	6.105	6.130	6.100	6.112	0.0161	10.345		0.0571			
	6.185	6.15	6.165	6.167	0.0176	6.100	6.100	6.095	6.098	0.0029	10.352	0.0628	0.0569	-0.3678		
S1B-14-W-70	6.15	6.16	6.15	6.153	0.0058	6.088	6.090	6.103	6.094	0.0081	10.569		0.0584			
	6.165	6.16	6.17	6.165	0.0050	6.255	6.295	6.275	6.275	0.0200	10.565	-0.0388	0.0564	-3.2945		
S1D-14-W-70	6.134	6.114	6.145	6.131	0.0157	6.115	6.110	6.125	6.113	0.0076	10.009		0.0555			
	6.16	6.16	6.16	6.160	0.0000	6.195	6.185	6.150	6.177	0.0236	10.069	0.6025	0.0547	-1.3778	-2.82	1.27
S1H-14-W-70	6.178	6.15	6.152	6.160	0.0156	6.124	6.140	6.126	6.130	0.0087	10.471		0.0573			
	6.19	6.17	6.18	6.180	0.0100	6.335	6.330	6.330	6.332	0.0029	10.473	0.0239	0.0552	-3.7877		
S1C-14-W-90	6.14	6.153	6.141	6.145	0.0072	6.083	6.094	6.095	6.091	0.0067	10.136		0.0561			
	6.135	6.145	6.17	6.150	0.0180	6.470	6.500	6.500	6.490	0.0173	9.7429	-3.8811	0.0506	-9.9517		
S1F-14-W-90	6.15	6.16	6.155	6.155	0.0050	6.120	6.117	6.125	6.121	0.0040	10.318		0.0567			
	6.31	6.325	6.43	6.355	0.0654	6.576	6.605	6.600	6.594	0.0155	10.111	-2.0110	0.0484	-14.6754	-1.03	20.6
S1I-14-W-90	6.115	6.142	6.165	6.141	0.0250	6.080	6.042	6.045	6.056	0.0211	10.089		0.0563			
	6.255	6.245	6.205	6.235	0.0265	6.810	6.885	6.790	6.828	0.0501	9.8485	-2.3828	0.0473	-16.0286		

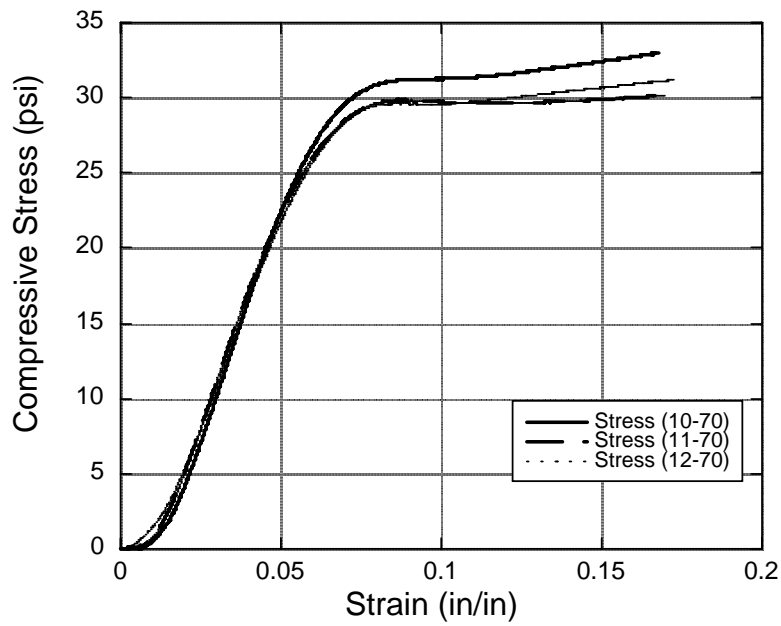
Sample ID	Dia (cm)					Height (cm)					Wt. (g)	% wt. change	Density g/cc	%Density Change	Avg. % Den. Change	SD
	D1 (cm)	D2 (cm)	D3 (cm)	Davg (cm)	SD (cm)	H1 (cm)	H2 (cm)	H3 (cm)	Havg (cm)	SD (cm)						
22-30-W-R	5.662	5.728	5.699	5.696	0.0331	6.030	6.013		6.022	0.0120	7.1199		0.0464			
	5.650	5.750	5.702	5.701	0.0500	6.050	6.053		6.052	0.0021	7.1503	0.4270	0.0463	-0.2228		
23-30-W-R	5.550	5.689	5.603	5.614	0.0701	6.074	6.080		6.077	0.0042	6.8738		0.0457			
	5.542	5.704	5.638	5.628	0.0815	6.070	6.065		6.068	0.0035	6.8955	0.3157	0.0457	-0.0265	-0.66	0.57
24-30-W-R	5.640	5.747	5.745	5.711	0.0612	6.005	6.010		6.008	0.0035	7.4178		0.0482			
	5.615	5.723	5.740	5.693	0.0678	6.036	6.030		6.033	0.0042	7.4695	0.6970	0.0487	0.9065		
25-30-W-70	5.495	5.680	5.570	5.582	0.0931	6.077	6.076		6.077	0.0007	6.8552		0.0461			
	5.601	5.650	5.550	5.600	0.0500	6.250	6.251		6.251	0.0007	6.8120	-0.6302	0.0443	-4.0393		
26-30-W-70	5.670	5.622	5.670	5.654	0.0277	6.030	6.035		6.033	0.0035	7.2335		0.0478			
	5.669	5.580	5.725	5.658	0.0731	6.210	6.205		6.208	0.0035	7.2929	0.8212	0.0468	-2.1596	-2.82	1.27
27-30-W-70	5.615	5.584	5.675	5.625	0.0463	5.926	5.935		5.931	0.0064	7.1290		0.0484			
	5.650	5.565	5.650	5.622	0.0491	6.126	6.110		6.118	0.0113	7.0997	-0.4110	0.0468	-3.3601		
28-30-W-90	5.603	5.640	5.671	5.638	0.0340	6.060	6.051		6.056	0.0064	6.6452		0.0440			
	5.600	5.700	5.500	5.600	0.1000	6.365	6.374		6.370	0.0064	6.4397	-3.0925	0.0411	-6.6152		
29-30-W-90	5.625	5.660	5.715	5.667	0.0454	5.962	5.956		5.959	0.0042	7.2992		0.0486			
	5.825	5.700	5.688	5.738	0.0759	6.420	6.413		6.417	0.0049	7.3028	0.0493	0.0440	-9.3696	-1.03	20.6
30-30-W-90	5.545	5.560	5.570	5.558	0.0126	5.982	6.007		5.995	0.0177	7.1636		0.0493			
	5.840	5.515	5.637	5.664	0.1642	6.710	6.600	6.525	6.612	0.0931	6.9666	-2.7500	0.0418	-15.0870		

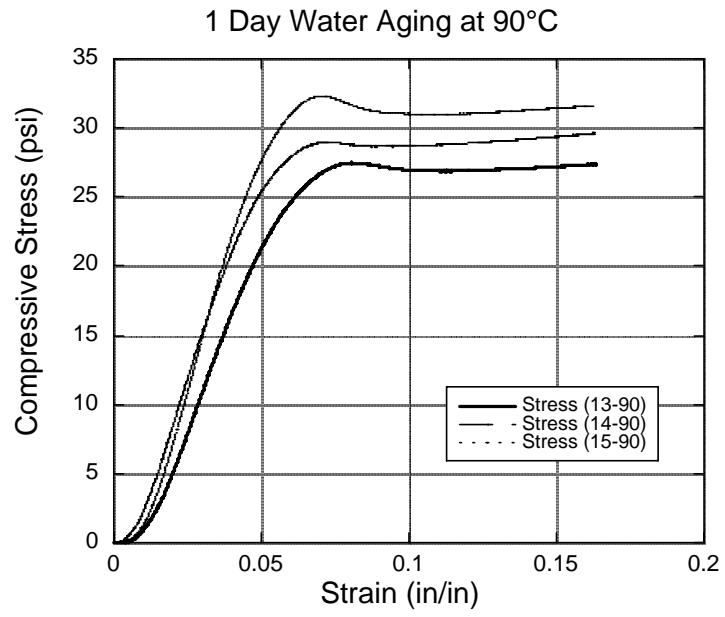
Sample ID	Dia (cm)					Height (cm)					Wt. (g)	% wt. change	Density g/cc	%Density Change	Avg. % Den. Change	SD
	D1 (cm)	D2 (cm)	D3 (cm)	Davg (cm)	SD	H1 (cm)	H2 (cm)	H3 (cm)	Havg (cm)	SD						
T1-60-W-R	6.140	6.125	6.150	6.138	0.0126	6.131	6.145	6.129	6.135	0.0087	10.9430		0.0603			
	6.165	6.205	6.150	6.173	0.0284	6.150	6.145	6.150	6.148	0.0029	10.9024	-0.3710	0.0593	-1.7111		
B1-60-W-R	6.107	6.083	6.084	6.091	0.0136	6.157	6.149	6.15	6.152	0.0044	10.4316		0.0582			
	6.153	6.128	6.170	6.150	0.0211	6.171	6.160	6.167	6.166	0.0056	10.3947	-0.3537	0.0568	-2.4783	-0.66	0.57
TC1-60-W-R	6.110	6.170	6.133	6.138	0.0303	6.130	6.133	6.125	6.129	0.0040	10.4715		0.0578			
	6.160	6.180	6.135	6.158	0.0225	6.150	6.125	6.135	6.137	0.0126	10.4296	-0.4001	0.0571	-1.1857		
T2-60-W-70	6.115	6.116	6.119	6.117	0.0021	6.115	6.130	6.145	6.130	0.0150	10.2932		0.0572			
	6.130	6.200	6.105	6.145	0.0492	6.410	6.390	6.395	6.398	0.0104	10.1664	-1.2319	0.0536	-6.2446		
B2-60-W-70	6.090	6.150	6.115	6.118	0.0301	6.080	6.110	6.108	6.099	0.0168	10.2990		0.0575			
	6.125	6.115	6.145	6.128	0.0153	6.380	6.436	6.381	6.399	0.0320	10.3029	0.0379	0.0546	-4.9579	-2.82	1.27
TC2-60-W-70	6.099	6.095	6.099	6.098	0.0023	6.090	6.125	6.117	6.111	0.0183	10.2556		0.0575			
	6.135	6.135	6.130	6.133	0.0029	6.486	6.350	6.400	6.412	0.0688	10.1170	-1.3515	0.0534	-7.0777		
T3-60-W-90	6.114	6.124	6.116	6.118	0.0053	6.070	6.057	6.055	6.061	0.0081	10.1863		0.0572			
	6.126	6.160	6.120	6.135	0.0216	6.470	6.468	6.400	6.446	0.0398	9.6444	-5.3199	0.0506	-11.4820		
B3-60-W-90	6.093	6.150	6.094	6.112	0.0326	6.098	6.083	6.099	6.093	0.0090	10.0270		0.0561			
	6.160	6.159	6.190	6.170	0.0176	6.400	6.392	6.365	6.386	0.0183	9.4709	-5.5460	0.0496	-11.5374	-1.03	20.6
TC3-60-W-90	6.115	6.095	6.099	6.103	0.0106	6.075	6.076	6.051	6.067	0.0142	10.1218		0.0571			
	6.142	6.185	6.135	6.154	0.0271	6.518	6.517	6.515	6.517	0.0015	9.6675	-4.4883	0.0499	-12.5418		

1 Day Water Aging at RT

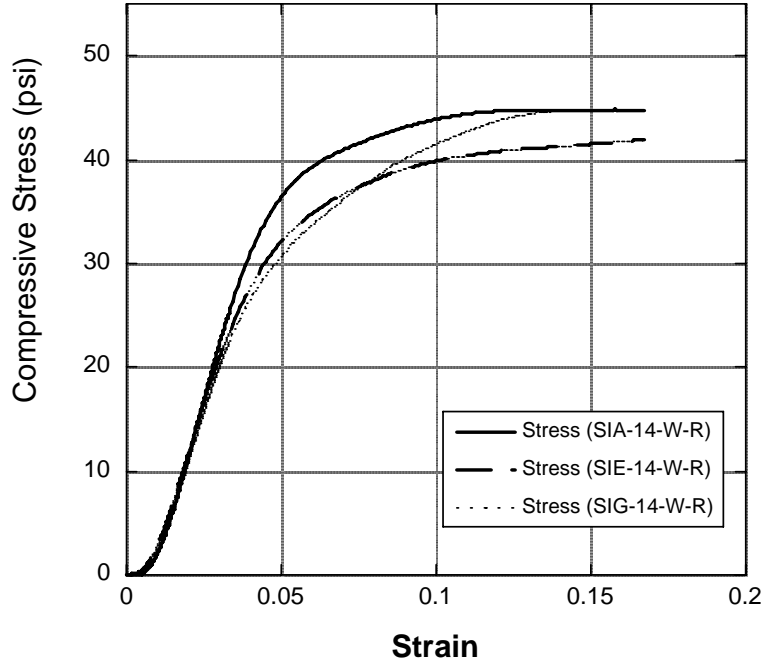


1 Day Water Aging at 70°C

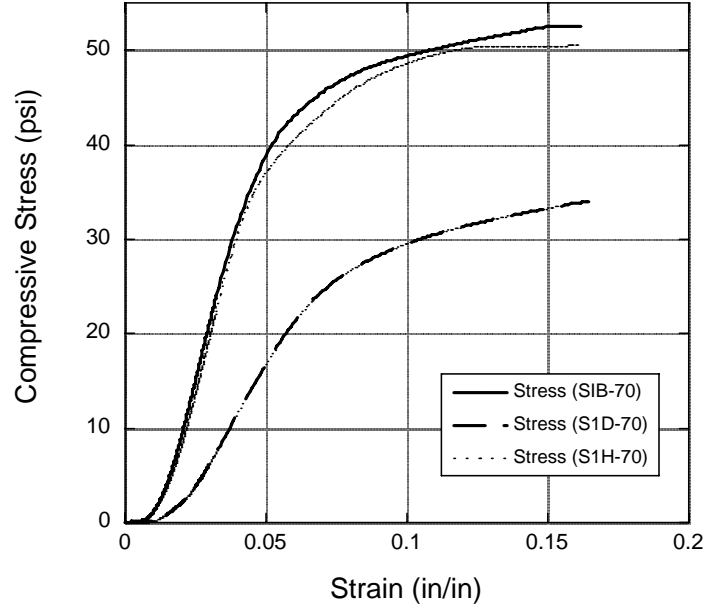




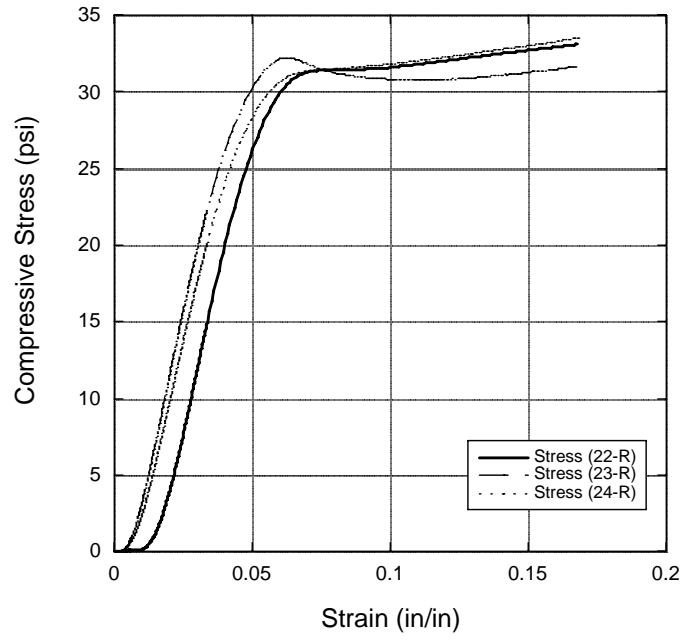
14 day water aging at RT



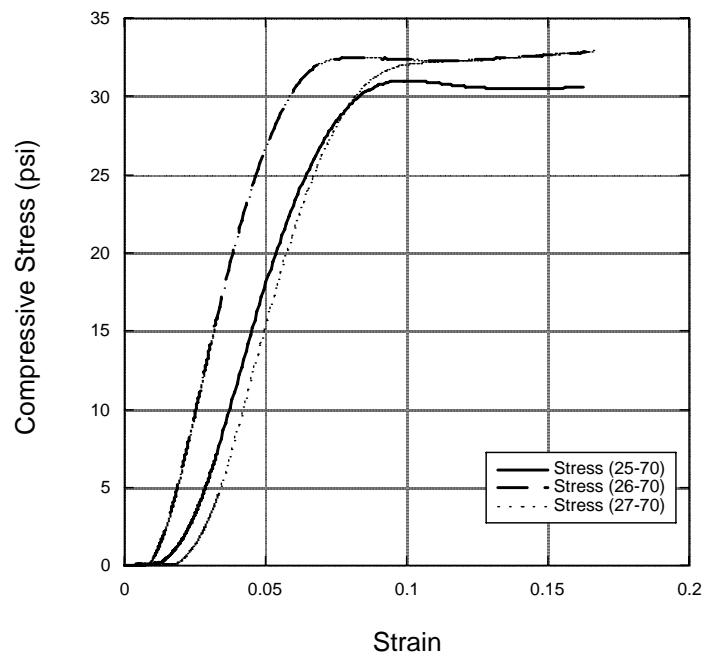
14 day water aging at 70°C

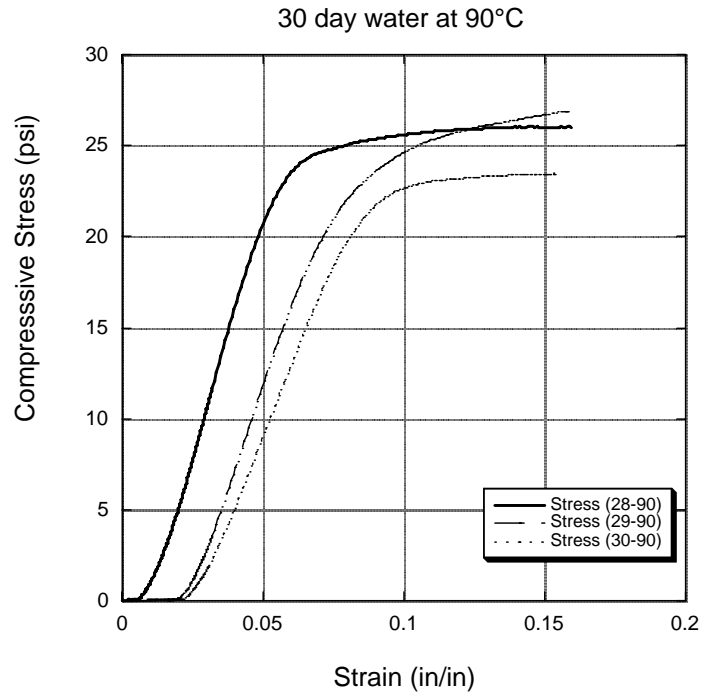


30 day water at RT

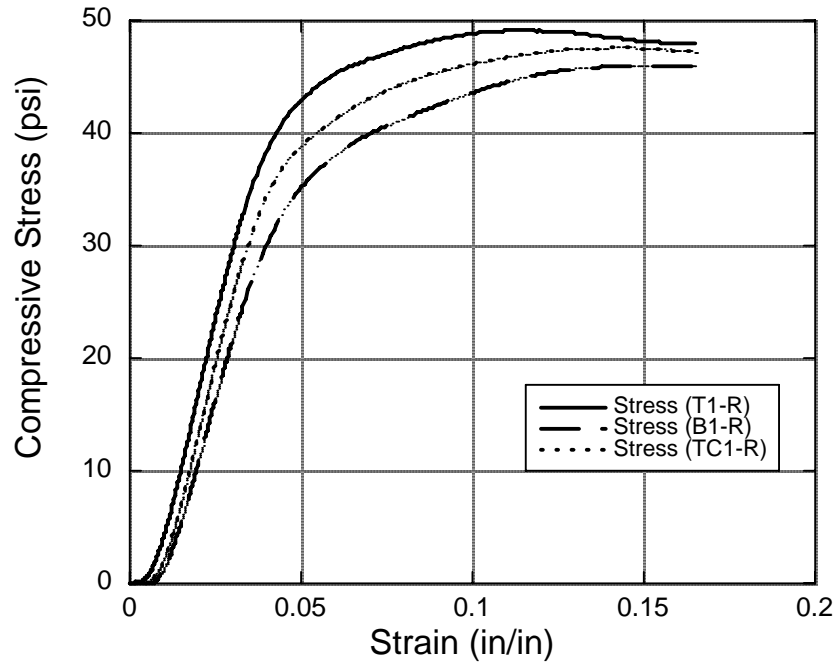


30 day water at 70°C

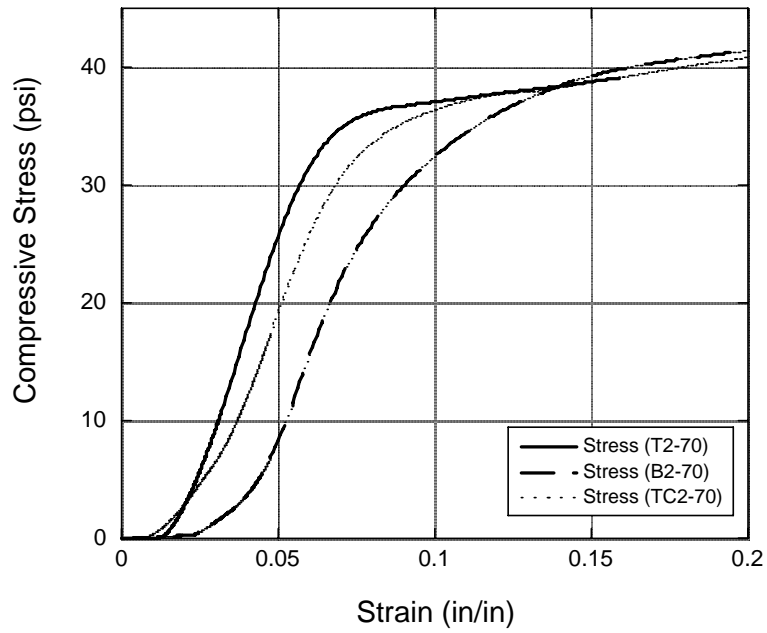


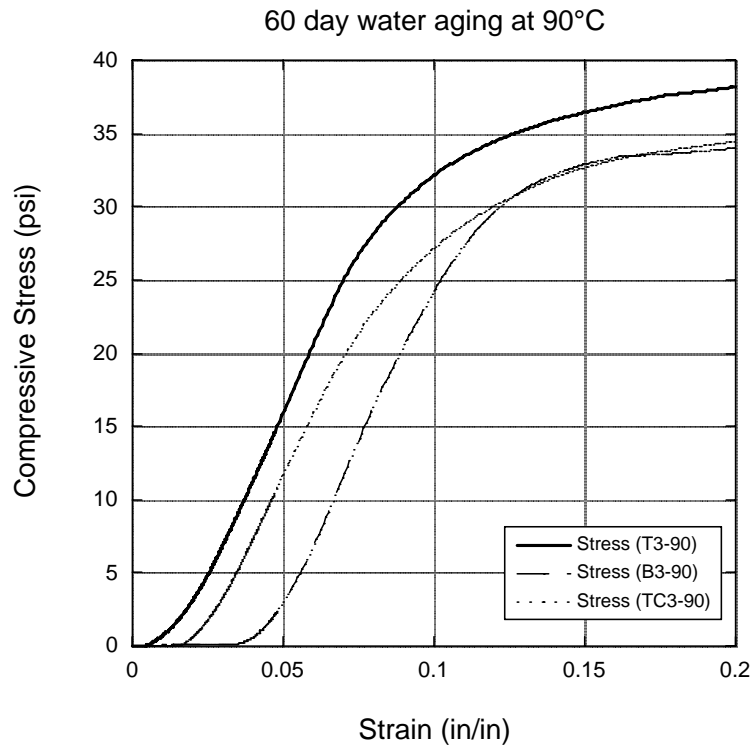


60 Day Water Immersion at RT



60 day water aging at 70°C





APPENDIX 5:

CONFINED COMPRESSION TEST ON 3.1 PCF FOAM

Sample	H1				
Time (min)	Deformation (mm)	Time (min)	Deformation (mm)	Sample Properties	
Pressure	1.1 TSF	Pressure	3.9 TSF		
0	0	0	0		
1	0.61	0.5	2.51		
2	0.61	1	2.76	Weight - gms	4.2
3	0.62	2	4.61	Diameter (cm)	6.25
10	0.62	2.25	4.71	Height (cm)	2.75
16	0.63	2.75	4.97	Sample with Mould (gms)	470.7
30	0.63	3	5.11	Final Height of Sample (cm)	1.88
45	0.63	3.25	5.16		
60	0.63	3.5	5.21	Time (min)	Deformation (mm)
120	0.63	4	5.4	Pressure	4.9 TSF
Pressure	2.3 TSF	4.25	5.49	0	0
0	0	4.5	5.59	1	1.02
1	0.52	5	5.68	2	1.05
2	0.57	5.5	5.79	15	1.08
5	0.57	6	5.89	30	1.1
10	0.57	7	5.98	60	1.1
15	0.57	8	6.19	120	1.1
25	0.58	9	6.29	Pressure	6.3 TSF
40	0.61	10	6.39	0	0
45	0.61	20	8.19	1	0.07
55	0.62	148	10.36	2	0.07
60	0.62	329	10.49	5	0.07
75	0.65	370	10.64	30	0.07
90	0.65	416	10.78	60	0.07
120	0.78	1440	11.01	Pressure	7.4 TSF
240	0.78			0	0
360	0.78			1	0.04
				2	0.05
				5	0.05
				30	0.05
				60	0.11

Sample	H2		
Time (minutes)	Deformation (mm)	Time (minutes)	Deformation (mm)
Pressure	1.1 TSF	Pressure	2.3 TSF
0	0	0	0
1	0.75	1	0.67
2	0.77	2	0.78
3	0.77	3	0.89
4	0.78	4	1.04
8	0.79	5	1.16
9	0.79	6	1.32
10	0.79	7	1.38
15	0.8	8	1.45
21	0.81	9	1.55
25	0.82	10	1.7
30	0.82	11	1.7
45	0.82	12	1.81
60	1.4	13	1.84
90	1.82	14	1.88
240	2.4	15	1.98
360	4.6	16	2
1440	5.82	17	2.09
Pressure	2.3 TSF	18	2.13
0	0	19	2.16
1	0.67	20	2.21
2	0.78	21	2.26
3	0.89	22	2.3
4	1.04	23	2.35
5	1.16	24	2.37
6	1.32	25	2.42
7	1.38	26	2.47
8	1.45	27	2.49
9	1.55	28	2.52
10	1.7	29	2.57
11	1.7	30	2.59
12	1.81	31	2.64
13	1.84	32	2.65
14	1.88	33	2.69
15	1.98	34	2.73
16	2	35	2.76
17	2.09	36	2.77
18	2.13	37	2.81
19	2.16	38	2.82
20	2.21	45	3
21	2.26	60	3.27
22	2.3	900	7
23	2.35		
24	2.37		
25	2.42		
26	2.47		
27	2.49		
28	2.52		
29	2.57		
30	2.59		
31	2.64		
32	2.65		
33	2.69		
34	2.73		
35	2.76		
36	2.77		
37	2.81		
38	2.82		
45	3		
60	3.27		
900	7		

Sample Properties

Weight - gms	4.2
Diameter (cm)	6.24
Height (cm)	2.72
Sample with Mould (gms)	478.2
Final Height of Sample (cm)	1.76

Time (minutes)	Deformation (mm)
Pressure	4.9 TSF
0	0
0.5	0.01
1	0.11
2	0.11
3	0.11
4	0.11
5	0.11
15	0.13
30	0.13
60	0.13
Pressure	6.3 TSF
0	0
0.25	0.07
1	0.08
2	0.08
15	0.09
30	0.09
60	0.09
Pressure	7.4 TSF
0	0
0.5	0.06
1	0.06
2	0.07
10	0.11
30	0.11
60	0.11
Pressure	3.9 TSF
0	0
0.5	0.99
1	1.03
2	1.03
3	1.03
4	1.04
5	1.04
6	1.04
10	1.06
20	1.07
60	1.07
150	1.11
280	1.13
360	1.13
416	1.13

Sample No H3				
Time (Minutes)	Deformation (mm)	Time (Minutes)	Deformation (mm)	Sample Properties
Pressure	1.1 TSF	Pressure	3.9 TSF	
0	0	0	0	
1	0.67	0.5	1.31	Weight - gms 4.1
2	0.69	1	1.39	Diameter (cm) 6.3
3	0.7	2	1.49	Height (cm) 2.8
10	0.71	3	1.54	Sample with Mould (gms) 471.5
15	0.74	4	1.58	Final Height of Sample (cm) 1.73
30	0.75	5	1.63	
45	0.75	6	1.68	
60	1.5	10	1.78	
120	2.34	30	1.82	
1440	4	150	1.89	
		280	1.91	
Pressure	2.3 TSF	360	1.91	
0	0	416	1.91	
2	0.72			
3	0.8	Pressure	4.9 TSF	
4	0.95	0	0	
5	1.18	0.5	0.78	
6	1.22	1	0.78	
7	1.43	5	0.81	
8	1.51	10	0.81	
9	1.56	15	0.81	
10	1.7	60	0.81	
11	1.8	120	0.81	
12	1.9			
13	2.05	Pressure	6.3 TSF	
14	2.11	0	0	
15	2.25	1	0.01	
16	2.35	2	0.01	
30	3	15	0.01	
45	3.5	30	0.01	
60	3.89	60	0.01	
76	4.17			
900	6.17	Pressure	7.4 TSF	
1440	8.19	0	0	
		1	0.01	
		2	0.02	
		5	0.02	
		30	0.04	
		60	0.04	
		120	0.04	

Sample	V1			Sample Properties	
Time (Minutes)	Deformation (mm)	Time (Minutes)	Deformation (mm)	Weight - gms	4
Pressure	1.1 TSF	Pressure	4.9 TSF	Diameter (cm)	6.04
0	0	0	0	Height (cm)	2.58
0.25	0.43	0.5	0.22	Sample with Mould (gms)	470.6
0.5	0.43	1	0.46	Final Height of Sample (cm)	1.7
1	0.44	2	0.48		
2	0.45	3	0.48		
5	0.46	4	0.48		
10	0.46	5	0.49		
15	0.47	10	0.49		
30	0.48	15	0.49		
16	0.49	30	0.49		
120	0.5	60	0.5		
240	0.5	90	0.5		
480	0.5	120	0.5		
Pressure	2.3 TSF	Pressure	6.3 TSF		
0	0	0	0		
0.5	0.24	0.5	0.02		
1	0.29	1	0.02		
2	0.31	2	0.02		
3	0.32	3	0.02		
5	0.33	4	0.02		
7	0.34	5	0.02		
10	0.35	30	0.02		
15	0.36	60	0.02		
30	0.38	Pressure	7.4 TSF		
60	0.4	0	0		
90	0.42	1	0		
120	0.42	2	0		
166	0.45	3	0		
1440	0.55				
Pressure	3.9 TSF				
0	0				
0.25	0.15				
0.5	0.4				
1	0.48				
2	0.54				
4	1.84				
4.5	2.15				
5	2.2				
8	2.93				
10	3.26				
30	4.72				
60	6.93				
120	7.4				
240	10.3				
900	14.43				
1440	14.43				

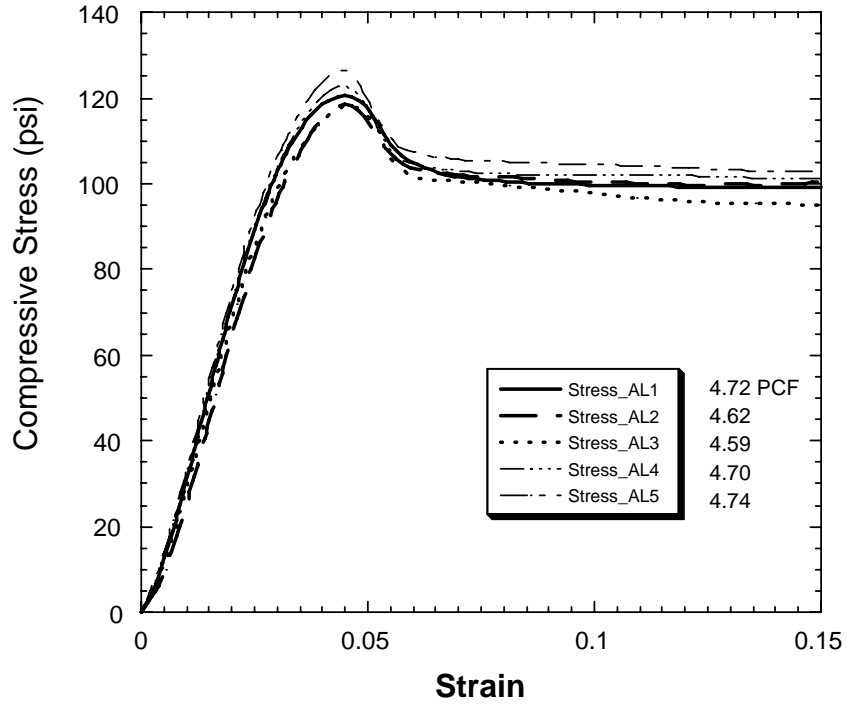
Sample	V2			
Time (Minutes)	Deformation (mm)	Time (Minutes)	Deformation (mm)	Sample Properties
Pressure	1.1 TSF	Pressure	6.3TSF	
0	0	0	0	Weight - gms 4.5
0.25	1.34	1	0.01	Diameter (cm) 6.27
1	1.35	2	0.01	Height (cm) 2.86
5	1.36	5	0.01	Sample with Mould (gms) 471.9
15	1.37	10	0.02	Final Height of Sample (cm) 1.716
30	1.38	30	0.02	
60	1.39	60	0.02	
120	1.39	120	0.02	
Pressure	2.3 TSF	Pressure	7.4 TSF	
0	0	0	0	
0.5	0.21	1	0.01	
1	0.25	5	0.01	
2	0.26	10	0.01	
4	0.27	15	0.01	
5	0.28	30	0.01	
15	0.29	Pressure	4.9 TSF	
30	0.31	0	0	
60	0.32	0.5	0.03	
90	0.32	1	0.15	
120	0.33	2	0.45	
166	0.34	3	1.2	
1440	0.39	4	1.3	
Pressure	3.9 TSF		5	1.5
0	0		6	2.35
0.25	0.14		7	2.65
0.5	0.18		8	3.1
1	0.2		9	3.7
2	0.21		10	4.5
4	0.26		15	6.45
5	0.27		30	7.94
8	0.28		60	10.08
10	0.32		65	10.51
15	0.33		90	11.11
30	0.41		120	11.11
60	0.41	1440	11.11	
90	0.46			
900	2.18			
1440	2.32			

Sample	V3			Sample Properties	
Time (Minutes)	Deformation (mm)	Time (Minutes)	Deformation (mm)		
Pressure	1.1 TSF	Pressure	6.3TSF		
0	0	0	0	Weight - gms	3.8
0.5	0.33	0.5	0.04	Diameter (cm)	6.08
1	0.34	1	0.04	Height (cm)	2.624
3	0.35	4	0.05		
10	0.36	5	0.05	Sample with Mould (gms)	477.8
15	0.37	10	0.05	Final Height of Sample (cm)	1.76
60	0.39	15	0.06		
120	0.4	30	0.06		
240	0.4	Pressure	7.4 TSF		
360	0.4	0	0		
Pressure	2.3 TSF	0.5	0.04		
0	0	5	0.05		
0.5	0.45	15	0.06		
1	0.55	30	0.07		
2	0.58	45	0.08		
3	0.6	60	1.14		
5	0.61	90	1.14		
6	0.63	120	1.14		
10	0.66	Pressure	4.9 TSF		
15	0.66	0	0		
30	0.73	0.25	3.04		
60	0.77	1	3.06		
90	0.77	2	3.07		
166	0.77	3	3.07		
1440	1.59	4	3.07		
Pressure	3.9 TSF	5	3.07		
0	0	10	3.08		
0.25	3.91	15	3.11		
0.5	4.9	30	3.12		
1	5.6	60	3.13		
2	6.5	90	3.14		
4	7.09	120	3.14		
4.5	7.16	240	3.14		
5	7.2				
8	7.29				
10	7.32				
30	7.49				
60	8.61				
900	9.48				

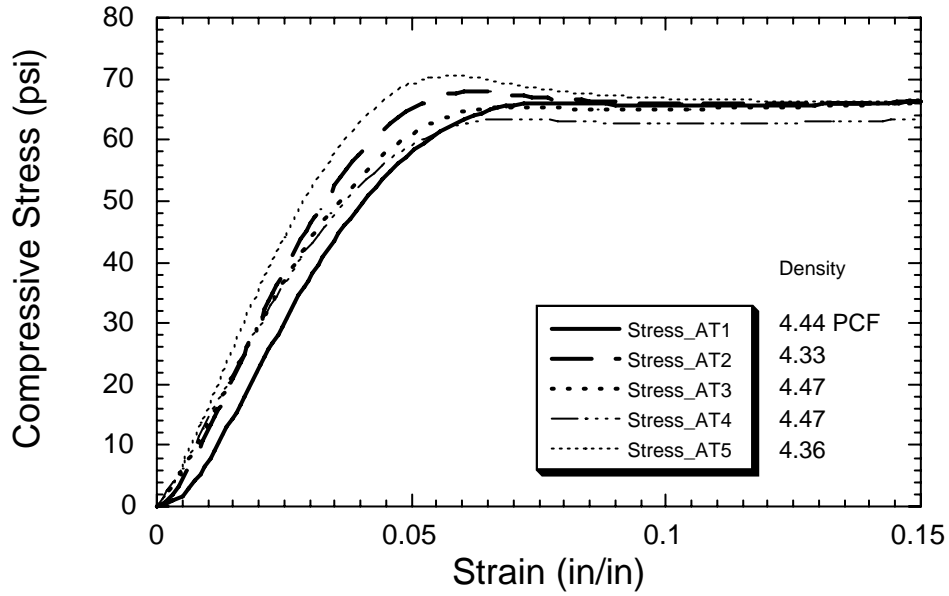
APPENDIX 6:

**COMPRESSION AND CREEP TESTING DATA (NEW HIGHER DENSITY FOAMS)
UNCONFINED COMPRESSION TESTS**

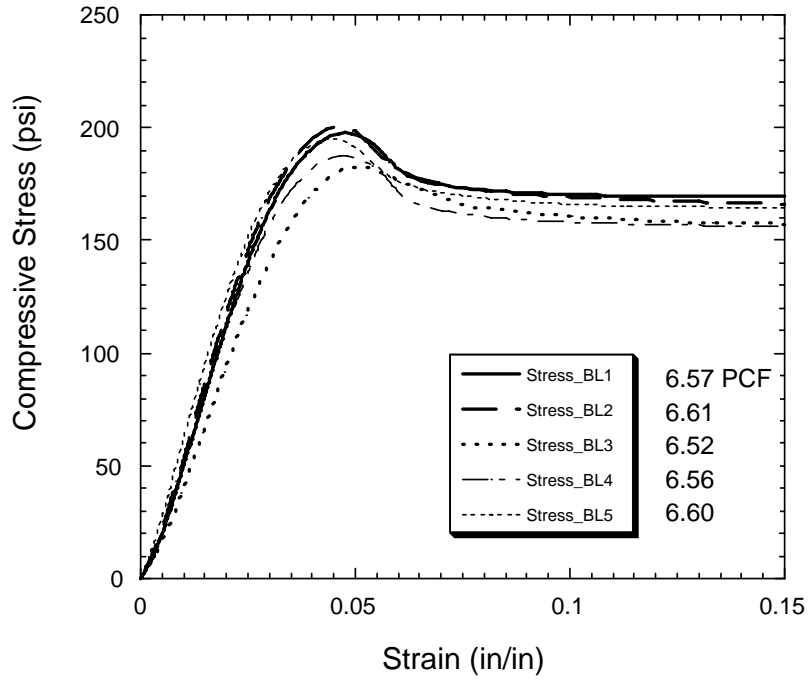
Foam A - Longitudinal



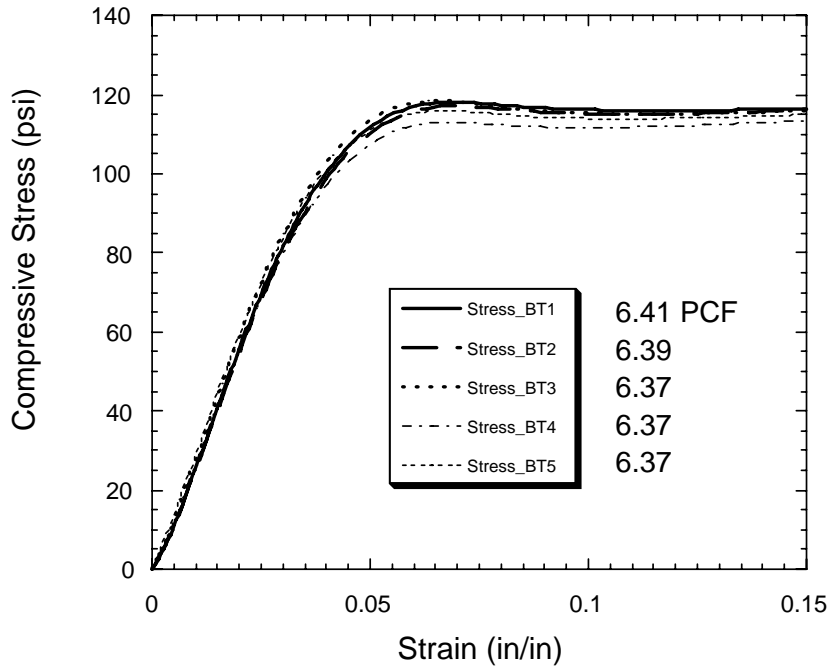
Foam A - Transverse



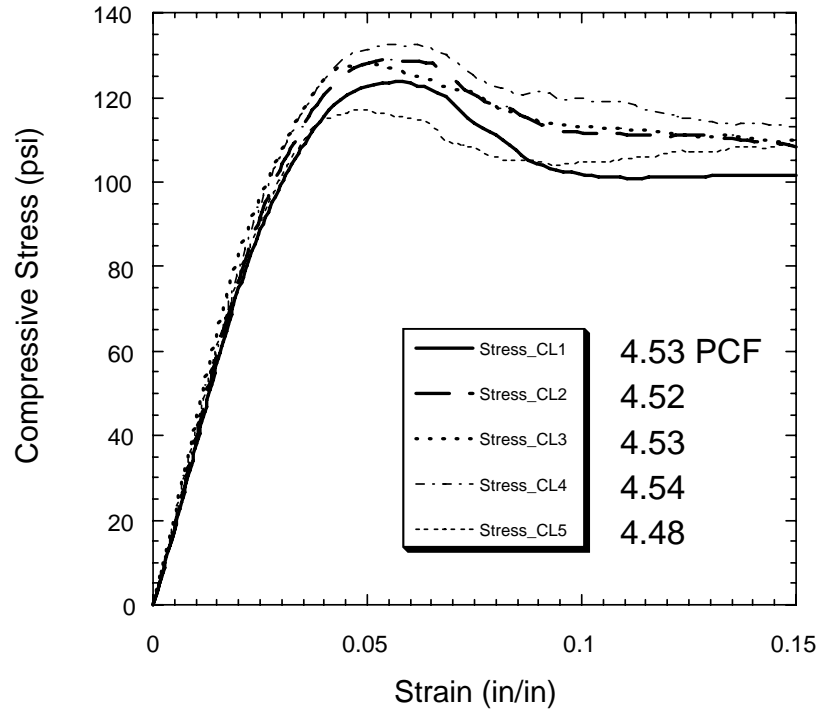
Foam B - Longitudinal



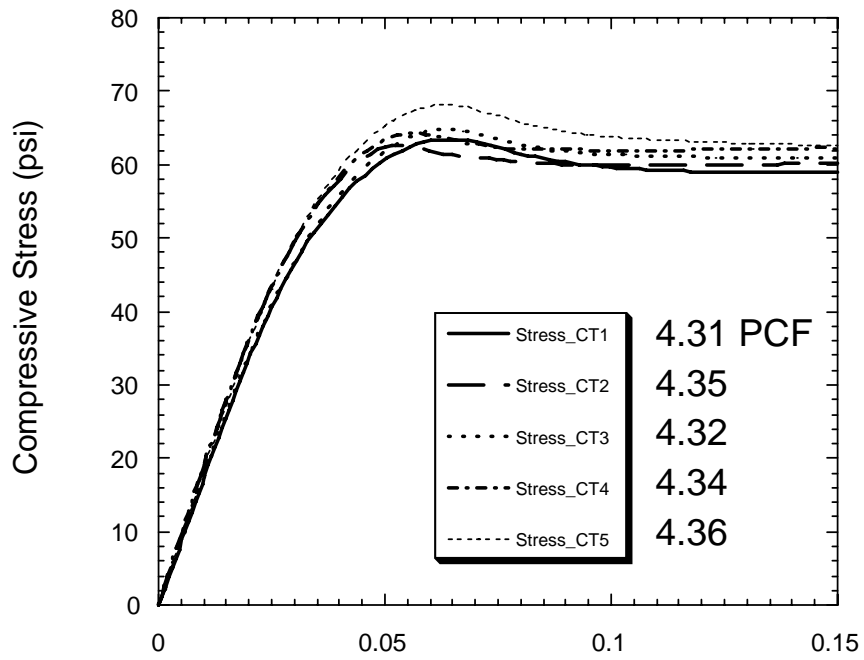
Foam B - Transverse



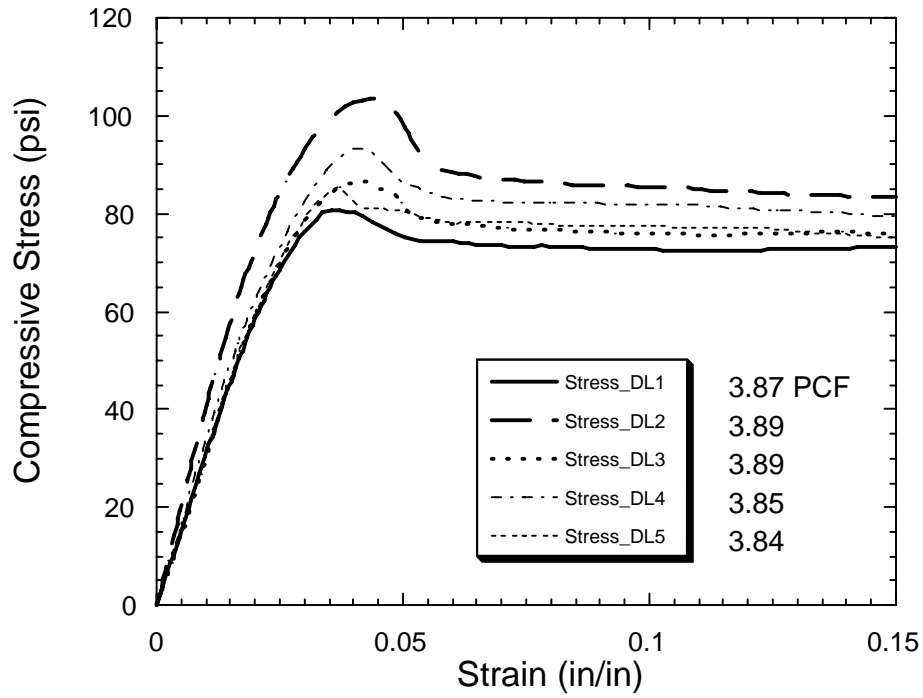
Foam C - Longitudinal



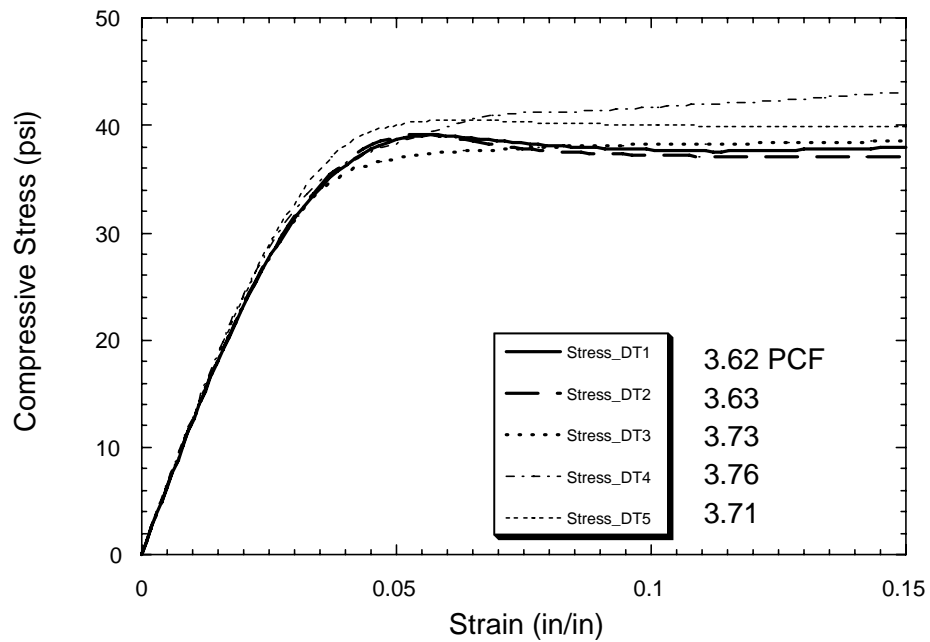
Foam C - Transverse



Foam D - Longitudinal



Foam D - Transverse



Confined Creep Testing: 64 psi (4.6 tsf)

BL-4				
dia.	6.3 cm			
h		2.608	2.58	2.6 cm
wt.	8.7414 gm			
Pressure	4.6 TSF			

Time (min)	deflection (mm)	Time (h)	Strain (%)
0	0	0.000	0.000
2	0.98	0.033	3.775
4	0.99	0.067	3.814
9	1	0.150	3.852
12	1.01	0.200	3.891
19	1.02	0.317	3.929
26	1.028	0.433	3.960
38	1.031	0.633	3.971
53	1.04	0.883	4.006
60	1.042	1.000	4.014
113	1.055	1.883	4.064
244	1.075	4.067	4.141
522	1.124	8.700	4.330
1350	1.152	22.500	4.438
1674	1.156	27.900	4.453
2918	1.166	48.633	4.492
3151	1.175	52.517	4.526
3464	1.181	57.733	4.549
4332	1.192	72.200	4.592
5001	1.197	83.350	4.611
5799	1.2	96.650	4.622
8440	1.216	140.667	4.684
10609	1.226	176.817	4.723
11545	1.236	192.417	4.761

STOPPED

BT-4				
dia.	6.3 cm			
h		2.644	2.636	2.636 cm
wt.		8.5785		
Pressure	4.6 TSF			

Time (min)	deflection (mm)	Time (h)	Strain (%)
0	0	0.000	0.000
2	0.96	0.033	3.639
4	0.97	0.067	3.677
8	0.98	0.133	3.715
15	0.99	0.250	3.753
30	1.01	0.500	3.829
60	1.02	1.000	3.867
123	1.03	2.050	3.904
222	1.04	3.700	3.942
720	1.08	12.000	4.094
1074	1.1	17.900	4.170
1450	1.11	24.167	4.208
2206	1.15	36.767	4.359
2758	1.23	45.967	4.663
2978	1.52	49.633	5.762
4321	1.55	72.017	5.876
5080	1.58	84.667	5.989
6539	1.58	108.983	5.989
8466	1.59	141.100	6.027
9348	1.6	155.800	6.065
10834	1.62	180.567	6.141
12269	1.63	204.483	6.179
14417	1.64	240.283	6.217
15200	1.642	253.333	6.224
16746	1.65	279.100	6.255
18321	1.65	305.350	6.255
19467	1.655	324.450	6.274
20930	1.67	348.833	6.331
22347	1.68	372.450	6.368
23915	1.715	398.583	6.501

STOPPED

AL-4					
dia.	6.3 cm				
h		2.62	2.61	2.630	2.62 cm
wt.	6.1279 gm				
Pressure	4.6 TSF				

Time (min)	deflection (mm)	Time (h)	Strain (%)
0	0	0.00	0.000
2	0.557	0.03	2.126
4	0.575	0.07	2.195
8	0.586	0.13	2.237
15	0.595	0.25	2.271
30	0.617	0.50	2.355
47	0.622	0.78	2.374
92	0.642	1.53	2.450
220	0.677	3.67	2.584
484	0.69	8.07	2.634
1308	0.737	21.80	2.813
1579	0.74	26.32	2.824
2820	0.765	47.00	2.920
3055	0.777	50.92	2.966
3368	0.785	56.13	2.996
4293	0.799	71.55	3.050
4965	0.807	82.75	3.080
5763	0.814	96.05	3.107
8403	0.845	140.05	3.225
10574	0.855	176.23	3.263
11508	0.885	191.80	3.378

STOPPED

AT-4

dia.	6.3 cm		
h		2.636	2.642 cm
wt.	8.7414 gm		
Pressure	4.6 TSF		

Time (min)	deflection (mm)	Time (h)	Strain (%)
0	0	0	0.000
2	1.69	0.033	6.404
4	1.79	0.067	6.783
6	1.92	0.100	7.275
13	2.08	0.217	7.882
28	2.32	0.467	8.791
58	2.62	0.967	9.928
133	3.13	2.217	11.861
223	3.61	3.717	13.679
718	6.15	11.967	23.304

STOPPED

AT-5

dia.	6.3 cm		
h		2.53	2.53
wt.		5.8	2.53 cm
Pressure	4.6 TSF		

Time (min)	deflection (mm)	Time (h)	Strain (%)
0	0	0.00	0.000
2	0.9	0.03	3.557
4	1.48	0.07	5.850
8	2	0.13	7.905
15	2.33	0.25	9.209
30	2.75	0.50	10.870
60	3.05	1.00	12.055
120	4.06	2.00	16.047
240	5.21	4.00	20.593
360	6.95	6.00	27.470
561	7.75	9.35	30.632
720	8.1	12.00	32.016

Creep Testing at 75 psi (5.4 tsf)

BL-5 Jay
 dia. 6.3 cm
 h 2.574 2.574 2.574 2.574 cm
 wt. 8.5 gm
 Pressure 5.4 TSF Dial reading 4.7

Time (min)	deflection (mm)	Strain (%)	Time (h)
0	0	0.00	4/19/06 0.00
2	0.67	2.60	4/19/06 0.03
4	0.68	2.64	4/19/06 0.07
8	0.69	2.68	4/19/06 0.13
15	0.7	2.72	4/19/06 0.25
30	0.71	2.76	4/19/06 0.50
60	0.72	2.80	4/19/06 1.00
120	0.74	2.87	4/19/06 2.00
240	0.75	2.91	4/19/06 4.00
360	0.77	2.99	4/19/06 6.00
531	0.77	2.99	4/19/06 8.85
720	0.79	3.07	4/19/06 12.00
1440	0.8	3.11	4/20/06 24.00
2880	0.83	3.22	4/21/06 48.00
4315	0.84	3.26	4/22/06 71.92
6241	0.85	3.30	4/23/06 104.02
7128	0.86	3.34	4/24/06 118.80
8614	0.88	3.42	4/25/06 143.57
10049	0.9	3.50	4/26/05 167.48
12194	0.9	3.50	4/27/06 203.23
12978	0.9	3.50	4/28/06 216.30
14524	0.9	3.50	4/29/06 242.07
16108	0.9	3.50	4/30/06 268.47
17253	0.9	3.50	1-May 287.55
18717	0.92	3.57	5/2/06 311.95
20134	0.925	3.59	5/3/06 335.57
21702	0.945	3.67	5/4/06 361.70
23014	0.96	3.73	5/5/06 383.57
24113	0.96	3.73	5/6/06 401.88
26070	0.96	3.73	5/7/06 434.50
27353	0.96	3.73	5/8/06 455.88
28785	0.96	3.73	5/9/06 479.75
30234	0.96	3.73	5/10/06 503.90
31655	0.96	3.73	5/11/06 527.58
33177	0.98	3.81	5/12/06 552.95
34987	0.98	3.81	5/13/06 583.12
36424	0.98	3.81	5/14/06 607.07
37403	0.98	3.81	5/15/06 623.38
38843	0.98	3.81	5/16/06 647.38
46043	0.99	3.85	5/18/06 767.38
46738	0.99	3.85	5/19/06 778.97

49687	0.99	3.85	5/21/06	828.12
51215	1	3.89	5/22/06	853.58
52707	1	3.89	5/23/06	878.45
54001	1	3.89	5/24/06	900.02
55601	1	3.89	5/25/06	926.68
56889	1	3.89	5/26/06	948.15
58694	1	3.89	5/27/06	978.23
59830	1	3.89	5/28/06	997.17
61133	1	3.89	5/29/06	1018.88
62490	1.01	3.92	5/30/06	1041.50
63938	1.01	3.92	31-May	1065.63
67214	1.02	3.96	6/2/06	1120.23
69829	1.025	3.98	6/4/06	1163.82
71049	1.03	4.00	6/5/06	1184.15
72490	1.03	4.00	6/6/06	1208.17
73918	1.03	4.00	6/7/06	1231.97
75369	1.03	4.00	6/8/06	1256.15
76794	1.03	4.00	6/9/06	1279.90
78536	1.04	4.04	6/10/06	1308.93
81145	1.04	4.04	6/12/06	1352.42
82564	1.04	4.04	6/13/06	1376.07
84023	1.04	4.04	6/14/06	1400.38
85419	1.04	4.04	6/15/06	1423.65
86945	1.04	4.04	6/16/06	1449.08
89007	1.04	4.04	6/18/06	1483.45

BT-5 Jay
 dia. 6.3 cm
 h 2.67 2.67 2.67 2.67 cm
 wt. 8.7 gm
 Pressure 5.4 TSF Dial reading 4.7

Time (min)	deflection (mm)	Strain (%)	Time (h)
0	0.00	0.00	4/25/06 0.00
2	0.25	0.94	4/25/06 0.03
4	0.31	1.16	4/25/06 0.07
8	0.33	1.24	4/25/06 0.13
15	0.35	1.31	4/25/06 0.25
30	0.40	1.50	4/25/06 0.50
60	0.42	1.57	4/25/06 1.00
126	0.45	1.69	4/25/06 2.10
240	0.48	1.80	4/25/06 4.00
360	0.52	1.95	4/25/06 6.00
608	0.55	2.06	4/25/06 10.13
720	0.56	2.10	4/25/06 12.00
1422	0.59	2.21	4/26/06 23.70
3568	0.72	2.70	4/27/06 59.47
4350	0.74	2.77	4/28/06 72.50
5898	0.76	2.85	4/29/06 98.30
7483	0.78	2.92	30-Apr 124.72
7559	0.78	2.92	4/30/06 125.98
8629	0.85	3.17	5/1/06 143.82
10092	0.86	3.23	5/2/06 168.20
11509	0.92	3.44	5/3/06 191.82
13076	0.98	3.67	5/4/06 217.93
14388	0.99	3.72	5/5/06 239.80
16206	1.01	3.79	5/6/06 270.10
17439	1.02	3.83	5/7/06 290.65
18722	1.08	4.03	5/8/06 312.03
20154	1.08	4.03	5/9/06 335.90
21603	1.08	4.05	5/10/06 360.05
23024	1.08	4.05	5/11/06 383.73
24546	1.08	4.05	5/12/06 409.10
26356	1.08	4.05	5/13/06 439.27
27792	1.08	4.05	5/14/06 463.20
28771	1.08	4.05	5/15/06 479.52
30227	1.15	4.30	5/16/06 503.78
33140	1.17	4.40	5/18/06 552.33
34556	1.18	4.41	5/19/06 575.93
37504	1.19	4.45	5/21/06 625.07
39030	1.20	4.49	5/22/04 650.50
40473	1.20	4.50	5/23/06 674.55
41772	1.20	4.51	5/24/06 696.20
43355	1.20	4.51	5/025/06 722.58

44645	1.21	4.54	5/26/06	744.08
46449	1.21	4.55	5/27/06	774.15
47585	1.22	4.58	5/28/06	793.08
48963	1.24	4.63	5/29/06	816.05
50359	1.24	4.66	5/30/06	839.32
51817	1.25	4.69	5/31/06	863.62
55095	1.28	4.78	6/2/06	918.25
57715	1.28	4.79	6/4/06	961.92
58932	1.28	4.80	6/5/06	982.20
60375	1.37	5.12	6/6/06	1006.25
61803	1.37	5.13	6/7/06	1030.05
63254	1.37	5.13	6/8/06	1054.23
64679	1.37	5.13	6/9/06	1077.98
66421	1.37	5.13	6/10/06	1107.02
69030	1.37	5.13	6/12/06	1150.50
70449	1.37	5.13	6/13/06	1174.15
71908	1.37	5.13	6/14/06	1198.47
73304	1.43	5.34	6/15/06	1221.73
74830	1.43	5.35	6/16/06	1247.17
76892	1.44	5.40	6/18/06	1281.53

BT-6 Jay
 dia. 6.3 cm
 h 2.550 2.556 2.540 2.549 cm
 wt. 7.9 gm
 Pressure 5.4 TSF Dial reading 4.7

Time (min)	deflection (mm)	Time (h)	Strain (%)	
0	0.000	0.000	0.000	5/4/06
2	1.270	0.033	4.984	5/4/06
4	1.285	0.067	5.044	5/4/06
8	1.316	0.133	5.164	5/4/06
15	1.331	0.250	5.224	5/4/06
30	1.349	0.500	5.293	5/4/06
60	1.369	1.000	5.373	5/4/06
180	1.440	3.000	5.652	5/4/06
252	1.453	4.200	5.702	5/4/06
360	1.458	6.000	5.722	5/4/06
480	1.463	8.000	5.742	5/4/06
701	1.483	11.683	5.822	5/4/06
1273	1.496	21.217	5.872	5/5/06
3092	1.585	51.533	6.220	5/6/06
4326	1.603	72.100	6.290	5/7/06
5608	1.608	93.467	6.310	5/8/06
7039	1.608	117.317	6.310	5/9/06
8489	1.608	141.483	6.310	5/10/06
9910	1.638	165.167	6.430	5/11/06
11436	1.656	190.600	6.500	5/12/06
13246	1.666	220.767	6.539	5/13/06
14682	1.671	244.700	6.559	5/14/06
15661	1.674	261.017	6.569	5/15/06
17118	1.681	285.300	6.599	5/16/06
19998	1.720	333.300	6.749	5/18/06
20696	1.722	344.933	6.759	5/19/06
23644	1.735	394.067	6.809	5/21/06
25171	1.750	419.517	6.868	5/22/06
26663	1.753	444.383	6.878	5/23/06
27961	1.755	466.017	6.888	5/24/06
29559	1.755	492.650	6.888	5/25/06
30848	1.755	514.133	6.888	5/26/06
32653	1.760	544.217	6.908	5/27/06
33789	1.775	563.150	6.968	5/28/06
35169	1.781	586.150	6.988	5/29/06
36531	1.793	608.850	7.038	5/30/06
37989	1.796	633.150	7.048	5/31/06
41144	1.821	685.733	7.147	6/2/06
43943	1.821	732.383	7.147	6/4/06
45160	1.821	752.667	7.147	6/5/06
46603	1.824	776.717	7.157	6/6/06

48031	1.824	800.517	7.157	6/7/06
49482	1.831	824.700	7.187	6/8/06
50907	1.836	848.450	7.207	6/9/06
52649	1.849	877.483	7.257	6/10/06
55257	1.859	920.950	7.297	6/12/06
56676	1.859	944.600	7.297	6/13/06
58136	1.859	968.933	7.297	6/14/06
59532	1.885	992.200	7.397	6/15/06
61058	1.890	1017.633	7.417	6/16/06
64560	1.900	1075.993	7.457	6/18/06
65988	1.908	1099.808	7.486	6/19/06
66781	1.913	1113.024	7.506	6/20/06
68278	1.913	1137.971	7.506	6/21/06
69721	1.915	1162.024	7.516	6/22/06
71038	1.923	1183.966	7.546	6/23/06
72734	1.930	1212.227	7.576	6/24/06
74670	1.930	1244.493	7.576	6/25/06
75506	1.930	1258.425	7.576	6/26/06
77589	1.935	1293.156	7.596	6/27/06
78686	1.941	1311.433	7.616	6/28/06
80507	1.946	1341.785	7.636	6/29/06
81134	1.948	1352.228	7.646	6/30/06
82955	1.948	1382.589	7.646	7/1/06
84753	1.951	1412.543	7.656	7/2/06
85464	1.953	1424.403	7.666	7/3/06
86995	1.958	1449.924	7.686	7/4/06
88314	1.958	1471.907	7.686	7/5/06
89848	1.958	1497.471	7.686	7/6/06
91243	1.958	1520.719	7.686	7/7/06
93070	1.961	1551.171	7.696	7/8/06
94727	1.961	1578.784	7.696	7/9/06
95508	1.961	1591.794	7.696	7/10/06
96984	1.963	1616.395	7.706	7/11/06
98399	1.966	1639.991	7.716	7/12/06
99838	1.966	1663.959	7.716	7/13/06
101316	1.967	1688.603	7.721	7/14/06
104144	1.976	1735.731	7.756	7/16/06
105613	1.979	1760.213	7.766	7/17/06
107096	1.984	1784.936	7.785	7/18/06
108481	1.994	1808.016	7.825	7/19/06

BL-6	Jay			
dia.	6.3 cm			
h		2.572	2.576	2.574 cm
wt.	8.5 gm			
Pressure	5.4 TSF	Dial reading 4.7		

Time (min)	deflection (mm)	Time (h)	Strain (%)	
0	0.000	0.000	0.000	5/4/2006
2	1.267	0.033	4.924	5/4/06
4	1.276	0.067	4.959	5/4/06
8	1.288	0.133	5.003	5/4/06
15	1.298	0.250	5.043	5/4/06
30	1.311	0.500	5.092	5/4/06
60	1.321	1.000	5.131	5/4/06
180	1.346	3.000	5.230	5/4/06
252	1.354	4.200	5.260	5/4/06
360	1.356	6.000	5.269	5/4/06
480	1.361	8.000	5.289	5/4/06
701	1.361	11.683	5.289	5/4/06
1273	1.361	21.217	5.289	5/5/06
3092	1.361	51.533	5.289	5/6/06
4326	1.361	72.100	5.289	5/7/06
5608	1.427	93.467	5.546	5/8/06
7039	1.427	117.317	5.546	5/9/06
8489	1.427	141.483	5.546	5/10/06
9910	1.427	165.167	5.546	5/11/06
11436	1.427	190.600	5.546	5/12/06
13246	1.427	220.767	5.546	5/13/06
14682	1.427	244.700	5.546	5/14/06
15661	1.427	261.017	5.546	5/15/06
17118	1.427	285.300	5.546	5/16/06
19998	1.427	333.300	5.546	5/18/06
20696	1.427	344.933	5.546	5/19/06
23644	1.539	394.067	5.980	5/21/06
25171	1.542	419.517	5.990	5/22/06
26663	1.544	444.383	6.000	5/23/06
27961	1.544	466.017	6.000	5/24/06
29559	1.544	492.650	6.000	5/25/06
30848	1.544	514.133	6.000	5/26/06
32653	1.547	544.217	6.010	5/27/06
33789	1.547	563.150	6.010	5/28/06
35169	1.549	586.150	6.019	5/29/06
36531	1.557	608.850	6.049	5/30/06
37989	1.560	633.150	6.059	5/31/06
41144	1.575	685.733	6.118	6/2/06
43943	1.575	732.383	6.118	6/4/06
45160	1.577	752.667	6.128	6/5/06
46603	1.580	776.717	6.138	6/6/06

48031	1.580	800.517	6.138	6/7/06
49482	1.580	824.700	6.138	6/8/06
50907	1.585	848.450	6.158	6/9/06
52649	1.590	877.483	6.177	6/10/06
55257	1.590	920.950	6.177	6/12/06
56676	1.590	944.600	6.177	6/13/06
58136	1.591	968.933	6.182	6/14/06
59532	1.593	992.200	6.187	6/15/06
61058	1.593	1017.633	6.187	6/16/06
64560	1.593	1075.992	6.187	6/18/06
65989	1.593	1099.816	6.187	6/19/06
66781	1.593	1113.022	6.187	6/20/06
68280	1.593	1137.992	6.187	6/21/06
69721	1.595	1162.018	6.197	6/22/06
71038	1.598	1183.971	6.207	6/23/06
72734	1.600	1212.230	6.217	6/24/06
74669	1.600	1244.491	6.217	6/25/06
75506	1.600	1258.431	6.217	6/26/06
77589	1.600	1293.151	6.217	6/27/06
78686	1.600	1311.429	6.217	6/28/06
80507	1.600	1341.789	6.217	6/29/06
81134	1.600	1352.225	6.217	6/30/06
82955	1.600	1382.583	6.217	7/1/06
84753	1.600	1412.550	6.217	7/2/06
85464	1.600	1424.396	6.217	7/3/06
86996	1.600	1449.929	6.217	7/4/06
88314	1.600	1471.899	6.217	7/5/06
89848	1.600	1497.460	6.217	7/6/06
91243	1.600	1520.722	6.217	7/7/06
93070	1.600	1551.175	6.217	7/8/06
94727	1.600	1578.789	6.217	7/9/06
95508	1.600	1591.797	6.217	7/10/06
96984	1.605	1616.393	6.237	7/11/06
98399	1.605	1639.990	6.237	7/12/06
99837	1.605	1663.954	6.237	7/13/06
101316	1.605	1688.603	6.237	7/14/06
104150	1.605	1735.829	6.237	7/16/06
105613	1.605	1760.213	6.237	7/17/06
107096	1.605	1784.929	6.237	7/18/06
108481	1.605	1808.018	6.237	7/19/06

APPENDIX 7:

BIODEGRADATION LITERATURE REVIEW

A7.1 Introduction

Polyurethane, which is a type of plastic, has been widely used for almost half a century in the health, automotive, and industrial fields. The unique chemical and physical properties of PU give it a range of characteristics and a wide range of applications in these fields. Many types of PU are polymers with diverse end use in the form of coatings, adhesives, constructional materials, fibers, elastomers, padding, paints, and medical implants. PUs could also be used in the environmental field, in the form of foams, for many remediation applications as an isolation material to prevent the release of hazardous materials into the environment. Hence, this class of materials has received wide attention for their synthesis, morphology, and chemical and mechanical properties (Chen et al., 2000).

Polyurethanes are synthesized from three basic components: a diisocyanate, a polyglycol, and an extender, usually a low-molecular-weight diol, diamine, or water. If the extender is a diol, the polyurethane consists entirely of urethane linkages. If the extender is water or diamine, both urethane and urea linkages are present, and the polyurethane is termed a “polyurethane urea.”

Polyurethanes are produced using low-molecular-weight prepolymers, i.e., various block copolymers. The terminal hydroxyl group allows for alternating blocks, called “segments,” to be inserted into the PU chain. Blocks providing rigid crystalline phase and containing isocyanate and the chain extender are referred to as “hard segments.” Those yielding generally either noncrystalline or a low crystallinity phase and containing polyester/polyether are called “soft segments.” Commercially, these block polymers are known as segmented PUs (Young and Lovell, 1994; Fried, 1995).

The morphology of polyurethane is a function of the following variables: structure of the soft segment, chain length of the soft segment, structure of the diisocyanate monomer, structure and chain length of the chain extender, amount and chain length of the hard segment, segment compatibility, type of the catalyst blowing agent, and thermal history (Frisch, 1997).

A7.2 Chemical Structure and Properties of PUs

PU is a polymer that has repeated units of a urethane moiety as shown in Fig. A7.1.

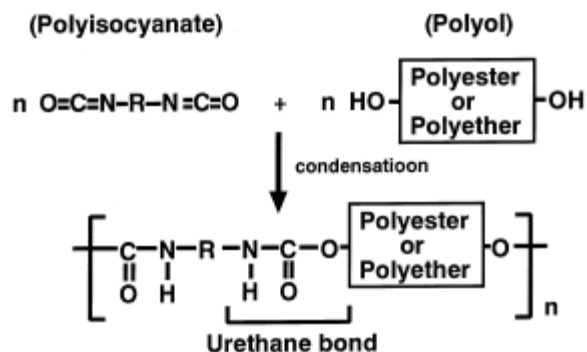


FIGURE A7.1 Structure of polyurethane (Nakajima-Kambe et al., 1999)

The simplest formula for PU is linear and represented by

$$(\text{R1} - \text{R2})_n$$

where:

n = number of repetitions

R1 = hydrocarbon containing the OH group, or soft segment, with a low glass transition temperature (i.e., $< 25^\circ\text{C}$)

R2 = hydrocarbon chain

It is possible to produce different kinds of PUs just by variations in the R group and substitutions of the amide hydrogen. As PU contains repeated urethane groups, other moieties also may be included, for example, urea, ester, ether (Saunders and Frisch, 1964) (Table A7.1). Urethane linkage is due to the synthesis by condensation of one isocyanate, $-\text{N}=\text{C}=\text{O}$, with an alcohol, $-\text{OH}$ (Dombrow, 1957; Kaplan et al., 1968). The hydrogen atom of the hydroxyl group is transferred to the nitrogen atom of the isocyanate (Bayer, 1947). PUs are usually classified into polyether and polyester polyurethanes, depending upon the group of polyols used as the soft segment during the synthesis (Urbansky et al., 1977; Ruiz et al., 1999).

One of the factors which determine the properties of the polymer is the ratio of hard and soft segments. Generally, the hard segment contributes to hardness, tensile strength, impact resistance, stiffness, and modulus. On the other hand, the soft segment contributes to water absorption, elongation, elasticity, and softness. Modification of these segments might result in changes in the degree of tensile strength and elasticity. Hence, it is possible to produce versatile PU polymers whose properties can be easily modified by varying their molecular structures of soft segment and hard segment (Zhang et al., 2003).

TABLE A7.1 Raw materials used during the synthesis of PUs

Polyisocyanate	2,4-Toluene diisocyanate (2,4-TDI) 2,4-TDI/2,6-TDI (80/20 mixture) 4-4'-Diphenylmethane diisocyanate 1,3-Xylylene diisocyanate Hexamethylene diisocyanate 1,5-Naphthalene diisocyanate
Polyol	
Polyester-type	Poly(butylene adipate) Poly(ethylene butylene adipate) Poly(ethylene adipate) Polycaprolactone Poly(propylene adipate) Poly(ethylene propylene adipate)
Polyol	
Polyether-type	Poly(oxytetramethylene) glycol Poly(oxypropylene) glycol Poly(oxypropylene)-poly(oxyethylene) glycol
Chain extension or crosslinking agent	1,4-Butanediol Ethylene glycol 2,2-Dimethyl-1,3-propanediol Trimethylolpropane 1,2,6-Hexanetriol 1,3- Butanediol Glycerol

Inorganic particles including talc, mica, SiO₂ and CaCO₃ are usually used during the synthesis as fillers to improve the properties of PUs, but limited improvements in the mechanical properties of PUs have been limited because of their larger size or small amount in aspect ratio (Zhang et al., 2003). Linear PUs are generally used in the production of fibers and molding (Urbanski et al., 1977); otherwise, flexible ones are used to produce coatings and binding agents (Saunders and Frisch, 1964). Modifications in the spacing, within branch chains, and also variations in the number of substitutions can produce PUs ranging from branched to linear or flexible to rigid.

Rigid PU foams are produced from polyisocyanates [usually polymeric methylenediphenyl diisocyanate (MDI)] and polyols of higher functionality, e.g., polyalkylene oxide adducts of polyethers such as sucrose, sorbitol, pentaerythritol, ethylenediamine, toluenediamine, and methylene bis(aniline), as well as combinations of these polyols, resulting in a network with high cross-link density. In recent years, aromatic polyesters also have been used extensively in combination with other polyols in rigid polyurethane (Frisch, 1997).

A7.3 Degradation of PUs

Physical, chemical and/or biological degradation of PUs is possible; the chemical and physical degradation of polymers implies that microorganisms, macroorganisms, or enzymes are not present and that the aging is totally dependent on physical, chemical, and/or mechanical influences.

Aging of PU might be slow but is irreversible, and it might result in the decrease of the essential properties of the polymeric material (Albertson and Karlsson, 1997). Many parameters, including processing conditions, additives, and morphology of the polymer, are effective in aging of PU. The application of the PU also might affect its fate in the environment. The chemical structure of polymers is especially important in determining the degradability of PUs. Low-molecular-weight compounds present in the chemical structure of the PU increase the degradation behavior because they are more accessible to biochemical reactions.

Air (oxygen), light, humidity, temperature variations, and biological agents are usually the most important factors affecting the degradation of the PUs (Albertson and Karlsson, 1997). It has been known that polyether PUs are more sensitive to the oxidative degradation than polyester PUs (Khatua and Hsieh, 1997). On the other hand, polyester PUs are more sensitive to hydrolytic degradation than polyether PUs (Labow et al., 2005).

The lifetime of polymers varies considerably, from a couple days to several years, depending on the type. Amorphous regions are more susceptible to hydrolysis reactions and microbial attacks than crystalline regions. Highly ordered crystalline regions are usually more difficult to penetrate than the amorphous part because microorganisms and enzymes cannot come into close enough contact in highly crystalline regions to cause aging. A hydrophobic polymer is often less degradable than a hydrophilic one, and the hydrophobicity substantially decreases the hydrolysis rate and the microbial attack. The characterization of the surface is an important factor in defining degradation of PUs in the environment (Albertson and Karlsson, 1997) because their hydrophobicity is also important during the biodegradation, which mainly takes place on the surface. It has been generally reported that as the hydrophobicity of PU increases, higher levels of bacterial adhesion and protein absorption on the surface are detected (Kim and Kim, 1998). From these statements, it can be concluded that hydrophobic and hydrophilic segments may decrease or increase the degradability. Hydrolyzable and/or oxidizable linkage affects the degradability of PU. Linear PUs are considered to be more susceptible to degradation than the branched polymer (Albertson and Karlsson, 1997).

The amount of hard segment in the structure of PU is also an important factor in its susceptibility to the microbial attack. Kim and Kim (1998) reported that polyurethane with a hard segment content of 11% is more biodegradable (41% of polyester PU degraded) than a hard segment content of 34.6% (~1% of PU degraded) under composting conditions. The soft segment part is normally a polyester or polyether of molecular weight between 500 and 3000, and the hard segment part is composed of a low-molecular-weight diol or diamine reacted with diisocyanate (Chen et al., 2000; Khatua and Hsieh, 1997). Hydrolytic and enzymatic degradation of hard segments containing aliphatic diisocyanate is higher than that of an aromatic hard segment containing diisocyanate (Kim and Kim, 1998). Furthermore, degradation of the hard

segment containing a higher amount of diol carbon chains in polyol (~16% of PU degraded) is higher than that of the hard segment containing less diol carbon chains (~5 % of PU degraded) under composting conditions (Kim and Kim, 1998). This difference could be due to less crystallinity and more flexibility as the number of diol carbon chains increases in the hard segment of PU (Frisch, 1997).

Many degradation mechanisms that occur simultaneously or subsequently are responsible from the abiotic and biotic aging of polymers. Abiotic and biotic ester formation, Norrish type I and type II photolytic degradation, and biodegradation of polyether are some reactions that can proceed when ester or ketone functions are present in the polymers (Albertson et al., 1987).

A7.4 Biodegradation of PU

Microbial degradation can mainly be divided in two big blocks: urethane bonds and polyol segments because they are the major constituents of PU.

Whatever the kind of polyurethane, microbial degradation of PU is dependent on the secretion of the extracellular enzymes. Urethane compounds of low molecular mass can be hydrolyzed by microorganisms, and this hydrolysis is catalyzed by an esterase (Matsumura et al., 1985; Marty and Vouges, 1987; Pohlenz et al., 1992; Owens et al., 1996; Oshiro et al., 1997). But the investigation on bond degradation is not very extensive, and it is not clear yet if PU bonds are hydrolyzed directly or following breakdown into low-molecular-mass compounds (Filip, 1978; Jansen et al., 1991).

The biodegradability of PU was first reported in 1966 by Ossefort and Testroet. As soon as the properties of PUs are modified, the tensile strength and elasticity change, determining the accessibility to degrading enzyme systems (Pathirana and Seal, 1983; Howard, 1999). It has been reported that polyester PUs are more biodegradable than polyether PUs (Darby and Kaplan, 1968). However, it is very difficult to compare the different results given by each researcher because the PU type and the microorganism type are different for each study. Many reports have been published on PU biodegradation in the laboratory under controlled conditions, especially biodegradation of polyester PU by microorganisms (main attention has been given to fungi) (Nakajima-Kambe et al., 1995). Table A7.2 summarizes PU degrading microorganisms in the literature. However, these results mostly come from lab studies, in many cases providing additional nutrients to microorganisms, and highly concentrated enzymes must be used for the biodegradation of PUs. The literature has no study on PU biodegradation in the environment. Field studies, nevertheless, are necessary in assessing the benefits and obstacles associated with the use of PUs as insulator materials for bioremediation applications in the environment.

TABLE A7.2 Polyurethane (PU)-degrading microorganisms (PE = polyether, PS = polyester) (Nakajima-Kambe et al., 1999)

Microorganisms	PU	Putative degrading enzymes	Reference
Fungi			
<i>Aspergillus niger</i>	PS, PE	Unknown	Darby and Kaplan 1968
<i>A. avus</i>	PS, PE	Unknown	Darby and Kaplan 1968
<i>A. fumigatus</i>	PS	Esterase	Pathirana and Seal 1984
<i>A. versicolor</i>	PS, PE	Unknown	Darby and Kaplan 1968
<i>Aureobasidium pullulans</i>	PS, PE	Unknown	Darby and Kaplan 1968
	PS	Unknown	Crabbe et al. 1994
<i>Chaetomium globosum</i>	PS, PE	Unknown	Darby and Kaplan 1968
	PS	PS Esterase, protease, urease	Pathirana and Seal 1984
<i>Cladosporium sp.</i>	PS	Unknown	Crabbe et al. 1994
<i>Curvularia senegalensis</i>	PS	Esterase	Crabbe et al. 1994
<i>Fusarium solani</i>	PS	Unknown	Crabbe et al. 1994
<i>Gliocladium roseum</i>	PS	PS Esterase, protease, urease	Pathirana and Seal 1984
<i>Penicillium citrinum</i>	PS	PS Esterase, protease, urease	Pathirana and Seal 1984
<i>P. funiculosum</i>	PS, PE	Unknown	Darby and Kaplan 1968
<i>Trichoderma sp</i>	PS, PE	Unknown	Darby and Kaplan 1968
Bacteria			
<i>Comamonas acidovorans</i>	PS	Esterase	Nakajima-Kambe et al. 1991
<i>Corynebacterium sp.</i>	PS	Esterase	Kay et al. 1991
<i>Enterobacter agglomerans</i>	PS	Unknown	Kay et al. 1991
<i>Serratia rubidaea</i>	PS	Unknown	Kay et al. 1991
<i>Pseudomonas aeruginosa</i>	PS	Unknown	Kay et al. 1991
<i>Staphylococcus epidermidis</i>	PS	Unknown	Jansen et al. 1991

A7.4.1 Biodegradation of Polyesters

Polyester PUs are considered to be susceptible to biodegradation by several kinds of fungi and bacteria. The biodegradation of PUs is due to their use as a sole source of carbon and/or nitrogen or co-metabolism by microorganisms under mostly aerobic conditions. Enzymatic attack on PUs could be due to hydrolases such as ureases attacking the urea bonds, proteases attacking the amide bonds, and esterases attacking the many ester bonds (Vega et al., 1999). Indeed, proteolytic enzymes (papain and urease) and cholesterol esterase have been shown to degrade PUs in vitro. Several reports have appeared in the literature on polyester PU degradation due to the hydrolysis of the ester bonds, but not because bacteria utilized them as a primary nutrient source nor as a result of co-metabolism (Kay et al., 1993). However, Nakajima-Kambe et al. (1997) reported a bacterial strain, *Comamonas acidovorans*, which uses the solid polyester PU as the sole carbon and nitrogen source. Akutsu et al. (1998) suggested that extracellular membrane-bound esterase activity is essential in PU degradation.

A7.4.2 Biodegradation of Polyethers

Although ester PUs are susceptible to microbial attacks, polyether PUs are relatively more resistant to this kind of attack. A study by Darby and Kaplan (1968) reports that polyether PUs are hardly susceptible to microbial degradation. This difference could be due to the PU biodegradation mechanism, which involves exo-type depolymerization in the ether PUs (Kawai et al. 1978, 1985), but endo-type depolymerization in the ester PUs (Nakajima-Kambe et al., 1999). However, it has been shown that degradation/deterioration of polyethylene PU can happen in many medical implants and tissue engineering materials made from this material, which are exposed to many hydrolytic enzymes and oxidants in the human body (Christenson et al., 2005; Ebert et al., 2005; Santerre et al., 2005). On the other hand, Brown et al. (1999) reported no sign of biodegradation of polyether PU foams under accelerated anaerobic conditions in a landfill simulator after 21 months of treatment.

The polyether PU preincubation with non-physiological enzyme (known as “papain”) decreased the mechanical stability of the materials, but specifically decreased their tensile strength and the fatigue lifetime (Stokes and McVennes, 1995; Zhao et al., 1987). In another study, Santerre et al. (2005) were able to assess the release of toluene diamine (TDA) from a polyether-urea-urethane by using radiolabeled diisocyanates when this PU was exposed to cholesterol esterase. The study revealed that the polymers containing the highest amount of labeled hard segments showed the least amount of chain cleavage by the enzyme and then TDA generation (Santerre et al., 2005). Santerre and Labrow (1997) also tested the consequence of hard segment size in the stability of polyether PUs against cleavage. They used three different polyether PUs, modifying the molar ratios of [¹⁴C]-diisocyanate to chain extender and constant polyether makeup. They observed that radiolabel release was quite dependent on the amount of hard segment contained in the PU. The PU with the lowest concentration of hard segment and higher number of carbonyl groups was disposed on the surface, whereas the increase of hard segment concentration does lead to restrictions in polymer chain mobility. Biodegradation of polycarbonated polyether PUs by esterase activity is mostly dependent on the hard segment chemistry and size (Tang et al., 2001). As mentioned before, the functional groups on polyether PU surfaces play an important role in susceptibility of PU to biodegradation. The rank order of chemical group susceptibility (Santerre et al., 2005) is given below:

*NON-HYDROGEN BONDED CARBONATED >NON-HYDROGEN BONDED URETHANE
>HYDROGEN BONDED CARBONATED >HYDROGEN BONDED URETHANE.*

The explanation of this could be based on the degree of the hydrogen bond, and because of that, this parameter is an important factor during the design of microbial resistant PU. Kanavel et al. (1996) also reported that sulfur-cured polyester and polyether PUs possessed some fungal inertness. These studies indicate that once the hard-segment density is known, it is easy to tailor PU structure and synthesis of nondegradable PUs.

The biodeterioration of PU is highly undesirable for long-term use of PU as an insulator material during the remediation applications. It could result in loss in the integrity of the material, which is weakened by microbial attacks, and hence, system failure could occur (Gu and Gu, 2005; Dannoux et al., 2005). One of the main problems is that no information exists in the

literature on the polyether PU half-life due to biodegradation or reported evidence of polyether PU biodegradation in the environment. The only reported information on the half-life of polyether PU foam concerns hydrolysis by superheated water, where the half-life is estimated as 400 years (Mahoney et al., 1974). Hence, in the present study, biodegradation of rigid PU samples by hydrolytic action under anaerobic conditions was investigated.

A7.5 References

Albertson C.-A., Andersson S.O., Karlsson S., 1987. The mechanism of the biodegradation of polyurethane. *Polymer Degradation Stability* 18: 73-79.

Akutsu Y., Nakajima-Kambe T., Nomura N., Nakahara T., 1998. Purification and properties of a polyester polyurethane degrading enzyme from *Comamonas acidovorans* TB-35. *Applied Environmental Microbiology* 64: 62-67.

Akutsu Y., Adachi Y., Yamada C., Toyoshima K., Uchiyama H., Nakajima-Kambe T., Nomura N., 2005. Isolation of a bacterium that degrades urethane compounds and characterization of urethane hydrolase. *Applied Microbiology Biotechnology* 70: 422-429.

Albertsson A.-C., Karlsson S., 1997. Controlled degradation by artificial and biological processes. In: *Macromolecular Design of Polymeric Materials*, Ed. Hatada E., Kitayama N., Vogl O., pp. 793-802, Marcel Dekker, Inc. New York.

Bayer O., 1947. Polyurethanes. *Modern Plastics* 24: 149-152.

Brown W.E., Bartlett C., Aul D.J., Blough M.S., D'Andrea M., Hauck J.T., Kennedy A.L., Minkley E.G., Bailey R.E., 1999. Monitoring potential degradation of polyurethanes in a landfill simulator. *Polyurethanes* 99: 369-472.

Chen Z., Ruifeng Z.R., Makoto K.M., Tadao N.T., 2000. Anticoagulant surface prepared by the heparinization of ionic polyurethane film. *Journal of Applied Polymer Science* 76: 382-390.

Christenson E.M., Wiggins M.J., Anderson J.M., Hiltner A., 2005. Surface modification of poly(ether urethane urea) with modified dehydroepiandrosterone for improved in vitro stability. *Journal of Biomedical Materials Research* 73A: 108-115.

Crabbe J.R., Campbell J.R., Thompson L., Walz S.L., Schultz W.W., 1994. Biodegradation of a colloidal ester based polyurethane by soil fungi. *International Biodeterioration & Biodegradation* 33: 103-113.

Dannoux A., Esnouf S., Begue J., Amekraz B., Moulin C., 2005. Degradation kinetics of poly(ether-urethane) estane induced by electron irradiation. *Nuclear Instruments and Methods in Physics Research B* 236: 488-494.

Darby R.T., Kaplan, A.M., 1968. Fungal susceptibility of polyurethanes. *Applied Microbiology* 16: 900-905.

Dombrow B.A., 1957. *Polyurethanes*. Reinhold Publishing, New York.

Ebert M., Ward B., Anderson J., McVenes R., Stokes K., 2005. In vivo stability of polyether polyurethanes with polyethylene oxide surface-modifying end groups: Resistance to biologic oxidation and stress cracking. *Journal of Biomedical Materials Research* 75A: 175-184.

Filip Z., 1978. Decomposition of polyurethane in a garbage landfill leakage water and soil microorganisms. *European Journal of Applied Microbiology Biotechnology* 5: 225-231.

Fried J.R., 1995. *Polymer Science and Technology*. Prentice-Hall, PTR, Englewood Cliffs, NJ.

Frisch K.C., 1997. High performance polyurethanes. In: *Macromolecular Design of Polymeric Materials*. Ed. Hatada E., Kitaiyama N., Vogl O., pp. 523-560, Marcel Dekker, Inc. New York.

Gu J.G., Gu J.D., 2005. Methods currently used in testing microbiological degradation and deterioration of a wide range of polymeric materials with various degree of degradability: A review. *Journal of Polymers and the Environment* 13: 65-74.

Howard G.T., Hilliard N.P., 1999. Use of Coomassie blue-polyurethane interaction in screening of polyurethanase proteins and polyurethanolytic bacteria. *International Biodeterioration & Biodegradation* 43: 23-30.

Jansen B., Schumacher-Perdreau F., Peters G., Pulverer G., 1991. Evidence for degradation of synthetic polyurethanes by *Staphylococcus epidermidis*. *Zentralblatt fuer Bakteriologie* 276: 36-45.

Kanavel G.A., Koons P.A., Lauer R.E., 1966. Fungus resistance of millable urethanes. *Rubber World* 154: 80-86.

Kaplan A.M., Darby R.T., Greenberger R., Rogers M.R., 1968. Microbial deterioration of polyurethane systems. *Developments in Industrial Microbiology* 9: 201-217.

Kawai F., Okamoto T., Suzuki T., 1985. Aerobic degradation of polypropylene glycol by *Corynebacterium* sp. *Journal of Fermentation Technology* 63: 239-244.

Kawai F., Kimura T., Fukaya M., Tani Y., Ogata K., Ueno T., Fukami H., 1978. Bacterial oxidation of polyethylene glycol. *Applied Environmental Microbiology* 35: 679-684.

Kay M.J., McCabe R.W., Morton L.H.G., 1993. Chemical and physical changes occurring in polyester polyurethane during biodegradation. *International Biodeterioration & Biodegradation* 31: 209-225.

Kay M.J., Morton L.H.G., Prince E.L., 1991. Bacterial degradation of polyester polyurethane. *International Biodeterioration* 27: 205-222.

Khatua S., Hsieh Y.L., 1997. Chlorine degradation of polyether-based polyurethane. *Journal of Polymer Science: Part A: Polymer Chemistry* 35: 3263-3273.

Kim D.Y., Kim S.C., 1997. Effect of chemical structure on the biodegradation of polyurethanes under composing conditions. *Polymer Degradation and Stability* 62: 343-352.

Labow R.S., Sa D., Matheson L.A., Santerre J.P., 2005. Polycarbonate-urethane hard segment type influence esterase substrate specificity for human-macrophage-mediated biodegradation. *Journal of Biomaterial Science: Polymer Edn.* 16: 1167-1177.

Mahoney L.R., Weiner S.A., Ferris F.C., 1974. Hydrolysis of polyurethane foam waste. *Environmental Science and Technology* 8: 135-139.

Marty J.L., Vouges J., 1987. Purification and properties of a phenylcarbamate herbicide degrading enzyme of *Pseudomonas alcaligenes* isolated from soil. *Agricultural and Biological Chemistry* 51: 3287-3294.

Matsumura E., Shin T., Murao S., Sakaguchi M., Kawano T., 1985. A novel enzyme, N-benzyloxycarbonyl amino acid urethane hydrolase IV. *Agricultural Biological Chemistry* 49: 3643-3645.

Nakajima-Kambe T., Shigeno-Akutsu Y., Nomura N., Onuma F., Nakahara T., 1999. Microbial degradation of polyurethane, polyester polyurethanes and polyether polyurethanes. *Applied Microbiology Biotechnology* 51: 134-140.

Nakajima-Kambe T., Onuma F., Akutsu Y., Nakahara T., 1997. Determination of the polyester polyurethane breakdown products and distribution of the polyurethane degrading enzyme of *Comamonas acidovorans* strain TB-35. *Journal of Fermentation Bioengineering* 83: 456-460.

Nakajima-Kambe T., Shigeno-Akutsu Y., Nomura N., Onuma F., Nakahara T., 1995. Isolation and characterization of a bacterium which utilizes polyester polyurethane as a sole carbon and nitrogen source. *FEMS Microbiology Letters* 129: 39-42.

Oshiro T., Shinji M., Morita Y., Takayama Y., Izumi Y., 1997. Novel l-specific cleavage of the urethane bond of t-butoxycarbonylamino acids by whole cells of *Corynebacterium aquaticum*. *Applied Microbiology Biotechnology* 48: 546-548.

Owens S., Otani T., Masaoka S., Ohe T., 1996. The biodegradation of low-molecular-weight urethane compounds by a strain of *Exophiala jeanselmei*. *Bioscience, Biotechnology & Biochemistry* 60: 244-248.

Pathirana R.A., Seal K.J., 1985. Studies on polyurethane deteriorating fungi. Part 3. Physico-mechanical and weight changes during fungal deterioration. *International Biodeterioration* 21: 41-49.

Pohlenz H.D., Boidol W., Schüttke I., Streber W.R., 1992. Purification and properties of an *Arthrobacter oxydans* P52 carbamate hydrolase specific for the herbicide phenmedipham and nucleotide sequence of the corresponding gene. *Journal of Bacteriology* 174: 6600-6607.

Ruiz , C., Hilliard, N., Howard G.T., 1999. Growth of *Pseudomonas chlororaphis* on a polyester-polyurethane and the purification and characterization of a polyurethanes-esterase enzyme. *International Biodeterioration & Biodegradation* 43: 7-12.

Santerre J.P., Labow R.S., 1997. The effect of hard segment size on the hydrolytic stability of the polyether-urea-urethanes when exposed to cholesterol esterase. *Journal of Biomedical Materials Research* 36: 223-232.

Santerre J.P., Labow R.S., Woodhouse K., Laroche G., 2005. Understanding the biodegradation of polyurethanes: From classical implants to tissue engineering materials. *Biomaterials* 26: 7457-7470.

Saunders J.H., Frisch K.C., 1964. *Polyurethanes: Chemistry and Technology, Part II: Technology*. Interscience Publishers, New York.

Smith T.L., 1976. Tensile strength of polyurethane and other elastomeric block copolymers. *Rubber Chemistry Technology* 49: 64-84.

Smith T.L., 1977. Strength of elastomers- a perspective. *Polymer Engineering Science* 17: 129-43.

Stokes K., McVennes R., 1995. Polyurethane elastomer biostability. *Journal of Biomaterials Applications* 9: 321-335.

Tang Y.W., Labow R.S., Santerre J.P., 2001. Enzyme-induced biodegradation of polycarbonate polyurethanes: Dependence on hard-segment concentration. *Journal of Biomedical Materials Research* 56: 516-528.

Urbansky J., Czerwinski W., Janicka K., Majewska F., Zowall H., 1977. *Handbook of Analysis of Synthetic Polymers and Plastics*. Ellis Horwood Lmt., Manchester, UK.

Vega R.T., Main T., Howard, G.T., 1999. Cloning and expression in *Escherichia coli* of a polyurethane-degrading enzyme from *Pseudomonas fluorescens*. *International Biodeterioration & Biodegradation* 43: 49-55.

Young R.J., Lovell P.A., 1994. *Introduction to Polymers*, 2nd edition. Chapman & Hall, London.

Zhang X., Xu R., Wu Z., Zhou C., 2003. The synthesis and characterization of polyurethane/clay nanocomposites. [*Polymer International*](#) 52: 790-794.

Zhao Q., Marchant R.E., Anderson J.M., Hiltner A., 1987. Long term biodegradation in vitro of poly(ether urethane urea): A mechanical property study. *Polymer* 35: 328-379.

QA/QC STUDIES

To validate the obtained weight loss data, quality assurance procedures were followed. The balance (sensitivity 0.1 mg) employed for weighing the PU foams was calibrated by using filter papers of known weight with precision of 0.1 mg. The percentage difference between the measured and control values ranged from 0 to 0.35% (Table. A7.3). Furthermore, effectiveness of the drying procedure used for the weight change determination was also tested on the untreated PU foams. The standard deviation ranged between 0.11 and 0.31% of the average value, with a standard deviation of 0.06% (Table A7.4).

TABLE A7.3 Sensitivity of analytical balance used for weighing the PU foams

Filter Paper	Reported (g)	Measured (g)	Difference	% Error
1	0.1154	0.1154	0	0.00
2	0.1152	0.1155	0.0003	0.26
3	0.1151	0.1153	0.0002	0.17
4	0.1129	0.113	0.0001	0.09
5	0.1134	0.1137	0.0003	0.26
6	0.114	0.114	0	0.00
7	0.1139	0.114	0.0001	0.09
8	0.1153	0.1155	0.0002	0.17
9	0.1152	0.1152	0	0.00
10	0.1155	0.1155	0	0.00
11	0.1152	0.1156	0.0004	0.35

TABLE A7.4 The effectiveness of the drying procedure used for the weight change determination

Foam	Run 1 (g)	Run 2 (g)	Run 3 (g)	Average	St. Dev.	% Difference
1	2.0713	2.0697	2.0596	2.0669	0.0063	0.31
2	2.1856	2.1825	2.1801	2.1827	0.0028	0.13
3	2.2005	2.2013	2.1967	2.1995	0.0025	0.11
4	1.7896	1.7873	1.7835	1.7868	0.0031	0.17
5	2.1108	2.1099	2.1025	2.1077	0.0046	0.22
6	2.4390	2.4378	2.4299	2.4356	0.0049	0.20
7	2.4080	2.4064	2.4007	2.4050	0.0038	0.16
8	2.8688	2.8632	2.8588	2.8636	0.0050	0.18
9	2.8078	2.8074	2.7980	2.8044	0.0055	0.20
10	2.5706	2.5697	2.5644	2.5682	0.0034	0.13
				Overall Avg.		0.18
				Overall Std.		0.06

APPENDIX 8: CORROSION TEST RESULTS

SAMPLES IN SOLUTION

Conditions	Sample ID	Temperature	A mm ²	W-0d (g)	W-2d (g)	W-7d (g)	W-14d(g)	W-27d(g)
Polished	13	Room	1805.6	29.6479	29.6388	29.6188	29.5932	29.5453
As cut	14	Room	1801.2	30.8881	30.8786	30.8589	30.8363	30.7947
Polished	15	60 °C	1847.9	30.8612	30.8476	30.823	30.7894	30.7272
As cut	16	60 °C	1696.4	29.722	29.7104	29.6875	29.6618	29.5999
Polished	17	80 °C	1913.7	33.0655	33.0548	33.0313	33.004	32.966
As cut	18	80 °C	1851.8	32.978	32.967	32.9507	32.9303	32.8856
W-90d (g)	W-120d (g)	W-147d (g)	ΔW(2) g	ΔW(7) g	ΔW(14) g	ΔW(27) g	ΔW(90) g	ΔW(120) g
29.2855	29.2024	29.1343	0.0091	0.0291	0.0547	0.1026	0.3624	0.4455
30.56	30.4711	30.4023	0.0095	0.0292	0.0518	0.0934	0.3281	0.417
30.2603	30.0912	29.9436	0.0136	0.0382	0.0718	0.134	0.6009	0.77
29.1552	28.983	28.8343	0.0116	0.0345	0.0602	0.1221	0.5668	0.739
32.9201	32.8905	32.852	0.0107	0.0342	0.0615	0.0995	0.1454	0.175
32.7779	32.6856	32.5778	0.011	0.0273	0.0477	0.0924	0.2001	0.2924
ΔW(147) g	CR-2mm/y	CR-7mm/y	CR-14mm/y	CR-27mm/y	CR 90-mm/y	CR 120-mm/y	CR 147-mm/y	
0.5136	0.1169	0.1068	0.1004	0.0976	0.1034	0.0954	0.0897	
0.4858	0.1223	0.1074	0.0953	0.0891	0.0939	0.0895	0.0851	
0.9176	0.1707	0.137	0.1287	0.1246	0.1676	0.161	0.1567	
0.8877	0.1586	0.1347	0.1176	0.1236	0.1722	0.1684	0.1651	
0.2135	0.1297	0.1184	0.1065	0.0893	0.0392	0.0353	0.0352	
0.4002	0.1378	0.0977	0.0853	0.0857	0.0557	0.061	0.0682	
Conditions	Sample ID	Temperature	A mm ²	W-0d (g)	W-3d (g)	W-5d (g)	W-22d(g)	W-78d(g)
Polished	19	Room	1798.59	31.8005	31.7839	31.76	31.7198	31.6403
As cut	20	Room	1991.67	35.303	35.2903	35.2822	35.2268	35.1374
	ΔW(5) g	W-148d(g)	W-197d(g)	ΔW(3) g	ΔW(22) g	ΔW(78) g	ΔW(148) g	ΔW(197) g
	0.0405	31.5026	31.3855	0.0166	0.0807	0.1602	0.2979	0.415
	0.0208	34.9878	34.8549	0.0127	0.0762	0.1656	0.3152	0.4481
	CR-3mm/y	CR -5mm/y	CR-22mm/y	CR-78mm/y	CR-148mm/y	CR-148mm/y		
	0.1446	0.2106	0.0946	0.053	0.0519	0.0543		
	0.0999	0.0977	0.0807	0.0494	0.0496	0.053		

Conditions	Sample ID	Temperature	A mm ²	W-0d (g)	W-60d (g)	W-120d (g)	W-150d(g)	W-180d(g)
Polished	1	Room	1800	32.1349	31.9684	31.8064	31.7289	31.6561
As cut	2	Room	1800	31.2098	31.0436	30.8946	30.8096	30.7353
Polished	5	60 °C	1800	31.6937	31.4408	31.1094	30.9283	30.7811
As cut	6	60 °C	1800	32.9407	32.6841	32.36	32.2099	32.0384
Polished	9	80 °C	1800	31.6836	31.5695	31.5217	31.4973	31.4643
As cut	10	80 °C	1800	32.7877	32.5776	32.4675	32.4026	32.2995
	ΔW(60) g	ΔW(120) g	ΔW(150) g	ΔW(180) g	CR-60mm/y	CR -120mm/y	CR -150mm/y	CR -180mm/y
	0.1665	0.3285	0.406	0.4788	0.0715	0.0705	0.0697	0.0685
	0.1662	0.3152	0.4002	0.4745	0.0714	0.0677	0.0687	0.0679
	0.2529	0.5843	0.7654	0.9126	0.1086	0.1255	0.1315	0.1306
	0.2566	0.5807	0.7308	0.9023	0.1102	0.1247	0.1255	0.1292
	0.1141	0.1619	0.1863	0.2193	0.0490	0.0348	0.0320	0.0314
	0.2101	0.3202	0.3851	0.4882	0.0902	0.0688	0.0661	0.0699

Conditions	Sample ID	Temperature	A mm ²	W-0d (g)	W-90d (g)	W-150d (g)	W-180d (g)
Polished	3	Room	1800	30.7693	30.5236	30.3614	30.2865
As cut	4	Room	1800	33.5223	33.2549	33.0902	33.0093
Polished	7	60 °C	1800	34.3921	33.9691	33.6091	33.4388
As cut	8	60 °C	1800	33.5731	33.1535	32.8282	32.6685
Polished	11	80 °C	1800	32.6911	32.2286	32.0661	32.0044
As cut	12	80 °C	1800	32.8371	32.4361	32.2922	32.1828
	ΔW(90) g	ΔW(150) g	ΔW(180) g	CR-90mm/y	CR -150mm/y	CR -180mm/y	
	0.2457	0.4079	0.4828	0.0703	0.0701	0.0691	
	0.2674	0.4321	0.513	0.0766	0.0742	0.0734	
	0.423	0.783	0.9533	0.1211	0.1345	0.1365	
	0.4196	0.7449	0.9046	0.1201	0.1280	0.1295	
	0.4625	0.625	0.6867	0.1324	0.1074	0.0983	
	0.401	0.5449	0.6543	0.1148	0.0936	0.0937	

SAMPLES IN SOIL

Conditions	Sample ID	A mm ²	Temperature	W-0d (g)	W-11d (g)	W-18d (g)	W-28d (g)	W-40d (g)	W-71d (g)	W-101d (g)	ΔW(18) g
As cut	1S	1889.7	Room	32.2361	32.2338	32.235	32.2443	32.2381	32.2435	32.2371	0.0011
As cut	2S	1848.9	60 °C	31.7452	31.7411	31.7282	31.7109	31.7012	31.6974	31.6949	0.017
As cut	3S	1819.6	80 °C	31.4427	31.4409	31.429	31.4285	31.4028	31.4039	31.4045	0.0137
	ΔW(11) g	ΔW(28) g	ΔW(40) g	ΔW(71) g	ΔW(101) g	CR-11mm/y	CR -18mm/y	CR-28mm/y	CR-40mm/y	CR-71mm/y	CR-101mm/y
	0.0023	-0.0082	-0.002	-0.0074	-0.001	0.0051	0.0015	-0.0072	-0.0012	-0.0026	-0.0002
	0.0041	0.0343	0.044	0.0478	0.0503	0.0093	0.0237	0.0307	0.0276	0.0169	0.0125
	0.0018	0.0142	0.0399	0.0388	0.0382	0.0042	0.0194	0.0129	0.0254	0.0139	0.0096

Conditions	Sample ID	A mm ²	Temperature	W-0d (g)	W-7d (g)	W-13d (g)	W-32d (g)	W-62d (g)	ΔW(13) g	ΔW(32) g	ΔW(32) g
As cut	5S	1901.06	Room	32.7791	32.7645	32.7611	32.76	32.7415	0.018	0.0191	0.0376
As cut	6S	1962.55	60 °C	34.4209	34.3956	34.3618	34.3247	34.3084	0.0591	0.0962	0.1125
As cut	7S	1914.85	80 °C	33.0526	33.0233	33.019	33.0137	33.0484	0.0336	0.0389	0.0042
	ΔW(7) g	CR-7mm/y	CR 13-mm/y	CR 32-mm/y	CR 32-mm/y						
	0.0146	0.0509	0.0338	0.0146	0.0148						
	0.0253	0.0854	0.1074	0.0710	0.0429						
	0.0293	0.1014	0.0626	0.0294	0.0016						

Conditions	Sample ID	A mm ²	Temperature	W-0d (g)	W-5d (g)	W-13d (g)	W-28d (g)	W-43d (g)	ΔW(5) g	ΔW(13) g	ΔW(28) g
As cut	8S	1823	Room	32.6619	32.6673	32.7109	32.6960	32.7018	-0.0054	-0.0490	-0.0341
As cut	9S	1962.7	Room	34.5486	34.5523	34.5300	34.5117	34.4998	-0.0037	0.0186	0.0369
As cut	10S	1844.05	Room	31.2709	31.2662	31.2637	31.2636	31.2648	0.0047	0.0072	0.0073
As cut	11S	1723.68	Room	28.7500	28.7564	28.7618	28.7643	28.7619	-0.0064	-0.0118	-0.0143
	ΔW(43) g	CR-5mm/y	CR 13-mm/y	CR-28mm/y	CR-43mm/y						
	-0.0399	-0.0275	-0.0959	-0.0310	-0.0236						
	0.0488	-0.0175	0.0338	0.0311	0.0268						
	0.0061	0.0236	0.0139	0.0066	0.0036						
	-0.0119	-0.0344	-0.0244	-0.0137	-0.0074						

Conditions	Sample ID	A mm ²	Temperature	W-0d (g)	W-12d (g)	W-19d (g)	W-26d (g)	W(33) g	W(40) g	ΔW(12) g	ΔW(19) g
Room	B1	1800	Room	28.949	28.9495	28.9492	28.9493	28.9495	28.9488	-0.0005	-0.0002
Room	B2	1800	Room	30.3825	30.3837	30.3836	30.3835	30.3836	30.3822	-0.0012	-0.0011
	ΔW(26) g	ΔW(33) g	ΔW(40) g	CR 12-mm/y	CR-19mm/y	CR 26-mm/y	CR 33-mm/y	CR 40-mm/y			
	-0.0003	-0.0005	0.0002	-0.0007	-0.0003	-0.0003	-0.0004	0.0001			
	-0.0010	-0.0011	0.0003	-0.0016	-0.0015	-0.0010	-0.0009	0.0002			



Nuclear Engineering Division

Argonne National Laboratory
9700 South Cass Avenue, Bldg. 212
Argonne, IL 60439-4838

www.anl.gov



THE UNIVERSITY OF
CHICAGO

A U.S. Department of Energy laboratory
managed by The University of Chicago